



Université catholique de Louvain
Faculté des Sciences
Département de Physique
Unité de physique théorique et de physique mathématique
Centre for Particle Physics and Phenomenology

A two-Higgs-doublet model: from twisted theory to LHC phenomenology

Doctoral dissertation presented by

Michel Herquet

in fulfilment of the requirements for the degree of Doctor in Sciences

Prof. Jean-Marc Gérard (Advisor)	UCL
Prof. Pierre Defrance (Chairman)	UCL
Prof. Abdelhak Djouadi	Université Paris-Sud
Prof. Michael Kramer	RWTH Aachen
Prof. Vincent Lemaître	UCL
Prof. Fabio Maltoni	UCL
Prof. Michel Tytgat	Université Libre de Bruxelles

Septembre 2008

“I can no other answer make, but, thanks, and thanks.”

William Shakespeare (1564-1616)

Je tiens tout d’abord à remercier chaleureusement le Professeur Jean-Marc Gérard de l’Université catholique de Louvain de m’avoir offert la possibilité de réaliser ce travail grâce à l’appui de l’Institut Interuniversitaire des Sciences Nucléaires, ainsi que d’avoir accepté d’en assurer la supervision. La clarté de son raisonnement, son ouverture d’esprit teintée d’humour et son étonnante intuition physique ne sont plus un secret pour tous ceux qui ont eu la chance de travailler à ses côtés.

Je voudrais également remercier particulièrement le Professeur Fabio Maltoni, sans qui une grande partie du présent travail n’aurait probablement jamais pu être réalisée. Son optimisme constant, son dynamisme communicatif et son approche novatrice de la phénoménologie ont marqué profondément ma formation tout au long de ces trois années passées dans la “MadGraph team”.

Mes remerciements vont également aux autres membres de mon Jury de soutenance, les Professeurs Pierre Defrance, Abdelhak Djouadi, Michael Kramer, Vincent Lemaître et Michel Tytgat, qui m’ont fait l’honneur d’évaluer ce travail malgré des circonstances parfois difficiles et qui, par leurs questions et remarques pertinentes, ont contribué à son amélioration.

La recherche en Physique des Particules, et singulièrement en phénoménologie, ne trouve bien souvent son accomplissement qu’au travers d’heureuses collaborations. La présente thèse ne fait pas exception à cette règle. Je remercie donc spécialement Simon de Visscher, non seulement d’avoir contribué largement, aussi bien scientifiquement que techniquement, à l’étude des conséquences expérimentales du modèle ici proposé, mais également de m’avoir apporté son aide inconditionnelle en toute circonstance, comme seul un ami pouvait le faire.

Je suis aussi redevable à tous les physiciens, jeunes et moins jeunes, proches et moins proches, qui ont influencé ma formation à l’occasion de collaborations ou de discussions, ou qui ont simplement contribué, grâce à leur amitié, à faire de ces années une expérience si enrichissante. Si l’espace me manque ici pour en dresser une liste exhaustive, je tiens néanmoins à citer les Professeurs Yves Brihaye, Denis Favart, Henry

Frisch, Jan Govaerts, Christophe Ringeval, Philippe Ruelle, et Tim Stelzer, mes premiers compagnons de route Nico, Bruno, Georges et Stéphane, mes “collègues mais néanmoins amis” du B322, Geoffroy et Vincent, ainsi qu’Augustin, François, Xavier, Jérôme, Wendy, Séverine, Pavel, Rikkert, Olivier, Pierre, Claude, Arnaud et Johan, à qui j’adresse un remerciement particulier pour m’avoir si souvent fait profiter de son expérience en de nombreux domaines, en ce compris la langue de Shakespeare. Merci aussi à Thomas et Fabrice, pour leur support technique qui se révéla plus d’une fois décisif, et à Cathy, Ginette et Carine de tolérer si patiemment l’excentricité des physiciens qui les entourent. . .

Enfin, ces remerciements ne seraient pas complets sans mentionner toutes ces personnes qui, dans mon entourage, ont contribué discrètement à la réussite de ce projet par leur patience, leur soutien et leur écoute, en particulier dans les moments plus difficiles. Je pense bien entendu à mes parents qui m’ont tant appris, à ma soeur Caroline, à Samuël, à mon adorable filleule Zoé, mais également aux amis que j’ai la chance d’avoir, trop nombreux pour être tous cités ici, mais qui, j’en suis sûr, se reconnaîtront. Merci enfin, et surtout, à ma merveilleuse épouse, Sabrina, qui m’a supporté jour après jour sans jamais se départir de son si joli sourire.

*A Sabrina, pour son amour et son soutien
qui ont rendu possible ce qui suit.*

Contents

Introduction	11
1 The Standard Model Way	15
1.1 From the Fermi interaction to the electroweak scale	15
1.2 Electroweak interactions before symmetry breaking	16
1.3 The Brout-Englert-Higgs mechanism	17
1.3.1 The abelian case	17
1.3.2 The BEH mechanism in the Standard Model	19
1.4 Standard Model Higgs boson phenomenology	20
1.4.1 Theoretical constraints	21
1.4.2 Indirect constraints from precision measurements	25
1.4.3 Direct searches at the LEP collider	28
1.4.4 Direct searches at the Tevatron collider	31
1.4.5 Direct searches at the Large Hadron Collider	33
2 Extended scalar sectors	35
2.1 Motivations	35
2.1.1 Higher symmetries	36

2.1.2	Phenomenological aspects	39
2.2	Generic extensions	43
2.2.1	Tree-level ρ parameter value	44
2.2.2	Gauge coupling constants unification	45
2.3	The general two-Higgs-doublet model	46
2.3.1	Potential in a generic basis	47
2.3.2	Basis invariance and the Higgs basis	49
2.3.3	Yukawa couplings	53
2.4	Global symmetries in the 2HDM	54
2.4.1	Custodial symmetry	55
2.4.2	CP symmetry	57
2.4.3	\mathbb{Z}_2 symmetry: type I versus type II scenario	60
2.5	The MSSM scalar sector	61
2.6	A twisted 2HDM	65
3	Constraints on the twisted 2HDM	69
3.1	Theoretical constraints	69
3.1.1	Vacuum stability and minimum constraints	69
3.1.2	Unitarity and perturbativity constraints	70
3.2	Indirect constraints	72
3.2.1	Electroweak precision parameters	72
3.2.2	Bottom quark physics	79
3.2.3	The muon anomalous magnetic moment	89
3.3	Direct constraints from collider experiments	92
3.3.1	The LEP experiment	92
3.3.2	The Tevatron experiment	96
3.4	Summary	98

4	Phenomenology at the LHC	103
4.1	Decays and production modes	104
4.1.1	Type I models	104
4.1.2	Type II models	108
4.1.3	Benchmark points	111
4.2	Signals with $h^0 \rightarrow A^0 A^0$	112
4.3	Signals with $H^0 \rightarrow A^0 Z^0$	116
4.3.1	Process $gg \rightarrow h^0 \rightarrow H^0 H^0 \rightarrow Z A^0 Z A^0$	116
4.3.2	Process $gg \rightarrow b\bar{b} H^0 \rightarrow b\bar{b} Z A^0$	119
4.4	Signals with $H^\pm \rightarrow A^0 W^\pm$	121
4.4.1	Process $gg \rightarrow h^0 \rightarrow H^+ H^- \rightarrow W^+ A^0 W^- A^0$	121
4.4.2	Process $pp \rightarrow tt \rightarrow W^\pm H^\mp bb \rightarrow W^+ W^- A^0 bb$	123
4.4.3	Process $pp \rightarrow tH^\pm(b) \rightarrow W^- bW^+ A^0(b)$	125
4.5	Summary	126
	Conclusion	127
	A Higgs boson Feynman rules in the twisted 2HDM	129
	B The 2HDM implementation into MadGraph/MadEvent v4	133
B.1	The implementation of the 2HDM into MadGraph	134
B.2	The implementation of the 2HDM into MadEvent	137
	C Higgs bosons production in association with single top	139

Introduction

“Dimidium facti qui coepit habet”

Quintus Horatius Flaccus (65 - 8 B.C.)

The forthcoming decade is widely expected to be another exciting era of modern high energy physics. While Run II at the Fermi National Accelerator Laboratory is now underway and is going to produce more than fifty times the amount of data used in discovering the top quark, the Large Hadron Collider (LHC) construction comes to its end and the first events are expected for the last months of 2008.

The end of the twentieth century has seen the success of the Standard Model (SM) of electroweak and strong interactions. Despite its original name (and maybe aim), this phenomenological model imposed itself over the years as a mathematically consistent *theory* describing all observed high-energy phenomena. This distinctive predictive power was first demonstrated by the observation of neutral weak currents in the late seventies, before being confirmed both by a huge amount of well understood experimental data and the incredible level of accuracy of several agreements, never reached in any other field of Science.

The reticence of the high-energy community to consider the Standard Model as the ultimate theory is mainly based on three classes of arguments. First, its mathematical consistency calls for the existence of a heavy scalar particle, the Brout-Englert-Higgs boson¹, which has so far escaped all direct detection attempts. The actual presence of

¹In the present work, the short name “Higgs boson” is often used, following the common usage in high energy physics publications. The contribution of Robert Brout and François Englert to the discovery of the spontaneous symmetry breaking mechanism should nevertheless be strongly underlined.

this new particle appears as more and more challenged over time, since the light mass region favoured by precision data is already excluded by the LEP experiment. Second, while being perfectly consistent, the SM may appear as *unnatural*, or at best heavily fine-tuned, for various reasons such as the stability of the Fermi scale and the lack of explanation for the fermion mass spectrum, in particular when considering the very small but non-zero neutrino masses. Finally, the quantum gauge field theory which is the mathematical ground of the Standard Model is ill-defined when applied to the classical theory of gravitation. Interestingly, these arguments are strongly dependent upon each other. For example, the hierarchy problem is related at the same time to the physical meaning of a very high scale where unknown quantum gravity effects are supposed to be non-negligible and to the presence of a fundamental scalar particle.

These various reasons lead the large majority of high energy physicists to contemplate the possibility of “Beyond the Standard Model” physics effects, which could arguably show up at the TeV scale in order to stabilise the Higgs boson mass and/or unitarise the gauge bosons scattering amplitudes at high energy. Several theories have been proposed among which the quite popular Supersymmetry and, more recently, Extra Dimensions, Little Higgs and Walking Technicolor theories are typical examples. In the Minimal Supersymmetric SM (MSSM), the Higgs mass is stabilized by compensating the SM loop contributions by opposite sign loops containing the new supersymmetric particles. In Little Higgs theories, the Higgs mass is protected by multiple approximate symmetries in a way similar to the pion mass. In technicolor-inspired theories, the Higgs boson appears as composite and, finally, in theories with extra dimensions the hierarchy between the weak scale and the Planck scale is explained by the geometry of the 4D branes arrangement along the new dimensions.

All these BSM theories are, in general, characterized by a set of new physical states interacting weakly and possibly strongly with the known SM particles. If their couplings are sizable and their masses are in the kinematical reach of the LHC, these particles are expected to be produced and to decay in the detectors (or to escape them), giving visible signatures (or missing transverse energy). Extracting these new physics imprints from the huge amount of data to be collected is going to be a real challenge, both from theoretical and experimental points of view. Indeed, compared to the situation in other experimental environments, *e.g.*, electron-positron collisions at LEP, the data flow describing events resulting from the head-on collision of two 7 TeV proton beams at LHC will be extremely complex. This is due to several effects: the space extended structure of the proton, the total amount of energy available in the rest frame of the collision and, last but not least, the high luminosity at which the machine has been designed to work.

This high luminosity is of course a necessity to probe New Physics characterized by rare events, but it has, however, two major drawbacks. First, the background rate is

in general orders of magnitude larger than the genuine signal. Even processes considered as rare at machines working at lower energies, such as top quark pair production at the Tevatron, will occur at relatively high rates (one every second) and will sometimes overwhelm interesting signals. Very strong cuts on kinematical variables will then be applied in order to reach discovery significance. This will require a detailed knowledge of Standard Model backgrounds in underpopulated regions of the phase space. Second, at high luminosity, several protons are expected to collide in a time scale smaller than the typical detector response delay. This phenomenon known as “pile-up” can only be described at the very last stage of the event simulation (i.e. at the detector level) and can sometimes play a non-trivial role in the sensitivity of a given analysis.

Considering the above difficulties together with the number of proposed BSM theories, the number of different scenarios for each of them, and the number of accessible points in the parameter spaces, it is hard to think about a systematic approach which can be managed by a scientific community with limited resources. The solutions usually proposed to face this situation can be classified into two distinctive categories. Top-down approaches focus on a particular theory and try to use the maximal amount of available theoretical, indirect and direct constraints in order to define specific benchmark points. The possible signatures of the theory for these particular benchmark points are then investigated in great detail. The hope is of course that the New Physics to be discovered is similar enough to one of these benchmark scenarios. Studies dedicated to MSSM are typical examples of such approach. The other possibility is to consider several signatures (“inspired” by realistic theories) from a model independent point of view and to scan the whole free parameter space to identify winning search strategies. Looking at particularly sensitive physical quantities, for example the top anti-top quark pair invariant mass distribution, in order to find deviations from the SM prediction is usually referred to as a “bottom-up” approach.

A third way, partially sharing the advantages of these two “extremes” approaches, could also be followed. Using the knowledge of the anatomy of various BSM theories, or of certain types of BSM theories, one can first identify recurring structures and define interesting generic SM extensions. Work along this line has been done, for example, in the “strongly-interacting light Higgs” approach by Giudice *et al.* where the typical structures common to Little Higgs and Technicolor theories are identified and studied from a model independent perspective. These generic extensions are however usually strongly constrained by precision constraints naturally satisfied in the Standard Model. In order to avoid unacceptably large fine-tuning, the (approximate) hidden global symmetries present in the SM and responsible for the suppression of particular rare effects should be implemented in the considered scenarios. This procedure has been, for example, followed by Isidori *et al.* to define the “Minimal Flavour

Violation” scheme which can be implemented in various BSM theories to naturally suppress the effects of unwanted flavour changing neutral currents.

The present work falls into this third approach of High Energy Physics phenomenology. The generic two-Higgs-doublet model is first identified as a recurring and common structure for the scalar sector of various BSM theories. The custodial, CP and Z_2 symmetries are then isolated as important features of the SM Higgs sector, before being generalised and implemented in the 2HDM. The phenomenology of the resulting model is finally studied, from the perspective of precision tests and for its signatures at high energy colliders.

This thesis is divided into four main parts. The first chapter is dedicated to a brief overview of the Standard Model, focusing in particular on the minimal implementation of the spontaneous symmetry breaking mechanism and on the associated accidental global symmetries. In the second chapter, various motivations for generic extensions of the SM scalar sector are reviewed and the two-Higgs-doublet model is introduced as an archetypal scenario. The custodial, CP and Z_2 symmetries accidentally present in the SM are generalised to the 2HDM case, and the possibility for a unusual “twisted” realisation of these symmetries is considered. The third chapter is devoted to an extensive study of the principal theoretical, indirect and direct constraints which may affect this exotic scenario. These constraints are used to restrict the model parameter space and to define various benchmark points in the beginning of the fourth chapter, where the most promising signatures at the LHC are examined. Three appendices complete this work, dedicated respectively to an exhaustive list of the model Feynman rules, to the generic 2HDM implementation in the MadGraph/MadEvent v4 Monte-Carlo event generator and to a study of the single top associated production of neutral Higgs boson(s).

Chapter 1

The Standard Model Way

“We can’t define anything precisely.”

Richard P. Feynman (1918 - 1988)

This first chapter is dedicated to an overview of the Standard Model for electroweak interactions, with a particular emphasis on the Brout-Englert-Higgs mechanism and on the Higgs boson phenomenology. This presentation is not supposed to be exhaustive but to introduce the concepts and notations used in the forthcoming chapters. The interested reader looking for more details is invited to consult other references like [1] or [2] on which part of the following is based.

1.1 From the Fermi interaction to the electroweak scale

Using the Fermi theory with four fermions interactions [3], one can describe the muon weak decay $\mu^- \rightarrow e^- \bar{\nu}_e \nu_\mu$ with the effective Lagrangian

$$L_F = -\frac{G_F}{\sqrt{2}} J^\mu J_\mu^\dagger \quad (1.1)$$

where J_μ is the $V - A$ leptonic current

$$J_\rho(x) = \bar{\psi}_e \gamma_\rho (1 - \gamma_5) \psi_{\nu_e} + \bar{\psi}_\mu \gamma_\rho (1 - \gamma_5) \psi_{\nu_\mu} \quad . \quad (1.2)$$

The Fermi constant G_F appearing in (1.1) is extracted from the muon lifetime τ_μ through the relation

$$\frac{1}{\tau_\mu} = \frac{G_F^2 m_\mu^5}{192\pi^3} \left(1 - \frac{8m_e^2}{m_\mu^2}\right) \left[1 + 1.810\frac{\alpha}{\pi} + (6.701 \pm 0.002) \left(\frac{\alpha}{\pi}\right)^2\right] \quad (1.3)$$

where higher order QED corrections have been included [4]. This leads to the precise value [5]

$$G_F = (1.16637 \pm 0.00001) \times 10^{-5} \text{ GeV}^{-2} \quad . \quad (1.4)$$

The very same constant appears in the description of other processes, like the neutron decay, hence the postulate of the *universality* of the weak interactions.

Nevertheless, the Fermi theory is unsatisfactory due to the nonrenormalizable¹ nature of the effective four-point interaction (1.1). Indeed, the coupling constant G_F has a negative canonical dimension such that the superficial degree of divergence grows with order of perturbation theory. Following a naive dimensional analysis argument, this description of the weak interaction is expected to be valid only up to scales much lower than the natural cutoff

$$\Lambda_{EW} \simeq \frac{1}{(\sqrt{2}G_F)^{1/2}} \simeq 250 \text{ GeV} \quad . \quad (1.5)$$

1.2 Electroweak interactions before symmetry breaking

The successful renormalizable theory proposed by Glashow, Weinberg and Salam[6, 7, 8] to describe electroweak phenomena at scales of order Λ_{EW} is a Yang-Mills theory [9] based on the gauge symmetry group $SU(2)_L \times U(1)_Y$. Vectorial fields are associated with each generator of the electroweak gauge group and mediate the corresponding interaction. The field B_μ is related to the generator Y of $U(1)_Y$ and the fields $W_\mu^{1,2,3}$ are related to the three generators $T^{1,2,3}$ of $SU(2)_L$, defined such as

$$[T^a, T^b] = i\epsilon^{abc}T_c \quad . \quad (1.6)$$

The strength tensors of these fields can be written

$$W_{\mu\nu}^a \equiv \partial_\mu W_\nu^a - \partial_\nu W_\mu^a + g_L \epsilon^{abc} W_\mu^b W_\nu^c \quad (1.7)$$

$$B_{\mu\nu} \equiv \partial_\mu B_\nu - \partial_\nu B_\mu \quad (1.8)$$

¹Here, the nonrenormalizable adjective is used to qualify a theory containing an unacceptably high number of divergences which would require an unnatural, infinite number of unrelated counterterms to be renormalized.

where g_L is the coupling constant of $SU(2)_L$. The purely gauge part of the Lagrangian reads

$$\mathcal{L}_G = -\frac{1}{4}W_{\mu\nu}^a W_a^{\mu\nu} - \frac{1}{4}B_{\mu\nu}B^{\mu\nu} \quad . \quad (1.9)$$

Regarding matter fields, the theory contains three generations of left and right-handed chiral quarks and leptons with $\psi_{L,R} \equiv 1/2(1 \mp \gamma_5)\psi$. Left-handed fermions transform as $SU(2)_L$ doublets (generically noted $Q_L = (u_L, d_L)^T$ for quarks and $L_L = (\nu_L, e_L)^T$ for leptons) and right-handed fermions transform as $SU(2)_L$ singlets (generically noted u_R and d_R for up-type and down-type quarks and e_R for charged leptons). The hypercharge Y associated with the gauge group $U(1)_Y$ is related to the third component I^3 of $SU(2)_L$ and to the electric charge Q through

$$Y = 2(Q - I^3) \quad . \quad (1.10)$$

Gauge and matter sectors are minimally coupled through the Dirac kinetic terms

$$\mathcal{L}_D = i\bar{Q}_L^i D_\mu \gamma^\mu Q_L^i + i\bar{u}_R^i D_\mu \gamma^\mu u_R^i + i\bar{d}_R^i D_\mu \gamma^\mu d_L^i \quad (1.11)$$

where i stands for the three generations of quarks and leptons and the covariant derivative D_μ is defined as

$$D_\mu \psi \equiv \left(\partial_\mu - ig_L T_a W_\mu^a - ig_Y \frac{Y}{2} B_\mu \right) \psi \quad (1.12)$$

with g_Y the coupling constant of $U(1)_Y$.

The Lagrangian $\mathcal{L}_G + \mathcal{L}_D$ is not sufficient by itself to completely describe electroweak interactions since it cannot account for the observed mass of fermions and W^\pm and Z^0 gauge bosons, the later being in turn also responsible for the limited range of the weak force and the smallness of the Fermi constant G_F . However, it is straightforward to show that adding a direct mass term for any of the associated fields would explicitly break the gauge invariance of the theory. As explained in the following section, this puzzling issue can be addressed, among others, in a simple and elegant way by the Brout-Englert-Higgs mechanism [10, 11, 12].

1.3 The Brout-Englert-Higgs mechanism

1.3.1 The abelian case

Let us first consider the simplified case of an abelian model with a single vector boson A_μ associated with a $U(1)$ local symmetry and a complex scalar field ϕ . Let us also

assume that the dynamic of this system is described by the Lagrangian

$$\mathcal{L} = -\frac{1}{4}F_{\mu\nu}F^{\mu\nu} + D^\mu\phi^*D_\mu\phi + \mu^2\phi^*\phi - \lambda(\phi^*\phi)^2 \quad (1.13)$$

where μ^2 and λ are real and positive parameters by hypothesis. The field strength $F^{\mu\nu}$ and the covariant derivative D^μ are defined in terms of A^μ with a coupling constant e as in (1.8) and (1.12). The complex field ϕ can be conveniently parameterized as

$$\phi(x) \equiv \frac{1}{\sqrt{2}}e^{i\xi(x)/v}(\rho(x) + v) \quad (1.14)$$

where $v = \sqrt{\mu^2/\lambda}$ corresponds to the classical minimum of potential (1.13). Any $U(1)$ local gauge transformation of the fields reads

$$\phi'(x) = e^{i\alpha(x)}\phi(x) \quad , \quad A'_\mu(x) = A_\mu(x) - \frac{1}{e}\partial_\mu\alpha(x) \quad (1.15)$$

where $\alpha(x)$ is an arbitrary function of space-time. Since the system is invariant under this transformation, one can always *fix* the gauge function to be

$$\alpha(x) = -\frac{1}{v}\xi(x) \quad . \quad (1.16)$$

With this particular choice, called the *unitary gauge*, the fields $\phi(x)$ and $A_\mu(x)$ now read

$$\phi'(x) = \frac{1}{\sqrt{2}}(\rho(x) + v) \quad , \quad A'_\mu(x) = A_\mu(x) - \frac{1}{ve}\partial_\mu\xi(x) \quad (1.17)$$

and the degree of freedom associated with the would-be Goldstone field $\xi(x)$ can now be seen as a longitudinal degree of freedom of the field $A_\mu(x)$. After replacing expressions (1.17) in (1.13), one can see that $\xi(x)$ disappears from \mathcal{L} and A^μ acquires a non zero mass:

$$m_A^2 = e^2v^2 \quad (1.18)$$

while the mode $\rho(x)$ appears as a physical scalar of positive mass

$$m_\rho^2 = 2\mu^2 \quad . \quad (1.19)$$

In summary, the Brout-Englert-Higgs (BEH) mechanism allows the gauge bosons to get a non zero mass at scales below v without explicitly breaking the gauge invariance of the theory. For each massive gauge boson, one Goldstone scalar must disappear from the physical spectrum in order to conserve the number of degrees of freedom. The “price to pay” for this mechanism to occur is the appearance of, at least, one physical scalar state called the Higgs boson.

1.3.2 The BEH mechanism in the Standard Model

In the Standard Model, three of the four electroweak gauge bosons have to be massive. This requires at least the presence of three scalars (to be absorbed as the longitudinal degrees of freedom of these vector fields) in addition to the extra scalar needed to trigger the BEH mechanism. The minimal solution is to group these four fields into one $Y = 1$ $SU(2)_L$ complex doublet

$$H \equiv \begin{pmatrix} H^+ \\ H^0 \end{pmatrix} \equiv \frac{1}{\sqrt{2}} \begin{pmatrix} i(\pi^1 + i\pi^2) \\ \sigma + i\pi^3 \end{pmatrix} . \quad (1.20)$$

The Higgs doublet couples to the gauge sector of the SM introduced in the previous section through the kinetic term of the most general gauge invariant renormalizable scalar Lagrangian

$$\mathcal{L}_H = (D^\mu H)^\dagger D_\mu H + \mu^2 H^\dagger H - \lambda(H^\dagger H)^2 . \quad (1.21)$$

The minimum of the potential in \mathcal{L}_S can always be rotated to

$$\langle H \rangle = \frac{1}{\sqrt{2}} \begin{pmatrix} 0 \\ v \end{pmatrix} \quad (1.22)$$

using a $SU(2)_L \times U(1)_Y$ gauge transformation. The gauge boson mass spectrum is then determined by

$$|D^\mu \langle H \rangle|^2 \quad (1.23)$$

where D^μ is the covariant derivative defined in (1.12), such that

$$D_\mu \langle H \rangle = \frac{-iv}{2\sqrt{2}} \begin{pmatrix} \sqrt{2}g_L W_\mu^+ \\ -g_L W_\mu^3 + g_Y B_\mu \end{pmatrix} \quad (1.24)$$

with

$$W_\mu^\pm \equiv \frac{1}{\sqrt{2}}(W_\mu^1 \mp iW_\mu^2) . \quad (1.25)$$

The W_μ^\pm bosons are clearly mass eigenstates with

$$m_W = \frac{1}{2}g_L v \quad (1.26)$$

while W_μ^3 and B_μ mix to give two physical bosons A_μ and Z_μ :

$$\begin{aligned} A_\mu &= \cos \theta_W B_\mu + \sin \theta_W W_\mu^3 \\ Z_\mu &= -\sin \theta_W B_\mu + \cos \theta_W W_\mu^3 \end{aligned} \quad (1.27)$$

with masses

$$m_A = 0 \quad \text{and} \quad m_Z = \frac{m_W}{\cos \theta_W} \quad (1.28)$$

where the weak angle is defined by $\tan \theta_W = g_Y/g_L$. The important role of the second relation in (1.28) is investigated more deeply in section 1.4.2.

The presence of a Higgs doublet in the Standard Model also allows for the following Yukawa terms in the Lagrangian

$$\mathcal{L}_Y = -\overline{Q}_L \lambda_d H d_R - \overline{Q}_L \lambda_u \tilde{H} u_R - \overline{L}_L \lambda_l H e_R + \text{h.c.} \quad (1.29)$$

where the $SU(2)_L$ doublet

$$\tilde{H} \equiv i\tau_2 H^* = \begin{pmatrix} (H^0)^\dagger \\ -H^- \end{pmatrix} \quad (1.30)$$

has an hypercharge $Y = -1$. After the spontaneous symmetry breaking of the electroweak symmetry, these Yukawa interactions provide (non flavor diagonal) mass terms $m_{u,d,l} = \lambda_{u,d,l} v / \sqrt{2}$ to all fermions except the neutrinos².

1.4 Standard Model Higgs boson phenomenology

In the SM, the mass of the W^\pm bosons can be related to the Fermi constant G_F by matching the effective four fermions description with the massive propagating W^\pm picture (with $p_W \ll m_W$), i.e.,

$$\frac{G_F}{\sqrt{2}} = \frac{g_L}{2\sqrt{2}} \times \frac{1}{M_W^2} \times \frac{g_L}{2\sqrt{2}} \quad (1.31)$$

The left coupling constant g_L and the W^\pm bosons mass both cancel between (1.26) and (1.31) so that the vacuum expectation value v can be estimated from the single low energy quantity G_F

$$v = \frac{1}{(\sqrt{2}G_F)^{1/2}} \simeq 246 \text{ GeV} \quad (1.32)$$

This parameter is then consistently identified with the natural cutoff scale Λ_{EW} in (1.5).

²Here we assume that neutrinos remain massless due to the absence of the associated right-handed components. Even if this assumption is in contradiction with experimental data, it does not play any role in the context of the present work.

After spontaneous symmetry breaking, the Higgs boson h^0 , i.e. the particle associated to the expansion of σ^0 around the vacuum in (1.20), $\sigma^0 \equiv v + h^0$, acquires a mass

$$m_{h^0}^2 = -\mu^2 + 3\lambda v^2 \quad (1.33)$$

which can then be simplified to

$$m_{h^0}^2 = 2\mu^2 = 2\lambda v^2 \quad (1.34)$$

using the potential minimization condition

$$\left. \frac{\partial V}{\partial \sigma^0} \right|_{\langle \sigma^0 \rangle = v} = 0 \quad \Leftrightarrow \quad v = \sqrt{\frac{\mu^2}{\lambda}} \quad (1.35)$$

Since v is precisely fixed by (1.32), the μ^2 and λ real parameters are completely fixed by the knowledge of the Higgs mass m_{h^0} , which in turns can be seen as the only free scale of the theory.

1.4.1 Theoretical constraints

The first type of constraints on the Higgs boson mass are coming from various requirements related to the self-consistency of the quantum theory.

Unitarity and perturbativity

A significant consequence of the nonrenormalizable nature of the Fermi theory introduced in section 1.1 is the violation of unitarity in interactions occurring at scales of order Λ_{EW} . In this effective theory the cross section is asymptotically proportional to the center of mass energy squared s , instead of being bounded by s^{-1} . The interaction probability then grows indefinitely with the available energy, and becomes bigger than unity at scales of order Λ_{EW} .

Even if this unwanted behavior can be cured for some particular processes (e.g. $e^- \bar{\nu}_e \rightarrow \mu^- \bar{\nu}_\mu$) by adding massive gauge bosons W^\pm “by hand” in the theory, it is in fact only postponed to other processes like $e^+ e^- \rightarrow W^+ W^-$. This issue can be solved in renormalizable theories by the presence of new particle(s) giving rise to additional negative interferences in the total amplitude. In the Standard Model, the Higgs boson plays this unitarizing role but its mass is in turn constrained to be of the order of the electroweak scale.

A more quantitative estimate of this bound can be extracted by applying the optical theorem to particular processes like, for example, the $W^+ W^- \rightarrow W^+ W^-$ scattering

at very high energies (see Ref. [13] and references therein for a detailed discussion). The optical theorem relates the total cross section σ and the imaginary part of the amplitude A in the forward direction $\theta = 0$ through

$$\sigma = \frac{1}{s} \text{Im}(A(\theta = 0)) \quad . \quad (1.36)$$

The scattering amplitude can be expanded into partial waves a_l of orbital momentum l

$$A \equiv 16\pi \sum_{l=0}^{\infty} (2l+1) P_l(\cos \theta) a_l \quad (1.37)$$

giving, for a $2 \rightarrow 2$ scattering process,

$$\sigma = \frac{16\pi}{s} \pi \sum_{l=0}^{\infty} (2l+1) |a_l|^2 \quad . \quad (1.38)$$

By substituting (1.37) and (1.38) in (1.36), the optical theorem becomes

$$\text{Re}(a_l)^2 + (\text{Im}(a_l) - \frac{1}{2})^2 = \frac{1}{4} \quad (1.39)$$

which is nothing else than the equation of circle of radius $\frac{1}{2}$ and center $(0, \frac{1}{2})$ in the $(\text{Re}(a_l), \text{Im}(a_l))$ plane. This leads trivially to a condition on the real part of a_l

$$|\text{Re}(a_l)| < \frac{1}{2} \quad . \quad (1.40)$$

The $l = 0$ partial wave for the amplitude of the $W^+W^- \rightarrow W^+W^-$ process can easily be estimated in the limit where $s \gg m_W^2, m_{h^0}^2$ and reads

$$a_0 \approx \frac{-m_{h^0}^2}{8\pi v^2} \quad . \quad (1.41)$$

The optical theorem condition (1.40) then gives the bound

$$m_{h^0} \lesssim 870 \text{ GeV} \quad (1.42)$$

for this particular channel. A combined analysis of all $2 \rightarrow 2$ scattering processes involving gauge and Higgs bosons gives a slightly more stringent bound of about 710 GeV. Another approach is to assume that m_{h^0} is much larger than \sqrt{s} , then requiring another mechanism to restore unitarity at the electroweak scale. A similar computation leads in this case to an upper bound of order 1.2 TeV on \sqrt{s} . Following this argument, if the Higgs boson does not exist or is too heavy to be observed by forthcoming experiments, BSM Physics signatures are anyway expected below or around the TeV scale.

Besides these limits related to unitarity, the requirement that all processes involving the Higgs boson can be consistently described with a perturbative expansion also leads to constraints on the λ parameter, hence on m_{h^0} . The Higgs partial decay width into pairs of gauge bosons, which grows proportionally to the cube of its mass, is a particularly sensible quantity in this context. The one loop corrections [14], for example, are of the same order as the Born tree-level contribution for $m_{h^0} \sim \mathcal{O}(10\text{TeV})$. And, even worse, the two-loops corrections can be larger than the one-loop correction already for $m_{h^0} \sim \mathcal{O}(1\text{TeV})$. More complete calculations [15] have led to a definitive upper limit of about 700 GeV, which appears to be in a surprisingly good agreement with the naive estimate obtained from a perturbative approach of unitarity.

Triviality

Due to the presence of the $\lambda(H^\dagger H)^2$ term in (1.21), the SM Higgs boson interacts with itself. The λ coefficient then varies with the energy scale Λ when Higgs loop corrections to the four Higgs vertex are taken into account. The first order Renormalization Group Equation (RGE) reads [16]

$$\frac{d}{d \log \Lambda^2} \lambda(\Lambda^2) = \frac{3}{4\pi^2} \lambda^2(\Lambda^2) + \mathcal{O}(\lambda^3) \quad (1.43)$$

and has the simple solution

$$\lambda(\Lambda^2) = \frac{\lambda(v^2)}{1 - \frac{3}{4\pi^2} \log \frac{\Lambda^2}{v^2}} \quad (1.44)$$

if the arbitrary reference scale is fixed to v . If $\Lambda \rightarrow 0$, λ goes to zero and the theory is *trivial*, i.e. it is not self-interacting anymore. If $\Lambda \gg v$, λ grows up rapidly and reach a Landau pole for the finite value

$$\Lambda = v \exp\left(\frac{4\pi^2}{3\lambda}\right) = v \exp\left(\frac{8\pi^2 v^2}{3m_{h^0}^2}\right) . \quad (1.45)$$

Different upper bounds on the Higgs mass can be obtained by requiring λ to stay finite below a given scale. If Λ is associated to the Planck scale, the bound is rather low, approximatively 200 GeV. At the contrary, if Λ is fixed to be the Higgs mass itself, the bound is much less stringent, of order 700 GeV. Of course, these naive estimates rely on the first order equation (1.43) which failed to be valid close to the Landau pole, but numerical simulations on lattice have shown similar results [17].

Vacuum stability

In equation (1.43), only the self interaction term in (1.21) is taken into account. Additional contributions to the λ parameter RGE arise from box diagrams involving heavy

fermions and gauge bosons. In the limit where the Higgs self coupling at a given scale is much smaller than the electroweak and Yukawa couplings, (1.43) becomes [16]

$$\frac{d}{d \log \Lambda^2} \lambda(\Lambda^2) = \frac{1}{16\pi^2} \left[-12 \frac{m_t^4}{v^4} + \frac{3}{16} (2g_L^4 + (g_L^2 + g_Y^2)^2) \right] \quad (1.46)$$

which has

$$\lambda(\Lambda^2) = \lambda(v^2) + \left[-12 \frac{m_t^4}{v^4} + \frac{3}{16} (2g_L^4 + (g_L^2 + g_Y^2)^2) \right] \log \frac{\Lambda^2}{v^2} \quad (1.47)$$

as a solution. Since the right hand side of (1.46) is negative, the parameter λ decreases monotonically with the energy. If $\lambda(v^2)$ is too small, its sign can change below the cutoff scale Λ and the potential is not stable anymore since it has no minimum. Depending on the actual value of Λ , a lower bound on m_{h^0} can then be extracted from the stability requirement. If Λ is associated to the Planck scale, the bound is rather high, around $m_{h^0} \gtrsim 130$ GeV, while for $\Lambda \approx 1$ TeV, one obtains $m_{h^0} \gtrsim 70$ GeV. Note that these bounds are much weaker if the vacuum is required to be metastable instead of strictly stable (e.g. see [18] and references therein). A summary of triviality and vacuum stability theoretical bounds on the Higgs boson mass as a function of Λ can be found on Figure 1.1.

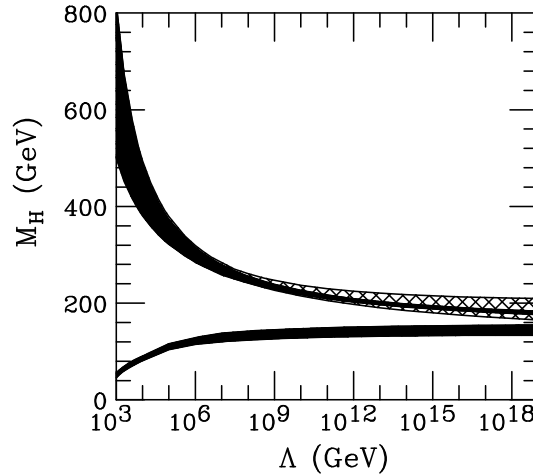


Figure 1.1: Triviality (upper band) and vacuum stability (lower band) bounds on the Standard Model Higgs boson mass as a function of the cutoff scale, using $m_t = 175$ GeV and $\alpha_s(m_Z) = 0.118$. The shaded areas show theoretical uncertainties and the cross-hatched area corresponds to the additional uncertainty when varying m_t from 150 to 200 GeV. From Ref. [19].

1.4.2 Indirect constraints from precision measurements

In order to constrain the Higgs boson mass by studying radiative corrections to precision electroweak parameters, one first needs to select a proper renormalization scheme. Marciano and Sirlin [20], for example, impose the tree-level relation $m_W = m_Z \cos \theta_W$ to remain valid at all order and introduce radiative corrections in the relation between G_F and m_W . In the context of the present work, we prefer the Veltman³ [21] scheme where the free parameters are g_L and $\sin \hat{\theta}_W$ and where the $m_W = m_Z \cos \hat{\theta}_W$ relation is no longer valid beyond the tree-level. The $\sin \hat{\theta}_W$ parameter is extracted from Z -pole and neutral current data at the scale $\mu = m_Z$.

The ρ parameter is defined as the ratio

$$\rho \equiv \frac{\hat{m}_W^2}{\hat{m}_Z^2 \cos^2 \hat{\theta}_W} . \quad (1.48)$$

As mentioned before, in the Veltman scheme, $\rho = 1$ only at the lowest order of perturbation theory but $\rho \neq 1$ in general due to radiative corrections. If the renormalized squared masses \hat{m}^2 differ from the bare masses m^2 by an amount δm^2 , one has

$$\begin{aligned} \Delta\rho &\equiv \rho - 1 \\ &= \frac{(m_W^2 + \delta m_W^2)}{(m_Z^2 + \delta m_Z^2) \cos^2 \hat{\theta}_W} - 1 \\ &= \frac{(m_W^2 + \delta m_W^2)}{m_W^2} \left(1 - \frac{\delta m_Z^2}{m_Z^2} \right) - 1 \\ &= \frac{1}{m_W^2} (\delta m_W^2 - \cos^2 \hat{\theta}_W \delta m_Z^2) \end{aligned} \quad (1.49)$$

or, if only low energy experiments are considered,

$$m_W^2 \Delta\rho = \Pi_{WW}(k^2 = 0) - \cos^2 \hat{\theta}_W \Pi_{ZZ}(k^2 = 0), \quad (1.50)$$

where the functions $\Pi_{WW,ZZ}(k^2)$ are the coefficients of the Minkowski metric in the gauge bosons propagators, i.e.

$$\Pi_{WW,ZZ}^{\mu\nu}(k^2) = \Pi_{WW,ZZ}(k^2) g^{\mu\nu} . \quad (1.51)$$

Custodial symmetry

The minimal Higgs sector of the Standard Model, as described by Lagrangian (1.21) has a important symmetry property. The simultaneous requirements of gauge invariance and renormalizability constrain (1.21) to be invariant under an ‘‘accidental’’ global symmetry.

³Equivalent, in this framework, to the \overline{MS} renormalization scheme.

Considering the definition (1.20) of the $SU(2)_L$ Higgs doublet in terms of scalar fields, the scalar Lagrangian (where only the partial derivative part of D^μ is considered) can be rewritten as a linear σ -model [22]

$$\mathcal{L}_S = \frac{1}{2}[(\partial_\mu \sigma)^2 + (\partial_\mu \vec{\pi})^2] + \frac{\mu^2}{2}(\sigma^2 + \vec{\pi}^2) - \frac{\lambda}{4}(\sigma^2 + \vec{\pi}^2)^2 \quad . \quad (1.52)$$

Considering $(\sigma, \vec{\pi})$ as a quadruplet, this Lagrangian is obviously invariant under the $SO(4)$ symmetry:

$$\begin{pmatrix} \sigma \\ \vec{\pi} \end{pmatrix} \rightarrow \begin{pmatrix} \sigma' \\ \vec{\pi}' \end{pmatrix} = O(\vec{\alpha}, \vec{\beta}) \begin{pmatrix} \sigma \\ \vec{\pi} \end{pmatrix} \quad (1.53)$$

with

$$O(\vec{\alpha}, \vec{\beta}) \equiv \exp \left[-i(\vec{\alpha} \cdot \vec{Q}_V + \vec{\beta} \cdot \vec{Q}_A) \right] \quad (1.54)$$

where the vectorial (\vec{Q}_V) and axial (\vec{Q}_A) generators obey the following commutation rules

$$[Q_V^i, Q_V^j] = [Q_A^i, Q_A^j] = i\varepsilon^{ijk} Q_V^k \quad , \quad [Q_V^i, Q_A^j] = i\varepsilon^{ijk} Q_A^k \quad . \quad (1.55)$$

The matrix $O(\vec{\alpha}, \vec{\beta})$ is given (at first order in α^i and β^i) by

$$O(\vec{\alpha}, \vec{\beta}) \approx \begin{pmatrix} 1 & -\beta_1 & -\beta_2 & -\beta_3 \\ \beta_1 & 1 & \alpha_3 & -\alpha_2 \\ \beta_2 & -\alpha_3 & 1 & -\alpha_1 \\ \beta_3 & \alpha_2 & \alpha_1 & 1 \end{pmatrix} \quad (1.56)$$

such that transformation(1.53) reads

$$\begin{aligned} \sigma &\rightarrow \sigma' \approx \sigma - \vec{\beta} \cdot \vec{\pi} \\ \vec{\pi} &\rightarrow \vec{\pi}' \approx \vec{\pi} - \vec{\alpha} \times \vec{\pi} + \vec{\beta} \sigma \quad . \end{aligned} \quad (1.57)$$

From these last relations, it is clear that only axial transformations mix σ and $\vec{\pi}$ fields. It follows that the vectorial $SO(3)$ subgroup of the original $SO(4)$ remains unbroken after the spontaneous breaking of the gauge symmetry by the non vanishing vacuum expectation value $\langle \sigma \rangle = v$.

This remaining $SO(3)$ global symmetry, called the ‘‘custodial symmetry’’ [23], has an important phenomenological consequence. Indeed, as demonstrated for example in [24], the ρ parameter defined in (1.48) can be linked in a suitable gauge to the ratio of the renormalization constants of the Goldstone fields $\pi^1 \pm i\pi^2$ and π^3 . Since these fields are transforming as a triplet under the $SO(3)$ symmetry, these renormalization constants are kept equal such that the $\rho = 1$ relation is enforced at all order of perturbation theory when only pure scalar self interactions are present.

The presence of an accidental custodial symmetry can also be revealed by considering the 2×2 matrix representation of the complex Higgs doublet H , namely

$$M \equiv \begin{pmatrix} H^0 & H^+ \\ -(H^+)^* & (H^0)^* \end{pmatrix} . \quad (1.58)$$

Using this representation, the scalar potential can be conveniently rewritten

$$\mathcal{L}_S = \text{Tr}(\partial^\mu M^\dagger \partial_\mu M) - \mu^2 \text{Tr}(M^\dagger M) + \lambda \text{Tr}^2(M^\dagger M) \quad (1.59)$$

which is manifestly invariant under a global chiral $SU(2)_L \times SU(2)_R$ transformation

$$M \rightarrow M' = U_L M U_R^\dagger , \quad U_L \in SU(2)_L \quad \text{and} \quad U_R \in SU(2)_R \quad (1.60)$$

due to the cyclicity of the trace. Since the vacuum $\langle M \rangle = v\mathbb{1}/\sqrt{2}$ is invariant only if $U_L = U_R$, the $SU(2)_L \times SU(2)_R$ symmetry is spontaneously broken to its vectorial subgroup $SU(2)_V$. The link with the real representation case described above is straightforward to draw by identifying $SU(2)_L \times SU(2)_R/\mathbb{Z}_2$ with $SO(4)$ (the \mathbb{Z}_2 symmetry corresponding to a simultaneous change of sign for both left and right unitary matrices) and $SU(2)_V$ with $SO(3)$.

Contrary to the pure scalar part of the Lagrangian, both gauge and Yukawa interactions (if up and down-type fermions are not degenerate) break the custodial symmetry. A quadratic dependance in both heavy fermions and gauge bosons masses is then expected in the one loop corrections to the ρ parameter while the Higgs mass only appears in a logarithmic contribution. This important feature, i.e. the fact that apparently dominant corrections cancel out in physical observables in the presence of a custodial symmetry, has been referred by Veltman [25] as the screening phenomenon. As demonstrated by Einhorn and Wudka [26], this concept can be systematically generalised to higher order corrections. For example, the two-loop corrections to the ρ parameter only contains terms proportional to $m_{h^0}^2$ although there are diagrams proportional to $m_{h^0}^4$.

Top and Higgs contributions to $\Delta\rho$ in the SM

For the explicit details of the $\Delta\rho$ corrections at one loop in the Standard Model framework, the interested reader is kindly invited to consult the original works [21, 27, 28] or [29]. The final results for the top quark and Higgs boson contributions, in the large top and Higgs masses limit, read respectively :

$$\Delta\rho_{\text{top}} \approx \frac{3G_F}{8\sqrt{2}\pi^2} m_t^2 \quad (1.61)$$

$$\Delta\rho_{\text{Higgs}} \approx -\frac{3G_F}{8\sqrt{2}\pi^2} \tan^2 \hat{\theta}_W m_W^2 \log \frac{m_{h^0}^2}{m_W^2} \quad (1.62)$$

As expected from previous argument, the top contribution behaves quadratically while the Higgs contribution only grows logarithmically. Equations (1.48), (1.61) and (1.62) link the m_t , m_{h^0} , m_W and $\sin^2 \hat{\theta}_W$ parameters in a non trivial way. A global fit of all the available electroweak precision data then allows to constrain the Higgs mass range. The preferred value is $m_H = 76_{-24}^{+33}$ GeV, with a 95% CL upper limit $m_H < 144$ GeV, raised to $m_H < 182$ GeV once the direct LEP limit is included [30].

As emphasized in [31], there are however some mild reasons of concern with this constraint. The two most precise measurements of $\sin^2 \hat{\theta}_W$ do not agree very well, leading to conflicting predictions for the Higgs mass. The rather large value obtained from the $b\bar{b}$ asymmetry at LEP favors a relatively heavy Higgs ($m_{h^0} = 420_{-190}^{+420}$ GeV), while the $\sin^2 \hat{\theta}_W$ value extracted from the lepton left-right asymmetry at SLD is much smaller, leading to very light Higgs prediction ($m_{h^0} = 31_{-19}^{+33}$ GeV) in contradiction with the LEP bound. Moreover, the world average of the W mass is still significantly larger than the value extracted from a global SM fit, again requiring the Higgs boson to be lighter than the LEP limit. The current situation is shown on Figure 1.2, where the predicted values of m_{h^0} from different measurements are shown.

1.4.3 Direct searches at the LEP collider

The main production mechanism for the SM Higgs boson at LEP is the s -channel Higgs-strahlung, $e^+e^- \rightarrow h^0 Z$, where h^0 is radiated from a Z boson. The final state Z can be either virtual (like at LEPI) or on-shell (like at LEPII). The cross section of this process as a function of \sqrt{s} and m_{h^0} is shown on Figure 1.3. The Higgs boson can also be produced by W^+W^- fusion, but this process is clearly marginal, except for masses beyond the Higgs-strahlung reach.

For Higgs masses below 140 GeV, the decay into fermion pairs is dominant and the $h^0 \rightarrow b\bar{b}$ mode has the highest branching ratio if $m_{h^0} > 2m_b$. The $\tau^+\tau^-$, $c\bar{c}$ and gg decays are also present but contribute to less than 10% of the total rate. In this region, the decay width is typically of order 1 MeV, well below the best experimental precision. For higher masses, the W^+W^- and ZZ modes are dominant and the decay width grows quickly with m_{h^0} (potentially up to a non perturbative regime, see section 1.4.1). A summary plot of the main branching ratios as a function of the Higgs mass can be found on Figure 1.3.

Considering the main Higgs boson production and decay modes, the most interesting final state topologies for a Higgs mass around 100 GeV are:

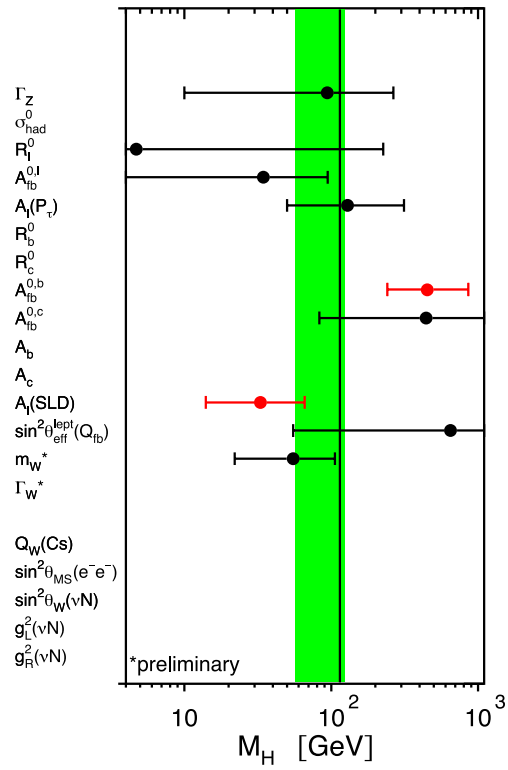


Figure 1.2: Values of the Higgs mass extracted from different electroweak observables. The average is shown as the green band. Predictions for which the central value is below 1 GeV or above 1 TeV with very large errors are not shown. The two extreme values discussed in the text appear in red. From Ref.[30].

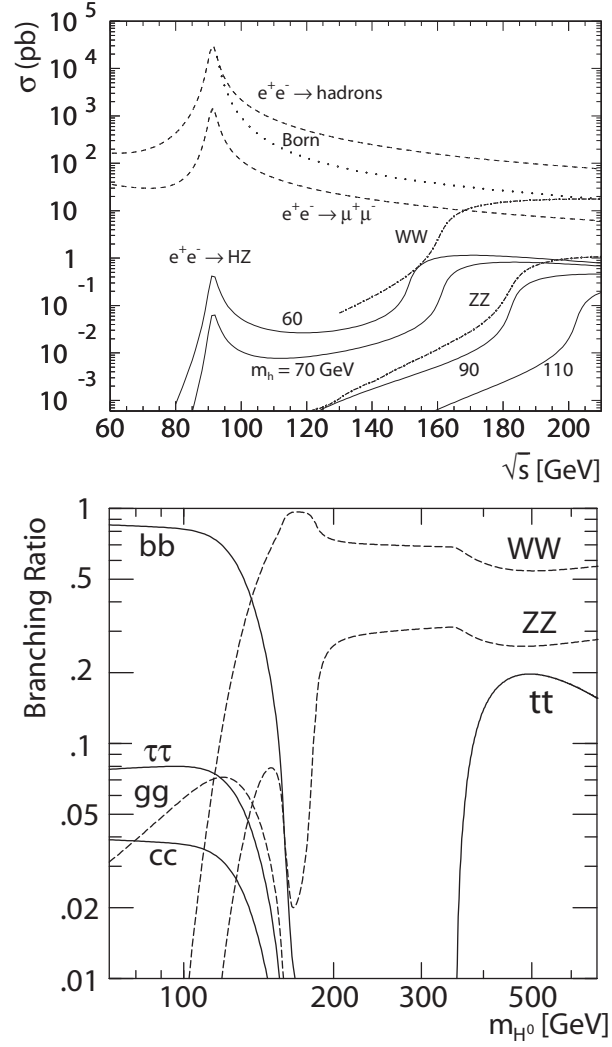


Figure 1.3: Top: Cross sections of the Higgs-strahlung production mechanism in e^+e^- collisions as a function of \sqrt{s} and m_{h^0} . The main background processes are also shown in dashed lines. Bottom: Branching ratios for the SM Higgs boson decay as a function of m_{h^0} . From Ref. [32].

- Four hadronic jets from $e^+e^- \rightarrow (h \rightarrow b\bar{b})(Z^0 \rightarrow q\bar{q})$. This important channel represents by itself 60% of the total branching ratio. The Higgs mass can be reconstructed with a precision of order 2.5 GeV.
- Missing transverse energy topology from $e^+e^- \rightarrow (h \rightarrow b\bar{b})(Z^0 \rightarrow \nu\bar{\nu})$. The “central” resolution is $\delta m_{h^0} \simeq 3$ GeV.
- Semi-leptonic topologies $e^+e^- \rightarrow (h \rightarrow b\bar{b})(Z^0 \rightarrow e^+e^-, \mu^+\mu^-)$. This channel has a rather small total branching ratio ($\simeq 6\%$) but has also a rather low background and a good energy resolution ($\delta m_{h^0} \simeq 1.5$ GeV).
- Topologies with τ^\pm leptons: $e^+e^- \rightarrow (h \rightarrow q\bar{q})(Z^0 \rightarrow \tau^+\tau^-)$ or $e^+e^- \rightarrow (h \rightarrow \tau^+\tau^-)(Z^0 \rightarrow q\bar{q})$.

At the LEP I experiment, only topologies with missing transverse energy and semi-leptonic final states were considered, due to their relatively low background. At the LEP II experiment, all topologies have been considered. The final result is an exclusion at a 95% confidence level of a Standard Model Higgs boson with a mass lower than 114.4 GeV [33].

1.4.4 Direct searches at the Tevatron collider

The Tevatron machine being a proton/anti-proton collider, the main production mode appears to be the direct production by gluon fusion (through a top quark loop) (see Figure 1.4). It is followed by the associated production with a gauge boson and the W^+W^- fusion process. However, regarding the backgrounds associated with the decay modes described in the previous section and the expected total integrated luminosity of the Tevatron (Run II), the Higgs-strahlung production with $h^0 \rightarrow b\bar{b}$ (or possibly $h^0 \rightarrow WW^*$) is the most promising discovery channel for $m_{h^0} \lesssim 150$ GeV. For higher masses, the direct production $gg \rightarrow h^0$ followed by a $h^0 \rightarrow W^+W^-$ decay also appears to be a competitive mode.

At the time of this work, the total integrated luminosity collected at the Tevatron collider is not yet sufficient to exclude a Standard Model Higgs boson at masses higher than the LEP II limit. Current data are used to put limits on the ratios to the expected SM cross sections as a function of the Higgs mass. The latest available results are shown on Figure 1.5. With an expected total luminosity of $\sim 5 \text{ fb}^{-1}$ by the end of the data acquisition phase, the Tevatron experiments should, in principle, be able to discover or exclude the SM Higgs in the $m_{h^0} \approx 160$ GeV mass region.

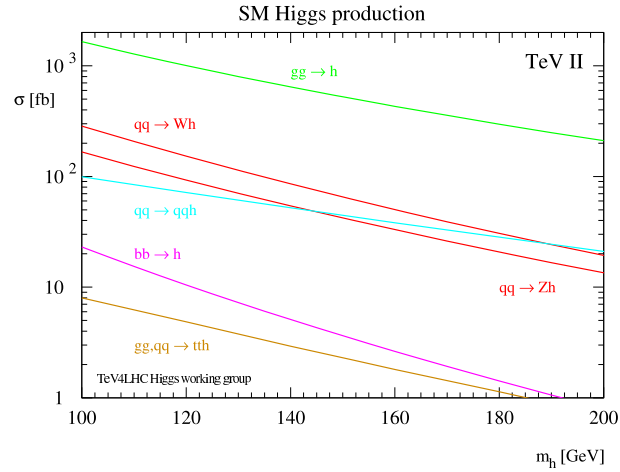


Figure 1.4: Summary of the best available estimations of the Standard Model Higgs boson production cross section at the Tevatron (Run II) as a function of its mass. From the TeV4LHC working group [34].

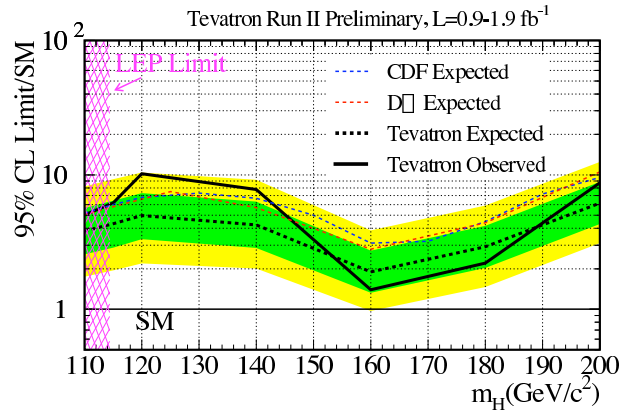


Figure 1.5: Observed and expected (median, for the background-only hypothesis) 95% C.L. upper limits on the ratios to the SM cross section, as functions of the Higgs test mass, for the combined CDF and D0 analyses. From Refs. [35]

1.4.5 Direct searches at the Large Hadron Collider

The principal SM Higgs boson production cross sections at the LHC are summarized on Figure 1.6. Whereas the main production mode is still the gluon fusion process

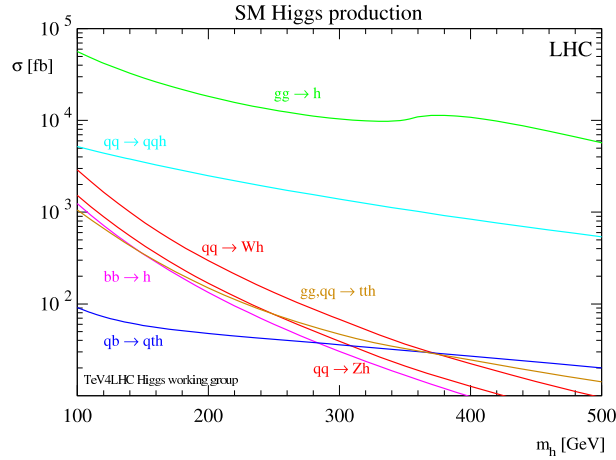


Figure 1.6: Summary of the best available estimations of the Standard Model Higgs boson production cross section at the LHC as a function of its mass. From the TeV4LHC working group [34].

like for the Tevatron, the gauge boson associated production is suppressed due to the absence of valence anti-quarks in the proton. The weak boson fusion replaces it as the second most important production mode on in the whole mass range. Other production mechanisms, e.g. in association with heavy quarks, have also sizable cross sections and could play a role in the study of the Higgs boson properties.

Depending on its mass, the Higgs boson first discovery channels at the LHC will be different. In the very low mass region, i.e. $m_{h^0} \lesssim 130$ GeV, the $gg \rightarrow h^0 \rightarrow \gamma\gamma$ process is probably the only viable discovery mode but suffers from a very reduced rate and a large background. In the mid-range region, i.e. from 130 GeV to 180 GeV, the $gg \rightarrow h^0 \rightarrow WW^*/WW \rightarrow l^+l^-\nu\bar{\nu}$ channel turns out to be the best alternative by offering a sizable rate together with good background rejection possibilities. Finally, above the $2m_Z$ threshold, the “gold-plated” mode $gg \rightarrow h^0 \rightarrow ZZ \rightarrow 4l$ should allow for Higgs detection up to masses of order 1 TeV. On the whole mass range, alternative processes can also play a role. Among others, the $t\bar{t}$ associated production (for low masses) and the weak boson fusion can be mentioned. Figure 1.7 summarizes the

expected significance of each channel in the CMS detector with a 30 fb^{-1} integrated luminosity.

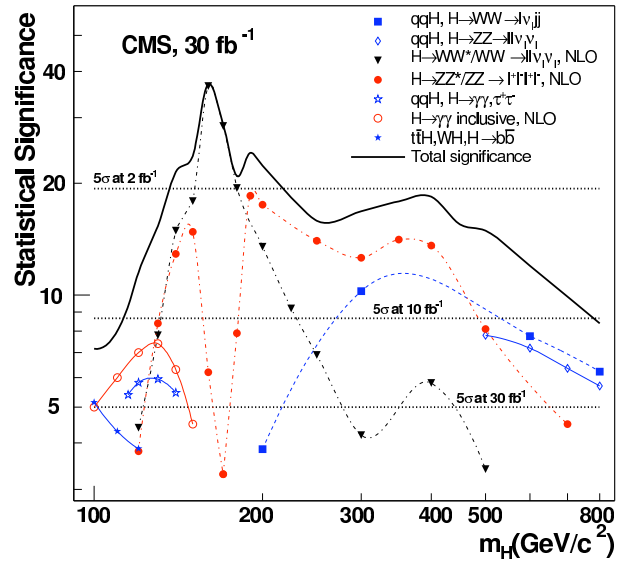


Figure 1.7: CMS discovery potential for the SM Higgs boson in the whole mass range. From Ref. [36].

Chapter 2

Extended scalar sectors

“If you are out to describe the truth, leave elegance to the tailor.”

Albert Einstein (1879-1955)

In this chapter, the theoretical motivations and implications of Standard Model scalar sector extensions are reviewed. The simplest of these extensions, namely the two-Higgs-doublet model (2HDM), is described into more details. After depicting the most general realization of this model, the principal aspects related to the custodial, CP and Z_2 symmetries are considered. The interplay between these global symmetries, and the possibility to define a “twisted” scenario satisfying naturally electroweak precision constraints are particularly emphasised.

2.1 Motivations

The scalar sector of the Standard Model described in section 1.3.2 is “minimal” in the sense that the associated Higgs representation (i.e., a single $SU(2)_L$ doublet) is the simplest possibility allowing for non vanishing mass terms for weak bosons and fermions after spontaneous symmetry breaking. Indeed, it is the smallest representation containing the three would-be Goldstone real fields associated with the three massive gauge bosons and the Higgs scalar required to trigger the spontaneous symmetry breaking mechanism. Nevertheless, more complex possibilities involving additional and/or larger representations may *a priori* be considered. Motivations for

such enlarged Higgs sectors are varied, but in general they fall into two (not mutually exclusive) categories. They can be associated with requirements of higher scale symmetries, like Supersymmetry or Grand Unification groups, or they can be justified by phenomenological arguments, like the possibility of new sources of CP violation needed, for example, to explain the matter predominance over anti-matter.

2.1.1 Higher symmetries

Supersymmetry

Supersymmetric (SUSY) theories are build on the assumption that fermionic and bosonic fields can be related through a non trivial extension of the Poincaré group. These theories share different advantages, the most important being undoubtedly their ability to solve the so-called “naturalness” problem. In the Standard Model, when radiative corrections to the Higgs mass are computed and the loop integral momenta cut off at a scale Λ , one has

$$m_{h^0}^2 = (m_{h^0}^0)^2 + \frac{3\Lambda^2}{8\pi^2 v^2} (m_{h^0}^2 + 2m_W^2 + m_Z^2 - 4m_t^2) \quad (2.1)$$

where $m_{h^0}^0$ is the Higgs bare mass. The amount of fine tuning required to get a physical Higgs mass of the order of the electroweak scale then grows quadratically¹ with Λ . Though the theory is still perfectly consistent in the absence of any physical meaning for the higher scale Λ , this provides a strong argument in favor of new Physics beyond the Standard Model.

In a supersymmetric theory, each SM particle comes with its superpartner of opposite statistic. Since fermions and bosons give loop contributions of opposite signs, the cutoff dependence in (2.1) exactly vanishes in the limit of exact SUSY. Of course, in realistic theories, the superpartners cannot be degenerate with their associated SM particles since they escaped all experimental detection attempts. Nevertheless, SUSY could be realized at the TeV scale so that the electroweak scale remains stabilized at higher scales. In the limited context of the present work, the complete theory associated with the supersymmetric extensions of the Standard Model is not detailed and the interested reader is invited to consult classical reviews like [38] for further references.

In the Minimal Supersymmetric Standard Model (MSSM), a minimum of two Higgs weak doublets, belonging to two different chiral supermultiplets, are required for the following reasons:

¹The Higgs mass can be chosen such that the second term of (2.1) exactly vanishes [37], but this cancellation can only be arranged at a fixed order in the perturbative expansion.

1. *Structure of the Yukawa couplings:* as seen from (1.30), in usual, non supersymmetric theories, a scalar doublet $Y = +1$ is equivalent to a $Y = -1$ doublet through C conjugation. In a supersymmetric theory, this is not true anymore since each doublet is forced to belong to a chiral supermultiplet which also includes a fermion multiplet of fixed chirality. Non vanishing mass terms for the up-type quarks then require the introduction of a new weak doublet with $Y = -1$ in the theory².
2. *Gauge anomaly cancelation:* In the SM, the $\text{Tr}(Y^3) = 0$ and $\text{Tr}((I^3)^2 Y) = 0$ conditions³ associated with triangular gauge anomalies cancelation are fulfilled through a somewhat mysterious conspiracy between quarks and leptons quantum numbers. The fermionic superpartner of the Higgs doublet being also a $Y = 1$ weak doublet, it would spoil that cancelation. A minimal solution is to add a second Higgs supermultiplet with $Y = -1$, in order to compensate for this extra contribution.

The explicit form of the MSSM scalar potential for the two Higgs doublets can be derived from first SUSY principles. It appears to be a special case of the more general two-Higgs-doublet model and is considered in section 2.5.

Although it provides a natural solution to stabilize the Higgs mass in the Standard Model, the MSSM also has its own drawbacks. The so called μ -problem, for example, corresponds to an unnatural fine tuning of the dimensional parameter μ appearing in F terms of the MSSM superpotential (see section 2.5). Since this parameter appears in the SUSY conserving part of the Lagrangian, its value is not expected to be related to the weak scale, contrary to what is required by phenomenological considerations.

Among all the possible scenarios proposed to solve the μ -problem, a particularly interesting and simple one is the Next to Minimal Supersymmetric Standard Model (NMSSM). In this model, the μ parameter is replaced by a dimensionless coupling λ multiplied by the vacuum expectation value $\langle S \rangle$ of a new scalar singlet under $SU(2)_L$. This new scale is in turn related to the SUSY breaking scale through minimization conditions, therefore removing the need for fine tuning. This model displays an interesting phenomenology which is not covered in the present work (e.g. see [40] for a recent overview), except for its light pseudoscalar signature $h^0 \rightarrow A^0 A^0$ which is considered for comparison in section 4.2.

²An original alternative solution [39] would be to consider a left handed slepton-lepton chiral supermultiplet as the $Y = -1$ Higgs-Higgsino supermultiplet. Unfortunately, this choice leads to unwanted phenomenological consequences like lepton number violation and a large mass for at least one neutrino.

³Here the trace runs over all left handed Weyl fermionic degrees of freedom.

Grand Unified Theories

Grand Unified Theories (GUTs) achieve by construction the ambitious aim of unifying strong and electroweak gauge interactions in a non-abelian gauge theory based on a single compact Lie group \mathcal{G} including the Standard Model group $SU(3)_C \times SU(2)_L \times U(1)_Y$. Several choices for \mathcal{G} have been considered all over the years, from the simplest Georgi-Glashow model [41] based on $SU(5)$ to E_6 models which arise naturally, for example, in the context of the $E_8 \times E_8$ heterotic string theory.

In general, all GUTs display the same kind of interesting features including gauge couplings unification at very high energy (leading to the well-known value $\sin^2 \theta_W = 3/8$ in $SU(5)$ [41]) and predictions for low energy observables like the Georgi-Jarlskog mass relations [42]. Due to the presence of new very massive gauge bosons, they also allow, in general, the proton decay. In order to achieve the breaking of \mathcal{G} to the SM group, different and often complicated Higgs representation are required. In general, this implies the presence of an extended scalar sector at the electroweak scale (e.g., a two-Higgs-doublet model in $SO(10)$).

But GUTs have also an important drawback, which is in essence very similar to the MSSM μ -problem. It arises due to the phenomenological need for a huge hierarchy between the high scale at which the original GUT group is broken down to the SM group, and the electroweak scale. This technical difficulty is sometimes referred to as the “doublet-triplet splitting” fine tuning problem since the GUT Higgs sector typically contains color singlet (weak doublet) and color triplet scalars. The former play the role of the SM Higgs and are then associated to the electroweak scale while the latter are required to fill up the GUT Higgs representation and must be extremely massive ($\sim M_{\text{GUT}}$) to satisfy experimental constraints on the proton lifetime.

A potential solution to the doublet-triplet splitting problem in the framework of $SO(10)$ theories (which are arguably the most natural ones nowadays) is known as the “Dimopoulos-Wilczek” mechanism [43]. It is based on a particular arrangement of the vacuum expectation values directions for the field responsible for the spontaneous breaking of the GUT symmetry, such that the VEV responsible for the color singlet masses and the one responsible for the color triplet masses are unrelated. The former can then be safely set to zero to naturally solve the hierarchy problem.

Little Higgs Theories

The essential idea behind Little Higgs (LH) theories [44, 45, 46] is to naturally solve the Standard Model naturalness problem by considering the Higgs as a pseudo-Goldstone boson of some approximate (spontaneously broken) global symmetries, exactly like

the pion in the chiral symmetry approach of QCD. The new particles introduced to ensure these symmetries are not broken too severely are precisely the states that cut off the quadratically divergent loop corrections to the Higgs mass.

In the simplest LH model [47], an $SU(3)$ group is broken to its subgroup $SU(2)_L$ and the four degrees of freedom associated with the SM Higgs doublet are part of the five pseudo-Goldstone bosons associated with the breaking⁴. The remaining degree of freedom corresponds to a real scalar field η , singlet under $SU(2)_L$, with a mass of order of the electroweak scale. So, even in the simplest cases, LH theories tend to predict an extension of the SM scalar sector. For more complex, and more realistic, scenarios, like the Minimal Moose [48] based on the coset $[SU(3)_L \times SU(3)_R/SU(3)_V]$ ⁴ or models with an additional custodial symmetry [49], the presence of two light Higgs doublets is a common feature. In general, these theories also predict a heavy fermionic state T , required to compensate the top quark loop contribution to the Higgs mass and to trigger the SSB of the electroweak symmetry *via* a Coleman-Weinberg mechanism [50].

2.1.2 Phenomenological aspects

New sources of CP violation

Besides being an interesting phenomenon by itself, due to its theoretical and experimental elusiveness, CP violation (see [51] for a general review) also plays a crucial role in cosmology. As shown by Sakharov [52], it is indeed a necessary ingredient to understand the genesis of the observed baryon asymmetry of the Universe, i.e. the overabundance of matter compare to antimatter. Another interesting consequence of CP violation would be the possibility for elementary particles to have a sizeable electric dipole moment. Indeed, electric dipole moments violate both P and T symmetries such that any attempt to introduce them without violating CP would imply a failure of the CPT theorem.

Even if CP violation arises in the Standard Model through a single non vanishing complex phase in the CKM matrix, it is by now clear that this mechanism cannot account by itself for the observed baryon asymmetry. The first reason is the fact that the electroweak phase transition is not strongly first order and, as a result, any baryon asymmetry generated during the transition would be subsequently washed out by B -violating processes in the broken phase [53]. The second reason is that the

⁴In fact, the requirement of SM-like $SU(2)_L$ interactions for the Higgs doublet together with vanishing quadratic divergences from gauge boson loops leads to a more complex picture. The $SU(3)$ global symmetry should be gauged and an additional set of Goldstone bosons has to be introduced to provide longitudinal degrees of freedom for the new gauge fields.

CP violating effects associated with the three generations CKM matrix are too small [54, 55].

Extensions of the SM scalar sector may provide a solution to this problem. In Multi-Higgs-doublet models (MHDMs), for example, the CP symmetry can be violated in the scalar sector, both explicitly and spontaneously (see for example [56]). It must be noted, however, that the requirement of Natural Flavour Conservation (NFC) (guaranteed by an additional reflection symmetry) restricts the possibilities for CP violation. Under this constraint, the two-Higgs-doublet only allows for explicit CP violation while the spontaneous breaking of this symmetry requires at least three Higgs doublets [57].

Strong CP problem

The strong CP problem is a side effect of the solution proposed by 't Hooft [58] to solve the $U(1)_A$ problem in QCD through the inclusion of topological effects called instantons. As shown by 't Hooft, the QCD Lagrangian must include a term

$$\mathcal{L}_\theta = \theta_{QCD} \frac{g_s^2}{32\pi^2} G^{a\mu\nu} \tilde{G}_{\mu\nu}^a \quad (2.2)$$

where $\tilde{G}_{\mu\nu}^a$ is the dual of the QCD field strength tensor and θ_{QCD} a free parameter. This term violates both P and T symmetries, and θ_{QCD} cannot be set to zero by hand by imposing the CP symmetry in the strong sector because it receives contribution from the weak sector, i.e.

$$\theta_{QCD} \rightarrow \bar{\theta} \equiv \theta_{QCD} + \theta_{EW} \quad (2.3)$$

where

$$\theta_{EW} = \arg \det(m_u m_d) \quad (2.4)$$

Since θ_{EW} is $\mathcal{O}(1)$ in the SM, and since there is *a priori* no link between θ_{QCD} and θ_{EW} , the resulting observable $\bar{\theta}$ is also expected to be $\mathcal{O}(1)$. However, experimental data on the neutron electric dipole moment [59] put a very strong constraint on this parameter, namely

$$\bar{\theta} \lesssim 10^{-10} \quad (2.5)$$

This serious fine tuning problem in the SM is known as the ‘‘strong CP problem’’.

Various solutions to this issue have been proposed, e.g. like considering the up quark to be massless⁵ such that $\bar{\theta}$ can be rotated out through a chiral transformation. Another

⁵This possibility is however excluded [60, 61] by the value of the m_u/m_d mass ratio extracted using chiral perturbation theory [62].

kind of solution, proposed by Peccei and Quinn [63], involves a new global chiral symmetry $U(1)_{PQ}$ under which the quarks and the Higgs multiplet(s) transform non-trivially. The parameter $\bar{\theta}$ becomes a dynamical variable (i.e. is associated to a field), and can be set dynamically to zero.

In order to provide this additional degree of freedom, the SM scalar sector must be extended, e.g. to a two-Higgs-doublet model. One of the new fields, named the axion a^0 , is the Goldstone boson associated with the breaking of the $U(1)_{PQ}$ symmetry. It acquires a small mass $m_{a^0} \approx f_\pi m_\pi / F$ due to the breaking of $U(1)_{PQ}$ at a high scale F . Such a very light (pseudo)scalar has been intensively searched without success by various experiments. The original Peccei-Quinn model (where $F \sim \Lambda_{EW}$ and $m_{a^0} \approx 100$ keV) is ruled out most easily by the non observation of the $K^\pm \rightarrow \pi^\pm a^0$ decay, while higher scales are excluded up to $F \gtrsim 10^9$ GeV by indirect arguments based on axions emitted by the sun, by HB stars and by supernovae. Note that model dependent cosmological limits on the axion lifetime also put an *upper* bound on F , around 10^{12} GeV, if inflation occurs at higher energy.

Fermions mass spectrum

The apparent lack of symmetry in the fermions mass spectrum is definitively one of the unsatisfying feature of the Standard Model. Since this spectrum is directly related to the Yukawa couplings between the Higgs field and the fermion multiplets, and these couplings being in turn completely arbitrary, there are unfortunately not so much theoretical “handles” in the SM itself to solve this issue.

A pragmatic approach to answer this question is the description of fermion mass “textures” using discrete or continuous underlying horizontal symmetries. Implementing these symmetries in a natural way at the Lagrangian level often requires extensions of the SM scalar sector, typically with additional Higgs doublets.

For example, the Koide non-linear mass relation

$$\sum_i m_i = \frac{2}{3} \left(\sum_i \sqrt{m_i} \right)^2 \quad (2.6)$$

where i is a generation indices, works surprisingly well for charged leptons [64, 65] but possibly also for quarks and neutrinos when weak mixing parameters are taken into account [66].

Relation (2.6) is quadratic with respect to the square root of the masses, and it is better satisfied at energies of the order of the electroweak scale. This suggests (see [67] and reference therein) that it could be related to the vacuum expectation values v_i of

3 Higgs-doublets ϕ_i through a seesaw like mechanism $m_i \propto v_i^2/V$. Relation (2.6) is then obtained from an internal S_3 permutation symmetry of the scalar potential ensuring

$$\sum_i v_i^2 = \frac{2}{3} \left(\sum_i v_i \right)^2 . \quad (2.7)$$

Dark matter

All modern astrophysical (galactic halo, ...) and cosmological observations use to agree not only on the presence of a sizable amount of Dark (i.e. non shining) Matter (DM) in the Universe, but also on the fact this new kind of matter is not made of ordinary atoms [68, 69]. Over the years, the exact nature of DM has become one of the most important question at the frontier of contemporary cosmology, astrophysics and particle physics. A popular hypothesis identifies the Lightest Supersymmetric Particle (LSP), in most cases a neutralino or a gravitino, as a good DM candidate since R -parity (which is in fact not predicted by SUSY itself) forbids its decay and makes it stable.

Recently, a simple, yet interesting, model for DM requiring a two-Higgs-doublet extension of the SM scalar sector has been proposed [70, 71, 72]. The main feature of this model, called the Inert Doublet Model (IDM), is a Z_2 symmetry

$$H_1 \rightarrow H_1 \quad , \quad H_2 \rightarrow -H_2 \quad (2.8)$$

which remains unbroken after SSB by enforcing $\langle H_2^0 \rangle = 0$ thanks to a positive mass term $\mu_2 > 0$. Assuming all the SM particles have an even Z_2 parity, the lightest neutral (pseudo)scalar (either H^0 or A^0) becomes stable and appears as an archetype candidate for Dark Matter.

A systematic analysis of the DM abundance and of the potentialities for direct and gamma indirect detection in this model is presented in [73]. The main conclusion is that the IDM dark matter candidate fiercely competes with the neutralino. This Weakly Interacting Massive Particle (WIMP) has a rich phenomenology and has a true potential for being constrained by DM detection experiments. The observed DM relic density can be reproduced in two regimes, i.e. for low ($\lesssim 100$ GeV) and high ($\gg 100$ GeV) masses. Prospects for direct detection of this kind of particle at the LHC have also been considered more recently in [74] and a light WIMP scalar (~ 50 GeV) appears to be detectable in invisible Higgs decays.

The IDM also allows for a slight improvement of the naturalness problem [71] by rising the SM Higgs mass up to ~ 600 GeV, i.e. close to the triviality limit (see Figure

1.1). Such an heavy SM Higgs could remain compatible with electroweak precision tests thanks to the additional contributions of the new scalars belonging to the inert doublet. This interesting feature can in fact be shared by many 2HDM scenarios (see [75, 76]) and is discussed into more details in section 3.2.1.

Neutrino masses

There is now convincing experimental evidence that, at variance with the SM prediction, neutrinos produced in solar, atmospheric and reactor processes change from one flavor to the other (see [5] for a review). Barring exotic possibilities, this in turns implies that neutrinos have small but non zero masses and that leptons mix. In the well known (type-I) seesaw mechanism, heavy right-handed Majorana neutrinos are introduced to naturally generate small neutrino masses.

Besides the type-I seesaw scenario, the triplet seesaw mechanism (sometimes refer to as type-II seesaw), which extends the SM with one scalar triplet ξ^a ($a \in \{1, 2, 3\}$) with $Y = 2$, gives another possible explanation to the smallness of neutrino masses. If the scalar triplet gets its mass after a SSB mechanism, the associated non zero VEV is strongly constrained by the ρ parameter (see section 2.2.1) and a massless Goldstone boson appears, the so-called ‘‘Majoron’’. The latest being excluded by the LEP measurement of Z invisible decay, this possibility is not considered here. The Yukawa potential of the model reads [77]

$$\mathcal{L} = \lambda_\xi^{ij} L_L^i \epsilon \tau^a L_L^j \xi^a + \lambda_H M_\xi H \epsilon \tau^a H \xi^a \quad (2.9)$$

where ϵ is the permutation matrix and τ^a the usual $SU(2)_L$ generators. Integrating out the heavy ξ triplet generates the effective Majorana mass operator ($L_L L_L H H$) leading to a Majorana mass term $m_L^{ij} = \lambda_\xi^{ij} \lambda_H / M_\xi^2$ for leptons after electroweak symmetry breaking. The main interest of this mechanism is that it requires a smaller number of unknown flavor parameters than models involving extra singlets or triplets of Majorana fermions.

2.2 Generic extensions

As mentioned in the previous section, there are many well motivated reasons to consider various type of SM scalar sector extensions involving additional doublets, singlets or even triplets. Before describing into more details the most common option, i.e. the two-Higgs-doublet model, two important consequences of generic extensions are reviewed.

2.2.1 Tree-level ρ parameter value

The ρ parameter defined in (1.48) is a sensible quantity with respect to the Higgs sector structure. As mentioned in section 1.4.2, in the context of the SM Higgs boson phenomenology, the one loop corrections to this parameter value involve the Higgs mass and can be used to put constraints on it. Yet, even the tree-level value of this parameter can be modified by the presence of additional scalar fields developing VEVs.

As shown in [78], the tree-level value of ρ can be easily computed for any set of complex scalar multiplets with neutral VEV v_i , $SU(2)_L$ isospins I_i , and hypercharges Y_i . Using (1.10) and a development similar to section 1.3.2, one easily obtains the tree-level values

$$\begin{aligned} m_Z^2 &= (g_L^2 + g_Y^2) \sum_i v_i^2 \frac{|Y_i|^2}{4} \\ m_W^2 &= \frac{g_L^2}{2} \sum_i v_i^2 \left(I_i(I_i + 1) - \frac{|Y_i|^2}{4} \right) \end{aligned} \quad (2.10)$$

such that⁶

$$\rho = \frac{\sum_i v_i^2 (4I_i(I_i + 1) - |Y_i|^2)}{2 \sum_i v_i^2 |Y_i|^2} . \quad (2.11)$$

Assuming the actual values of the VEVs v_i are unrelated, and that each numerator contribution is compensated by an identical contribution in the denominator, the $\rho \approx 1$ requirement translates as

$$(2I_i + 1)^2 - 3Y_i^2 = 1 \quad \forall i. \quad (2.12)$$

Since I_i and Y are respectively half-integer and integer numbers, this equation has only a discrete set of solutions (I_i, Y) , among which $(0, 0)$ (neutral singlets) and $(1/2, \pm 1)$ (SM-like doublets) are the most evident choices. Other possibilities are generally discarded since the associated representations are rather complicated (the simplest example is a $Y = 4$ $SU(2)_L$ septuplet).

The previous argument tends to exclude any model involving triplet Higgs representation, like the one required by the type-II seesaw mechanism for neutrino masses (see section (2.1.2)) or by Left-Right symmetric models [79, 80, 81]. This restriction can in fact be circumvented by two means. Either the vacuum expectation value of the additional triplet(s) is very small compare to the usual SM doublet VEV so that the

⁶In case of real representations with $Y = 0$, the denominator of this expression comes with an extra factor of two.

associated tree-level contribution to ρ is suppressed⁷, either a specific arrangement of the additional representations together with the associated VEV leads to an exact compensation of the new contributions. A well known example [1] of such an arrangement is the combination of one $Y = 1$ complex doublet with VEV v_d , one real $Y = 0$ triplet and one $Y = 2$ complex triplet with *the same* VEV v_t (e. g. because of an additional custodial symmetry in the potential). One then has

$$\rho = \frac{2|v_d|^2 + 4|v_t|^2 + 4|v_t|^2}{2|v_d|^2 + 8|v_t|^2} = 1 \quad . \quad (2.13)$$

2.2.2 Gauge coupling constants unification

Since extended scalar sectors contain new heavy particles which may couple to the SM gauge boson, the RGE associated with the gauge coupling constants α_i

$$\alpha_1(M_Z) = \frac{5}{3} \frac{\alpha(M_Z)}{\cos^2(\theta_W)}, \quad \alpha_2(M_Z) = \frac{\alpha(M_Z)}{\sin^2(\theta_W)} \quad \text{and} \quad \alpha_3(M_Z) = \alpha_s(M_Z) \quad (2.14)$$

are in general modified⁸. These equations read

$$\mu \frac{d\alpha_i(\mu)}{d\mu} = \beta(\alpha_i) \quad (2.15)$$

where μ is an arbitrary energy scale and $\beta(\alpha_i)$ is the Callan-Symanzik function which can be expanded in the perturbative regime

$$\beta(\alpha_i) = \frac{1}{2\pi} \sum_{n \geq 1} (b_n)_i \alpha_i^{n+1} \quad . \quad (2.16)$$

At one loop, (2.15) becomes

$$\frac{d\alpha_i(\mu)}{d\mu} = \frac{b_i}{2\pi} \frac{\alpha_i^2}{\mu} \quad (2.17)$$

and has the solution

$$\alpha_i^{-1}(\mu) = \alpha_i^{-1}(\mu_0) - \frac{b_i}{2\pi} \ln \frac{\mu}{\mu_0}. \quad (2.18)$$

The b_i coefficients can be computed using [84]

$$b_i = -\frac{11}{3} C(G_i) + \frac{2}{3} T(R_i^f) + \frac{1}{6} T(R_i^s) \quad (2.19)$$

where

⁷Assuming the presence of only one Higgs triplet, a limit of 0.01 to 0.1 (depending on Y) for $v_{\text{triplet}}/v_{\text{doublet}}$ can be derived from experimental data [82, 83].

⁸The hypercharge normalization is fixed such that $\text{Tr}(Y^2) = 2$.

- $C(G)$ is the quadratic Casimir associated with the gauge group G , i.e.

$$C(G)\delta^{AB} = \sum_{C,D} f^{ACD} f^{BCD}, \quad (2.20)$$

where f^{ABC} are the structure constants of the group

- $T(R)$ is associated to the representation R with generators T_R^A , under which the fermions (R^f) and real scalar fields (R^s) transform, through

$$T(R)\delta^{AB} = \text{Tr}(T_R^A T_R^B). \quad (2.21)$$

In the case of a general extension of the SM scalar sector involving scalar singlets, doublets and triplets (up to $Y = 4$), these coefficients read

$$\begin{aligned} b_1 &= 4 + \frac{1}{10}(2N_{0,2} + 8N_{0,4} + N_{1/2,1} + 9N_{1/2,3} + 6N_{1,2}) \\ b_2 &= -\frac{10}{3} + \frac{1}{6}(N_{1/2,1} + N_{1/2,3} + 4(N_{1,0} + N_{1,2})) \\ b_3 &= -7 \end{aligned} \quad (2.22)$$

where $N_{I,Y}$ gives the number of representations with the weak-isospin I and hypercharge Y . The coupling constants evolution in different models is illustrated on Figure 2.1.

It turns out that, for some specific combinations, the poor coupling constant unification observed in the SM can be improved [85, 86]. The typical unification scale M_U obtained in these models is lower than comfortable (to say the least) for the proton decay (see Table 2.1) but this needs not be a problem if the coupling constant unification is not associated with true group unification. Simple solutions imply the presence of additional triplets (with small or vanishing VEVs to guarantee $\rho = 1$ at tree-level, see previous section) while achieving coupling constant unification in a multi-Higgs-doublet model require at least seven doublets. As noted in [86], this conclusion may however be circumvented if the number of colors N increases with the energy. For $N = 7$, it can even be realized with a single Higgs doublet.

2.3 The general two-Higgs-doublet model

Following the conclusions of sections 2.1 and 2.2.1, the two-Higgs-doublet model (2HDM) appears as an interesting, simple yet natural, starting point for studying the

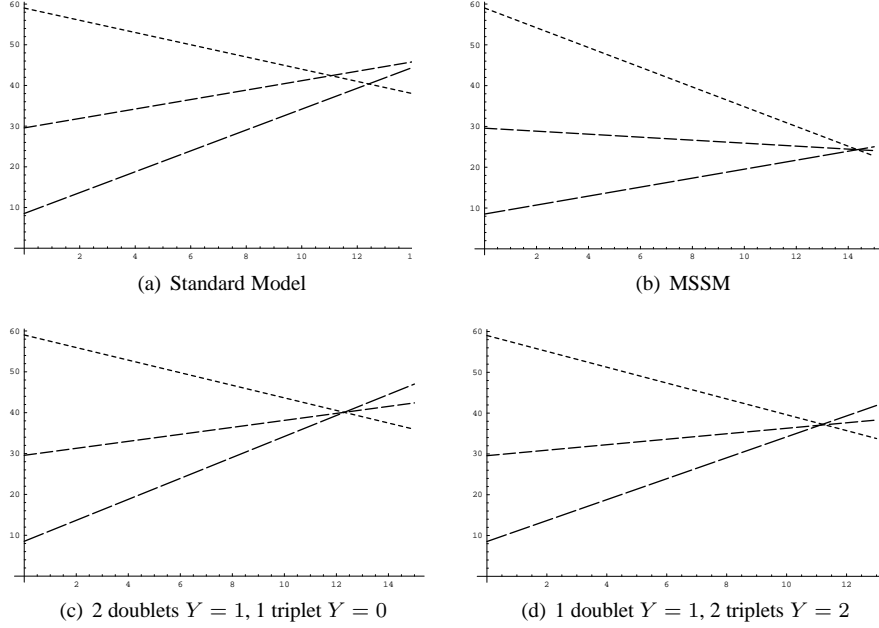


Figure 2.1: Examples of α_1^{-1} , α_2^{-1} and α_3^{-1} (from top to bottom) evolution with respect to $\log(\mu/m_Z)$ for different scalar sector contents.

phenomenological impact of extending the SM scalar sector. In this section, the properties of the most general, unconstrained model are reviewed before introducing more specific realizations.

2.3.1 Potential in a generic basis

Consider a 2HDM based on two $SU(2)_L$ doublets ϕ_1 and ϕ_2 with same hypercharge $Y = +1$. Gauge invariance allows us to define four hermitian operators

$$\begin{aligned}
 \hat{A} &= \phi_1^\dagger \phi_1 \\
 \hat{B} &= \phi_2^\dagger \phi_2 \\
 \hat{C} &= \text{Re}(\phi_1^\dagger \phi_2) = \frac{1}{2}(\phi_1^\dagger \phi_2 + \phi_2^\dagger \phi_1) \\
 \hat{D} &= \text{Im}(\phi_1^\dagger \phi_2) = -\frac{i}{2}(\phi_1^\dagger \phi_2 - \phi_2^\dagger \phi_1)
 \end{aligned} \tag{2.23}$$

$N_{0,2}$	$N_{0,4}$	$N_{1/2,1}$	$N_{1,0}$	$N_{1,2}$	$\alpha_s(M_Z)$	M_U (GeV)
0	0	1	0	2	0.121	1.7×10^{13}
0	0	2	1	0	0.117	1.8×10^{14}
0	0	4	0	1	0.117	2.8×10^{13}
0	1	3	1	0	0.113	4.6×10^{13}
1	0	3	1	0	0.122	1.0×10^{14}
1	1	1	1	1	0.121	1.7×10^{13}
0	0	1	0	0	0.071	1.1×10^{13} (SM)
0	0	2	0	0	0.117	2.0×10^{16} (MSSM)
0	0	7	0	0	0.113	4.6×10^{13} (7HDM)

Table 2.1: Models with less than five additional multiplets such that $\alpha_s(m_Z) \in [0.105, 0.125]$ (extracted from the requirement of exact unification) and $M_U > 10^{13}$ GeV. Here $\alpha^{-1}(m_Z) = 128.91$ and $\sin^2 \theta_W(m_Z) = 0.2311$. SM, MSSM and a model with seven doublets are shown for reference.

such that the most general renormalisable scalar potential contains fourteen (four linear and ten quadratic) terms

$$V(\phi_1, \phi_2) = -m_1^2 \hat{A} - m_2^2 \hat{B} - m_3^2 \hat{C} - m_4^2 \hat{D} + \lambda_1 \hat{A}^2 + \lambda_2 \hat{B}^2 + \lambda_3 \hat{C}^2 + \lambda_4 \hat{D}^2 \\ + \lambda_5 \hat{A} \hat{B} + \lambda_6 \hat{A} \hat{C} + \lambda_7 \hat{A} \hat{D} + \lambda_8 \hat{B} \hat{C} + \lambda_9 \hat{B} \hat{D} + \lambda_{10} \hat{C} \hat{D} \quad (2.24)$$

The potential being hermitian, the m_i^2 and λ_i parameters are restricted to be real numbers.

Let us assume from now that the vacuum respects the electromagnetic gauge symmetry, i.e. that the vacuum expectation values of ϕ_1 and ϕ_2 are aligned in the $SU(2)_L$ space such that a single $SU(2)_L$ gauge transformation suffices to rotate them to the neutral components. This phenomenologically motivated assumption is in fact rigorously justified in the context of the restricted CP conserving models to be considered in the following sections (e.g. see [87, 88]). After a suitable $U(1)_Y$ transformation to set the phase of the vacuum expectation value of ϕ_1^0 to zero, one has

$$\langle \phi_1 \rangle = \frac{1}{\sqrt{2}} \begin{pmatrix} 0 \\ v_1 \end{pmatrix} \quad \text{and} \quad \langle \phi_2 \rangle = \frac{1}{\sqrt{2}} \begin{pmatrix} 0 \\ v_2 e^{i\theta} \end{pmatrix} \quad (2.25)$$

with v_1 and v_2 two real parameters such that $v^2 = v_1^2 + v_2^2$.

The corresponding potential minimum conditions can be obtained by imposing

$$\left. \frac{\partial V}{\partial \eta_i} \right|_{\langle \eta_i \rangle} = 0 \quad (2.26)$$

where η_i are the eight real components of the two doublets. They translate to three independent equations relating m_1^2 , m_2^2 and m_4^2 to the other parameters of the potential and to the three VEV parameters v_1 , v_2 and θ :

$$\begin{aligned}
\frac{m_1^2}{v^2} &= \lambda_1 c_\beta^2 + \frac{(\lambda_3 + \lambda_5)}{2} s_\beta^2 \\
&\quad + \frac{t_\beta}{2c_\theta} \left[\lambda_6 c_\beta^2 \left(1 + \frac{c_{2\theta}}{2}\right) + \frac{\lambda_7}{2} c_\beta^2 s_{2\theta} + \frac{\lambda_8}{2} s_\beta^2 + \lambda_{10} s_{2\beta} s_\theta - \frac{m_3^2}{v^2} \right] \\
\frac{m_2^2}{v^2} &= \lambda_2 s_\beta^2 + \frac{(\lambda_3 + \lambda_5)}{2} c_\beta^2 \\
&\quad + \frac{1}{2t_\beta c_\theta} \left[\lambda_8 s_\beta^2 \left(1 + \frac{c_{2\theta}}{2}\right) + \frac{\lambda_9}{2} s_\beta^2 s_{2\theta} + \frac{\lambda_6}{2} c_\beta^2 + \lambda_{10} c_{2\beta} s_\theta - \frac{m_3^2}{v^2} \right] \\
\frac{m_4^2}{v^2} &= \frac{1}{2} \left[(\lambda_4 - \lambda_3) s_\theta s_{2\beta} + \left(\frac{2m_3^2}{v^2} - \lambda_6 s_\beta^2 - \lambda_8 c_\beta^2 \right) t_\theta \right. \\
&\quad \left. \lambda_7 c_\beta^2 + \lambda_9 s_\beta^2 + \frac{\lambda_{10}}{2} \frac{c_{2\theta} s_{2\beta}}{c_\theta} \right] \tag{2.27}
\end{aligned}$$

where $\tan \beta \equiv v_2/v_1$ and s , c and t are the usual abbreviations for \sin , \cos and \tan .

2.3.2 Basis invariance and the Higgs basis

An important aspect of the 2HDM is the freedom to redefine the two scalar fields ϕ_1 and ϕ_2 using arbitrary $U(2)$ transformations acting in the ‘‘flavor’’ space, i.e.

$$\Psi \rightarrow \Psi' \equiv U\Psi \quad , \quad U \in U(2) \quad . \tag{2.28}$$

where Ψ is the isodoublet

$$\Psi \equiv \begin{pmatrix} \phi_1 \\ \phi_2 \end{pmatrix} \tag{2.29}$$

Indeed, transformation (2.28) leaves the canonically normalized, gauge-covariant kinetic energy terms

$$\frac{1}{2} |D^\mu \Psi|^2 = \frac{1}{2} |D^\mu \phi_1|^2 + \frac{1}{2} |D^\mu \phi_2|^2 \tag{2.30}$$

invariant. In this sense, this global $U(2)$ symmetry appears as a *symmetry of the physics* but *not* of the Lagrangian, i.e. transformation (2.28) modifies in general the explicit form of (2.24), but cannot alter the value of physical observables. Note however that the diagonal subgroup $U(1)$ of $U(2)$ corresponding to a global phase redefinition can be identified with the gauge group $U(1)_Y$, which corresponds to a true

internal symmetry of the Lagrangian. This relevant notion of *basis invariance* has been first emphasized in [51] and considered into great details more recently in [89] and [90, 91].

In order to study the meaningful observables associated with the most generic 2HDM and avoid considering unphysical, basis dependent quantities, two strategies can be identified. In the first one, the explicit parameters appearing in (2.24) and (2.25) are considered as basis dependent components of various two- and four-tensors which transform covariantly under the $U(2)$ flavor transformations [51, 90]. By fully contracting these tensors indices, different basis invariant quantities can be defined and related to physical predictions. Nevertheless, as shown explicitly in [90], these invariants are linked through trivial relations to the potential parameters in the specific set of basis, the so-called ‘‘Higgs basis’’, where one of the two VEV vanishes. So, a possible, somehow simpler, alternative approach to tensor techniques then consists in taking advantage of the $U(2)$ reparametrization freedom to fix from the beginning $v_2 = 0$, and to infer physical results directly from parameters values in this particular basis, or *vice versa*.

A possibly sensible issue regarding this procedure is the ambiguous definition of the Higgs basis. Starting from an arbitrary generic basis (2.25), the Higgs basis can always be reached using the unitary transformation

$$\begin{aligned} \begin{pmatrix} H_1 \\ H_2 \end{pmatrix} &= \exp(i\beta\tau^2) \exp(-i\theta(\mathbb{1} + \tau^3)) \Psi \\ &= \begin{pmatrix} \cos\beta & \sin\beta \\ -\sin\beta & \cos\beta \end{pmatrix} \begin{pmatrix} 1 & 0 \\ 0 & e^{-i\theta} \end{pmatrix} \begin{pmatrix} \phi_1 \\ \phi_2 \end{pmatrix} . \end{aligned} \quad (2.31)$$

However, any subsequent phase transformation

$$\begin{pmatrix} H_1 \\ H_2 \end{pmatrix} \rightarrow \begin{pmatrix} 1 & 0 \\ 0 & e^{i\xi} \end{pmatrix} \begin{pmatrix} H_1 \\ H_2 \end{pmatrix} \quad (2.32)$$

corresponding to a combination of $U(1)_Y$ and diagonal $SU(2)$ transformations conserves the Higgs basis defining properties, namely $\langle H_1 \rangle = v/\sqrt{2}$ and $\langle H_2 \rangle = 0$. The Higgs basis is then *defined up to an arbitrary complex phase ξ acting on H_2 and all physical observables should be a priori independent of ξ* . As developed in (2.4.1) and (2.4.2), this remnant $U(1)$ symmetry plays a key role when considering a generic definition of the CP and custodial symmetries. In the following, the ξ dependence is explicitly included in order to emphasize the symmetrical nature of the $H_i \leftrightarrow \phi_i$ basis change. The inversion of all forthcoming relations is in particular simply obtained by making the replacements $\theta \leftrightarrow \xi$ and $\beta \leftrightarrow -\beta$.

In a Higgs basis, potential (2.24) reads

$$V(H_1, H_2) = -\mu_1^2 \hat{A} - \mu_2^2 \hat{B} - \mu_3^2 \hat{C} - \mu_4^2 \hat{D} + \Lambda_1 \hat{A}^2 + \Lambda_2 \hat{B}^2 + \Lambda_3 \hat{C}^2 + \Lambda_4 \hat{D}^2 \\ + \Lambda_5 \hat{A} \hat{B} + \Lambda_6 \hat{A} \hat{C} + \Lambda_7 \hat{A} \hat{D} + \Lambda_8 \hat{B} \hat{C} + \Lambda_9 \hat{B} \hat{D} + \Lambda_{10} \hat{C} \hat{D} \quad (2.33)$$

where \hat{A} , \hat{B} , \hat{C} and \hat{D} are defined in terms of H_1 and H_2 as in (2.23). They are linked to the \hat{A} , \hat{B} , \hat{C} and \hat{D} operators as

$$\begin{aligned} \hat{A} &= c_\beta^2 \hat{A} + s_\beta^2 \hat{B} + s_{2\beta}(c_\theta \hat{C} + s_\theta \hat{D}) \\ \hat{B} &= s_\beta^2 \hat{A} + c_\beta^2 \hat{B} - s_{2\beta}(c_\theta \hat{C} + s_\theta \hat{D}) \\ \hat{C} &= -\frac{s_{2\beta}}{2} c_\xi (\hat{A} - \hat{B}) + (c_\theta c_{2\beta} c_\xi + s_\theta s_\xi) \hat{C} + (s_\theta c_{2\beta} c_\xi - c_\theta s_\xi) \hat{D} \\ \hat{D} &= -\frac{s_{2\beta}}{2} s_\xi (\hat{A} - \hat{B}) + (c_\theta c_{2\beta} s_\xi - s_\theta c_\xi) \hat{C} + (s_\theta c_{2\beta} s_\xi + c_\theta c_\xi) \hat{D} \end{aligned} \quad (2.34)$$

while parameters μ_i and Λ_i are related the generic basis parameters through

$$\begin{aligned} \mu_1^2 &= m_1^2 c_\beta^2 + m_2^2 s_\beta^2 + (m_3^2 c_\theta + m_4^2 s_\theta) \frac{s_{2\beta}}{2} \\ \mu_2^2 &= m_1^2 s_\beta^2 + m_2^2 c_\beta^2 - (m_3^2 c_\theta + m_4^2 s_\theta) \frac{s_{2\beta}}{2} \\ \mu_3^2 &= (m_2^2 - m_1^2) s_{2\beta} c_\xi + (m_3^3 c_\theta + m_4^2 s_\theta) c_{2\beta} c_\xi + (m_3^3 s_\theta - m_4^2 c_\theta) s_\xi \\ \mu_4^2 &= (m_2^2 - m_1^2) s_{2\beta} s_\xi + (m_3^3 c_\theta + m_4^2 s_\theta) c_{2\beta} s_\xi - (m_3^3 s_\theta - m_4^2 c_\theta) c_\xi \end{aligned} \quad (2.35)$$

and

$$\begin{aligned} \Lambda_1 &= \lambda_1 c_\beta^4 + \lambda_2 s_\beta^4 + (\lambda_3 c_\theta^2 + \lambda_4 s_\theta^2 + \lambda_5 + \lambda_{10} s_\theta c_\theta) s_\beta^2 c_\beta^2 \\ &\quad + (\lambda_6 c_\theta + \lambda_7 s_\theta) s_\beta c_\beta^3 + (\lambda_8 c_\theta + \lambda_9 s_\theta) s_\beta^3 c_\beta \\ \Lambda_2 &= \lambda_1 s_\beta^4 + \lambda_2 c_\beta^4 + (\lambda_3 c_\theta^2 + \lambda_4 s_\theta^2 + \lambda_5 + \lambda_{10} s_\theta c_\theta) s_\beta^2 c_\beta^2 \\ &\quad + (\lambda_6 c_\theta + \lambda_7 s_\theta) s_\beta^3 c_\beta + (\lambda_8 c_\theta + \lambda_9 s_\theta) s_\beta c_\beta^3 \\ \Lambda_3 &= (\lambda_1 + \lambda_2) c_\xi^2 s_{2\beta}^2 + (\lambda_3 c_\theta^2 + \lambda_4 s_\theta^2 + \lambda_{10} s_\theta c_\theta) c_\xi^2 c_{2\beta}^2 \\ &\quad + (\lambda_3 s_\theta^2 + \lambda_4 c_\theta^2 - \lambda_{10} s_\theta c_\theta) s_\xi^2 + \frac{1}{2} ((\lambda_3 - \lambda_4) s_{2\theta} - \lambda_{10} c_{2\theta}) c_{2\beta} s_{2\xi} \\ &\quad - \lambda_5 c_\xi^2 s_{2\beta}^2 - ((\lambda_{68} s_\theta - \lambda_{79} c_\theta) s_{2\beta} s_{2\xi} + (\lambda_{68} c_\theta + \lambda_{79} s_\theta) s_{4\beta} c_\xi^2) \end{aligned}$$

$$\begin{aligned}
\Lambda_4 = & (\lambda_1 + \lambda_2)s_\xi^2 s_{2\beta}^2 + (\lambda_3 c_\theta^2 + \lambda_4 s_\theta^2 + \lambda_{10} s_\theta c_\theta)s_\xi^2 c_{2\beta}^2 \\
& + (\lambda_3 s_\theta^2 + \lambda_4 c_\theta^2 - \lambda_{10} s_\theta c_\theta)c_\xi^2 - \frac{1}{2}((\lambda_3 - \lambda_4)s_{2\theta} - \lambda_{10} c_{2\theta})c_{2\beta} s_{2\xi} \\
& - \lambda_5 s_\xi^2 s_{2\beta}^2 + ((\lambda_{68} s_\theta - \lambda_{79} c_\theta)s_{2\beta} s_{2\xi} - (\lambda_{68} c_\theta + \lambda_{79} s_\theta)s_{4\beta} s_\xi^2)
\end{aligned}$$

$$\begin{aligned}
\Lambda_5 = & (\lambda_1 + \lambda_2 - \lambda_3 c_\theta^2 - \lambda_4 s_\theta^2 - \lambda_{10} s_\theta c_\theta)s_\beta^2 c_\beta^2 + \lambda_5 (c_\beta^4 + s_\beta^4) \\
& + \lambda_{68} s_{2\beta} c_{2\beta} c_\theta + \lambda_{79} s_{2\beta} c_{2\beta} s_\theta
\end{aligned}$$

$$\begin{aligned}
\Lambda_6 = & -4(\lambda_1 c_\beta^3 s_\beta - \lambda_2 c_\beta s_\beta^3)c_\xi + \frac{1}{2}(\lambda_3 c_\theta^2 + \lambda_4 s_\theta^2 + \lambda_{10} s_\theta c_\theta)s_{4\beta} c_\xi \\
& + (\lambda_3 - \lambda_4 - \lambda_{10})s_\theta c_\theta s_\beta c_\beta c_\xi + \frac{\lambda_5}{2}c_\xi s_{4\beta} \\
& + (\lambda_6 c_\beta^2 + \lambda_8 s_\beta^2)(2c_{2\beta} c_\theta c_\xi + s_\theta s_\xi) - (\lambda_6 c_\beta^2 - \lambda_8 s_\beta^2)c_\theta c_\xi \\
& + (\lambda_7 c_\beta^2 + \lambda_9 s_\beta^2)(2c_{2\beta} s_\theta c_\xi - c_\theta s_\xi) - (\lambda_7 c_\beta^2 - \lambda_9 s_\beta^2)s_\theta c_\xi
\end{aligned}$$

$$\begin{aligned}
\Lambda_7 = & -4(\lambda_1 c_\beta^3 s_\beta - \lambda_2 c_\beta s_\beta^3)s_\xi + \frac{1}{2}(\lambda_3 c_\theta^2 + \lambda_4 s_\theta^2 + \lambda_{10} s_\theta c_\theta)s_{4\beta} s_\xi \\
& + (\lambda_3 - \lambda_4 - \lambda_{10})s_\theta c_\theta s_\beta c_\beta c_\xi + \frac{\lambda_5}{2}s_\xi s_{4\beta} \\
& + (\lambda_6 c_\beta^2 + \lambda_8 s_\beta^2)(2c_{2\beta} c_\theta s_\xi + s_\theta c_\xi) - (\lambda_6 c_\beta^2 - \lambda_8 s_\beta^2)c_\theta s_\xi \\
& + (\lambda_7 c_\beta^2 + \lambda_9 s_\beta^2)(2c_{2\beta} s_\theta s_\xi - c_\theta c_\xi) - (\lambda_7 c_\beta^2 - \lambda_9 s_\beta^2)s_\theta s_\xi
\end{aligned}$$

$$\begin{aligned}
\Lambda_8 = & -4(\lambda_1 s_\beta^3 c_\beta - \lambda_2 s_\beta c_\beta^3)c_\xi - \frac{1}{2}(\lambda_3 c_\theta^2 + \lambda_4 s_\theta^2 + \lambda_{10} s_\theta c_\theta)s_{4\beta} c_\xi \\
& - (\lambda_3 - \lambda_4 - \lambda_{10})s_\theta c_\theta s_\beta c_\beta s_\xi - \frac{\lambda_5}{2}c_\xi s_{4\beta} \\
& + (\lambda_6 s_\beta^2 + \lambda_8 c_\beta^2)(2c_{2\beta} c_\theta c_\xi + s_\theta s_\xi) - (\lambda_6 s_\beta^2 + \lambda_8 c_\beta^2)c_\theta c_\xi \\
& + (\lambda_7 s_\beta^2 + \lambda_9 c_\beta^2)(2c_{2\beta} s_\theta c_\xi - c_\theta s_\xi) - (\lambda_7 s_\beta^2 - \lambda_9 c_\beta^2)s_\theta c_\xi
\end{aligned}$$

$$\begin{aligned}
\Lambda_9 = & -4(\lambda_1 s_\beta^3 c_\beta - \lambda_2 s_\beta c_\beta^3)s_\xi - \frac{1}{2}(\lambda_3 c_\theta^2 + \lambda_4 s_\theta^2 + \lambda_{10} s_\theta c_\theta)s_{4\beta} s_\xi \\
& - (\lambda_3 - \lambda_4 - \lambda_{10})s_\theta c_\theta s_\beta c_\beta c_\xi - \frac{\lambda_5}{2}s_\xi s_{4\beta} \\
& + (\lambda_6 s_\beta^2 + \lambda_8 c_\beta^2)(2c_{2\beta} c_\theta s_\xi + s_\theta c_\xi) - (\lambda_6 s_\beta^2 + \lambda_8 c_\beta^2)c_\theta s_\xi \\
& + (\lambda_7 s_\beta^2 + \lambda_9 c_\beta^2)(2c_{2\beta} s_\theta s_\xi - c_\theta c_\xi) - (\lambda_7 s_\beta^2 - \lambda_9 c_\beta^2)s_\theta s_\xi
\end{aligned}$$

$$\begin{aligned}
\Lambda_{10} = & (\lambda_1 + \lambda_2)s_{2\beta}^2s_{2\xi}^2 - ((\lambda_3 - \lambda_4)s_{2\theta} - \lambda_{10}c_{2\theta})(c_{2\beta}c_{2\xi} - \frac{1}{4}(c_{4\beta} + 3)c_{2\theta}) \\
& - \frac{1}{2}(\lambda_3 + \lambda_4)s_{2\beta}^2s_{2\xi}^2 - \lambda_5s_{2\beta}^2s_{2\xi} + \lambda_{68}(2c_{2\xi}s_{2\beta}s_{\theta} - c_{\theta}s_{4\beta}s_{2\xi}) \\
& - \lambda_{79}(2c_{2\xi}s_{2\beta}c_{\theta} + s_{\theta}s_{4\beta}s_{2\xi})
\end{aligned} \tag{2.36}$$

where $\lambda_{68} = (\lambda_6 - \lambda_8)/2$ and $\lambda_{79} = (\lambda_7 - \lambda_9)/2$.

Since $\langle H_2 \rangle$ vanishes by definition, the potential minimization conditions (2.27) now reduce to

$$\mu_1^2 = \Lambda_1 v^2 \quad , \quad \mu_3^2 = \frac{\Lambda_6 v^2}{2} \quad \text{and} \quad \mu_4^2 = \frac{\Lambda_7 v^2}{2} \quad . \tag{2.37}$$

Besides the usual three massless would-be Goldstone bosons, the physical spectrum contains a charged pair with mass

$$m_{H^\pm} = \frac{\Lambda_5 v^2}{2} - \mu_2^2 \tag{2.38}$$

and three neutral states with the squared mass matrix

$$\mathcal{M}^2 = \frac{1}{2} \begin{pmatrix} 4\Lambda_1 v^2 & \Lambda_6 v^2 & \Lambda_7 v^2 \\ \Lambda_6 v^2 & (\Lambda_3 + \Lambda_5)v^2 - 2\mu_2^2 & \frac{\Lambda_{10} v^2}{2} \\ \Lambda_7 v^2 & \frac{\Lambda_{10} v^2}{2} & (\Lambda_4 + \Lambda_5)v^2 - 2\mu_2^2 \end{pmatrix} . \tag{2.39}$$

The symmetric matrix \mathcal{M} is diagonalized by an orthogonal matrix T . The diagonalization yields masses m_i for the three physical neutral scalars S^i of the model

$$\mathcal{M}^2 \equiv T \text{diag}(m_1^2, m_2^2, m_3^2) T^T \quad . \tag{2.40}$$

2.3.3 Yukawa couplings

In the most generic model, both Higgs doublets can couple to the SM fermions such that (1.29) becomes

$$\begin{aligned}
\mathcal{L}_Y = & -\frac{\sqrt{2}}{v} \overline{Q}_L (\Delta_d \phi_1 + \Gamma_d \phi_2) d_R - \frac{\sqrt{2}}{v} \overline{Q}_L (\Delta_u \tilde{\phi}_1 + \Gamma_u \tilde{\phi}_2) u_R \\
& - \frac{\sqrt{2}}{v} \overline{L}_L (\Delta_l \phi_1 + \Gamma_l \phi_2) e_R + \text{h.c.}
\end{aligned} \tag{2.41}$$

where $\Delta_{d,u,l}$ and $\Gamma_{d,u,l}$ are six complex 3×3 matrices. The very same terms in a Higgs basis read

$$\begin{aligned}
\mathcal{L}_Y = & -\frac{\sqrt{2}}{v} \overline{Q}_L (M_d H_1 + Y_d H_2) d_R - \frac{\sqrt{2}}{v} \overline{Q}_L (M_u \tilde{H}_1 + Y_u \tilde{H}_2) u_R \\
& - \frac{\sqrt{2}}{v} \overline{L}_L (M_l H_1 + Y_l H_2) e_R + \text{h.c.}
\end{aligned} \tag{2.42}$$

where $M_{d,u,l}$ are the SM-like mass matrices which can be bi-diagonalized in the usual way while $Y_{d,u,l}$ are *a priori* arbitrary 3×3 matrices. The two representations are linked through

$$\begin{aligned} M_u &= c_\beta \Delta_u + s_\beta \Gamma_u e^{-i\theta} \\ M_{d,l} &= c_\beta \Delta_{d,l} + s_\beta \Gamma_{d,l} e^{i\theta} \end{aligned} \quad (2.43)$$

and

$$\begin{aligned} Y_u &= e^{i\xi} (-s_\beta \Delta_u + c_\beta \Gamma_u e^{-i\theta}) \\ Y_{d,l} &= e^{-i\xi} (-s_\beta \Delta_{d,l} + c_\beta \Gamma_{d,l} e^{i\theta}) \quad . \end{aligned} \quad (2.44)$$

Contrary to what happens in the Standard Model, the Yukawa interactions of physical scalars are not necessarily flavor diagonal in the 2HDM. Indeed, since the M and Y matrices are in principle unrelated, they are not expected to be (bi-)diagonalized by the same unitary transformations acting on the fermion fields. This leads in general to the apparition of tree-level Flavour Changing Neutral Currents which are strongly constrained by low energy experimental data. This issue can be easily addressed by introducing a \mathbb{Z}_2 symmetry acting on both the Higgs doublets and the fermion fields. This parity restricts the allowed couplings, as described in section 2.4.3.

2.4 Global symmetries in the 2HDM

The most general 2HDM described in the previous section is build on the only requirements of gauge invariance and renormalizability. In the Standard Model, these requirements accidently imply invariance of the scalar potential under larger global symmetries like the custodial symmetry (see section 1.4.2) or the CP symmetry. These symmetries, which have important phenomenological consequences, are in general not naturally present in the context of extended scalar sectors. Nevertheless, they can arise in the limit of particular values of the parameters in the potential or could be imposed “by hand” and constrain these parameters. In the following, a generic definition is proposed for each of the most common global symmetries, namely the custodial, the CP and the \mathbb{Z}_2 symmetries.

2.4.1 Custodial symmetry

Similarly to the Standard Model case reviewed in section 1.4.2, let us first introduce the $[1/2, 1/2]$ representations M_i of the Higgs doublets H_i

$$M_i \equiv \begin{pmatrix} H_i^0 & H_i^+ \\ -(H_i^+)^* & (H_i^0)^* \end{pmatrix} . \quad (2.45)$$

on which a $SU(2)_L \times SU(2)_R$ symmetry may act. As detailed previously, we can also assume without loss of generality to be in a Higgs basis where only H_1 gets a non zero VEV. From section 1.4.2, we know that the invariance of the vacuum under the diagonal subgroup $SU(2)_{L+R}$ is necessary to ensure that the relation $\rho = 1$ does not suffer from large (i.e., quadratic in the Higgs bosons masses) corrections at the one-loop level. For the $[1/2, 1/2]$ representation M_1 of H_1 , we thus impose

$$M_1 \rightarrow U_L M_1 U_R^\dagger \quad (2.46)$$

However, at this stage the chiral transformation for the $[1/2, 1/2]$ representation M_2 of H_2 is not yet completely fixed [76]. Indeed, only $SU(2)_L \times U(1)_Y$ is a local symmetry of the Lagrangian. By analogy with Left-Right symmetric models (e.g., see [1]), the conserved electric charge turns out to be $Q = T_L^3 + T_R^3$ in the bosonic sector of the theory, with T_R^3 the diagonal generator of the global $SU(2)_R$. So we still have the freedom to impose the invariance under

$$M_2 \rightarrow U_L M_2 V_R^\dagger \quad (2.47)$$

with

$$V_R = X^\dagger U_R X \quad (2.48)$$

if the two-by-two unitary matrix X commutes with $\exp(iT_3^R)$, namely

$$X = \begin{pmatrix} \exp(i\frac{\gamma}{2}) & 0 \\ 0 & \exp(-i\frac{\gamma}{2}) \end{pmatrix} . \quad (2.49)$$

It is straightforward to see that both \hat{A} and \hat{B} operators are invariant under the chiral transformations (2.46) and (2.47) while \hat{C} and \hat{D} are not if γ is an arbitrary parameter. Nevertheless the linear combination

$$\begin{aligned} \hat{C}' &\equiv \frac{1}{2} \text{Tr}(M_1 X M_2^\dagger) = \frac{1}{2} \text{Tr}(M_2 X^\dagger M_1^\dagger) \\ &= \cos\left(\frac{\gamma}{2}\right) \hat{C} + \sin\left(\frac{\gamma}{2}\right) \hat{D} \end{aligned} \quad (2.50)$$

is always invariant, no matter the value of γ . Therefore, the most general custodial-invariant potential contains only three linear and six quadratic terms in \hat{A} , \hat{B} and \hat{C}' :

$$V_{CS} = -\mu_1^2 \hat{A} - \mu_2^2 \hat{B} - \mu_3'^2 \hat{C}' + \Lambda_1 \hat{A}^2 + \Lambda_2 \hat{B}^2 + \Lambda_3' \hat{C}'^2 + \Lambda_5 \hat{A} \hat{B} + \Lambda_6' \hat{A} \hat{C}' + \Lambda_8' \hat{B} \hat{C}' \quad . \quad (2.51)$$

The squared mass of the charged pair H^\pm is given by (2.38). A suitable $\gamma/2$ rotation acting on $(\text{Re}(H_2^0), \text{Im}(H_2^0))$ allows us to reduce the full three-by-three mass matrix for the neutral fields (2.39) into a single mass term

$$m_{S_3} = m_{H^\pm} \quad (2.52)$$

for the state

$$\frac{S^3}{\sqrt{2}} \equiv -\sin\left(\frac{\gamma}{2}\right) \text{Re}(H_2^0) + \cos\left(\frac{\gamma}{2}\right) \text{Im}(H_2^0) \quad (2.53)$$

and a two-by-two mass matrix

$$\mathcal{M}^2 = \begin{pmatrix} 2\Lambda_1 v^2 & \frac{\Lambda_6' v^2}{2} \\ \frac{\Lambda_6' v^2}{2} & m_{H^\pm}^2 + \frac{\Lambda_3'}{2} v^2 \end{pmatrix} \quad (2.54)$$

for

$$\begin{aligned} \frac{S^1}{\sqrt{2}} &\equiv \text{Re}(H_1^0) - \frac{v}{\sqrt{2}} \\ \frac{S^2}{\sqrt{2}} &\equiv \cos\left(\frac{\gamma}{2}\right) \text{Re}(H_2^0) + \sin\left(\frac{\gamma}{2}\right) \text{Im}(H_2^0) \quad . \end{aligned} \quad (2.55)$$

S_3 is thus degenerate with H^\pm in a triplet of $SO(3)$, a clear signature of the custodial character of potential (2.51). The $S^{1,2}$ scalars are singlet under this symmetry but mix if $\Lambda_6' \neq 0$.

At this stage, it is important to note that γ is *not physically observable* in the framework of the fully generic two-Higgs-doublet model. Indeed, one can always use the reparametrization freedom of the Higgs basis (2.32) to rotate out this additional phase. However, this statement is only valid in the absence of any external constraints which may “freeze” the actual value of the second doublet phase, e.g. by fixing the Λ_i parameters or the Y Yukawa coupling matrices. In such a case, the misalignment between γ and the second doublet phase becomes a physical observable which can be measured in high energy processes. A typical example where such a situation occurs is described in section 2.6.

2.4.2 CP symmetry

In the present work, we follow the standard approach advocated in [51] to study CP invariance and violation. The starting point of this scheme is to require all the gauge-kinetic terms to be invariant *by definition*. This can always be achieved since all pure gauge Lagrangians are necessarily CP invariant [92] in the absence of topological effects.

The CP transformation of the photon field $A^\mu(t, \vec{x})$ is fixed by first principles. It transforms as $A_\mu(t, \vec{x}) \rightarrow A^\mu(t, -\vec{x})$ under parity, like all vector fields, and changes its sign under charge conjugation to ensure invariance of the electromagnetic interaction $A_\mu j^\mu$. This gives

$$(CP)A_\mu(t, \vec{x})(CP)^\dagger = -A^\mu(t, -\vec{x}) \quad . \quad (2.56)$$

The CP transformation of an arbitrary (possibly charged) spin-0 field ϕ is less constrained. Assuming the invariance under P and C transformations of the Klein Gordon Lagrangian, consistently with electromagnetism, leads to

$$P\phi(t, \vec{x})P^\dagger = e^{i\alpha_P} \phi(t, -\vec{x}) \quad (2.57)$$

and

$$C\phi(t, \vec{x})C^\dagger = e^{i\alpha_C} \phi^\dagger(t, \vec{x}) \quad (2.58)$$

where α_P and α_C are two free phases. It follows that the CP transformation of any scalar field is *a priori* defined up to an arbitrary phase $\alpha = \alpha_P + \alpha_C$. For example, the charged components H^\pm of a Higgs doublet transform as

$$\begin{aligned} (CP)H^+(t, \vec{x})(CP)^\dagger &= e^{i\alpha} H^-(t, -\vec{x}) \\ (CP)H^-(t, \vec{x})(CP)^\dagger &= e^{-i\alpha} H^+(t, -\vec{x}) \quad . \end{aligned} \quad (2.59)$$

In the SM, it turns out that relations (2.56) and (2.59) together with the requirement of invariance under CP of the kinetic part of (1.21) completely fix the CP transformation of all other bosonic fields. They read

$$\begin{aligned} (CP)W_\mu^+(t, \vec{x})(CP)^\dagger &= -e^{i\alpha} W^{-\mu}(t, -\vec{x}) \\ (CP)W_\mu^-(t, \vec{x})(CP)^\dagger &= -e^{-i\alpha} W^{+\mu}(t, -\vec{x}) \end{aligned} \quad (2.60)$$

and

$$\begin{aligned} (CP)Z_\mu(t, \vec{x})(CP)^\dagger &= -Z^\mu(t, -\vec{x}) \\ (CP)\sigma(t, \vec{x})(CP)^\dagger &= \sigma(t, -\vec{x}) \\ (CP)\pi^3(t, \vec{x})(CP)^\dagger &= -\pi^3(t, -\vec{x}) \quad . \end{aligned} \quad (2.61)$$

These relations imply that the SM scalar potential in (1.21) is always CP invariant, both explicitly and after spontaneous symmetry breaking. Due to this, the only possible sources of CP violation in the Standard Model are the complex coefficients appearing in the Yukawa sector, the fermionic kinetic terms being conventionally CP invariant.

In the generic base of the two-Higgs-doublet model, the most generic CP transformation of the Higgs fields reads

$$\begin{aligned} (CP)\phi_a^+(t, \vec{x})(CP)^\dagger &= U_{ab}^{CP} e^{i\alpha} \phi_b^-(t, -\vec{x}) \\ (CP)\phi_a^0(t, \vec{x})(CP)^\dagger &= U_{ab}^{CP} \phi_b^{0*}(t, -\vec{x}) \end{aligned} \quad (2.62)$$

where the two-by-two matrix U^{CP} must satisfy

$$\begin{aligned} v_1 &= U_{11}^{CP} v_1 + U_{12}^{CP} v_2 e^{-i\theta} \\ v_2 e^{i\theta} &= U_{21}^{CP} v_1 + U_{22}^{CP} v_2 e^{-i\theta} \end{aligned} \quad (2.63)$$

in order to fulfill the gauge-kinetic terms CP invariance. Since the phase α is not physically observable, i.e. it cancels in all interaction vertices involving charged scalar(s), we shall set it to zero from now on without losing generality. The two equations in (2.62) may then be grouped as

$$(CP)\phi_a(t, \vec{x})(CP)^\dagger = U_{ab}^{CP} \phi_b^*(t, -\vec{x}) \quad . \quad (2.64)$$

In the Higgs basis where $v_1 = v$ and $v_2 = 0$, equations (2.63) constrains U^{CP} to be of the form

$$U^{CP} = \begin{pmatrix} 1 & 0 \\ 0 & e^{i\delta} \end{pmatrix} \quad (2.65)$$

which consistently reflects the Higgs basis definition phase ambiguity emphasized in equation (2.32), as one can see by identifying $\xi = 2\delta$. The diagonal structure of (2.65) also guarantees that, in the Higgs basis, all the fields belonging to the first doublet H_1 transform under CP exactly as the fields belonging to H in the Standard Model, i.e. like in Eqs. (2.59) and (2.61). The neutral combinations

$$\begin{aligned} \frac{H^0}{\sqrt{2}} &\equiv \cos\left(\frac{\delta}{2}\right) \text{Re}(H_2^0) + \sin\left(\frac{\delta}{2}\right) \text{Im}(H_2^0) \\ \frac{A^0}{\sqrt{2}} &\equiv -\sin\left(\frac{\delta}{2}\right) \text{Re}(H_2^0) + \cos\left(\frac{\delta}{2}\right) \text{Im}(H_2^0) \end{aligned} \quad (2.66)$$

belonging to the second doublet are respectively CP -even and odd but are not necessarily physical mass eigenstates if the CP symmetry is violated. Assuming the

Yukawa couplings of H_2 in (2.42) are CP -invariant, one can always define the Y matrix in such a way H^0 couples to the CP -even fermionic field bilinear $\bar{\psi}\xi$ where ψ and ξ are two arbitrary Dirac spinors, while A^0 couples to the CP -odd $\bar{\psi}\gamma_5\xi$.

Starting from relations (2.64) and (2.65), it is straightforward to show that both operators \hat{A} and \hat{B} remain even under the CP symmetry, no matter the value of δ , while the orthogonal combinations

$$\begin{aligned}\hat{C}'' &= \cos\left(\frac{\delta}{2}\right)\hat{C} + \sin\left(\frac{\delta}{2}\right)\hat{D} \\ \hat{D}'' &= -\sin\left(\frac{\delta}{2}\right)\hat{C} + \cos\left(\frac{\delta}{2}\right)\hat{D}\end{aligned}\quad (2.67)$$

are respectively even and odd. Therefore, the most general CP -invariant potential always reads, in the Higgs basis,

$$\begin{aligned}V_{CP} &= -\mu_1^2\hat{A} - \mu_2^2\hat{B} - \mu_3^{2''}\hat{C}'' + \Lambda_1\hat{A}^2 + \Lambda_2\hat{B}^2 + \Lambda_3''\hat{C}''^2 + \Lambda_4''\hat{D}''^2 \\ &\quad + \Lambda_5\hat{A}\hat{B} + \Lambda_6''\hat{A}\hat{C}'' + \Lambda_8''\hat{B}\hat{C}'' \quad .\end{aligned}\quad (2.68)$$

The explicit CP (non-)invariance of the potential can be discussed from two distinct but somehow equivalent points of view. Either the phase δ is fixed by an unknown mechanism, like a new interaction beyond the SM (technicolor, ...), in such a way that Eq. (2.68) represents the most general CP invariant potential. Either the potential expression is fixed by additional constraints, like an other unknown symmetry, and it is said to be CP invariant if and only if there exists a basis change, and in particular a phase δ , such that it can be written as (2.68). From this point of view, it is easy to show that, in the 2HDM, invariance under the custodial symmetry implies invariance under CP , since one can always choose $\delta = \gamma$ in (2.51). This last result is consistent with the one obtained in [93].

In the second approach, the CP definition may also not be *unique* if the potential form (2.68) remains invariant for different values of δ . This is for example the case in the limit where $\Lambda_{6,8}'' \rightarrow 0$ (leading to $\mu_3^{2''} \rightarrow 0$, from Eq. (2.37)). In this case, the absence of terms linear in \hat{C}'' allows for a second solution corresponding to the phase shift $\delta \rightarrow \delta + \pi$ which exchanges the CP parity of \hat{C}'' and \hat{D}'' . Let us emphasize this new possibility really corresponds to a physically distinguishable configuration. Indeed, the phase shift $\delta \rightarrow \delta + \pi$ also affects the expressions of the two CP eigenstates H^0 and A^0 in terms of $\text{Re}(H_2^0)$ and $\text{Im}(H_2^0)$ in (2.66), which are in turn related to the physical mass eigenstates for a fixed set of parameters.

2.4.3 \mathbb{Z}_2 symmetry: type I versus type II scenario

As mentioned in section 2.3.3, and contrary to the SM case, the requirements of gauge invariance and renormalizability for the Yukawa sector of the 2HDM are not sufficient to guarantee the absence of tree-level Flavour Changing Neutral Currents (FCNCs). The later being strongly constrained by current experimental data on heavy hadrons mixing and decay, a mechanism to naturally suppress them is an essential ingredient of any viable phenomenological model.

A simple, yet elegant, example of such mechanism has been proposed by Glashow and Weinberg in [94]. By requiring that *fermions of a given charge receive their mass through the coupling of precisely one Higgs doublet*, one ensures that the Yukawa couplings of the Higgs field are diagonalized simultaneously with the mass matrices. This condition can be naturally implemented in the two-Higgs-doublet model if there exists a generic basis where the two doublets transform under an extra \mathbb{Z}_2 symmetry as

$$\phi_1 \rightarrow \phi_1 \quad , \quad \phi_2 \rightarrow -\phi_2 \quad . \quad (2.69)$$

Assuming the right handed fermion fields in (2.41) are even or odd under this symmetry, while the left handed fermion fields are even, the Glashow-Weinberg criterium is naturally enforced. If all fermions have the same \mathbb{Z}_2 parity, they receive their mass through their interaction with a single Higgs field like in the SM and the model is called “type I”. If the right handed up-type quarks are \mathbb{Z}_2 -odd, while the right handed down-type quarks and charged leptons are \mathbb{Z}_2 -even, they receive their mass through interactions with different Higgs fields and the model is called “type II”. This last possibility could provide a natural explanation for the heavy fermions mass spectrum, i.e. by relating the top/bottom mass hierarchy to a VEVs ratio, $m_t/m_b \approx v_2/v_1$.

While the presence of this new symmetry in the Yukawa sector of the theory is required to suppress tree-level FCNCs, it must also hold in other sectors of the theory in order to avoid large contributions from higher orders. This restricts the number of parameters in potential 2.24 from fourteen to eight, by forbidding all terms linear in \hat{C} or \hat{D} which are both \mathbb{Z}_2 -odd. However, the so-called “soft-breaking terms”, i.e. quadratic terms like $-m_3^2 \hat{C} - m_4^2 \hat{D}$, do violates the \mathbb{Z}_2 symmetry but only in long range interactions, and their presence may remain compatible with all phenomenological constraints. The most generic 2HDM potential invariant under a (softly broken) \mathbb{Z}_2 symmetry then reads, in a generic basis,

$$\begin{aligned} V_{\mathbb{Z}_2} = & -m_1^2 \hat{A} - m_2^2 \hat{B} - m_3^2 \hat{C} - m_4^2 \hat{D} + \lambda_1 \hat{A}^2 + \lambda_2 \hat{B}^2 + \lambda_3 \hat{C}^2 + \lambda_4 \hat{D}^2 \\ & + \lambda_5 \hat{A} \hat{B} + \lambda_{10} \hat{C} \hat{D} \quad . \end{aligned} \quad (2.70)$$

Contrary to the custodial and CP cases, the \mathbb{Z}_2 symmetry is in general defined in a generic basis where both VEV are non zero in order to allow for non vanishing mass terms for all fermions in a type II scenario. Indeed, if the \mathbb{Z}_2 symmetry is only manifest in a Higgs basis, the sole remaining option is a type I scenario where all fermions couples to H_1 . All the new physical fields belonging to H_2 , this provides a natural candidate for dark matter, as discussed in section 2.1.2, but restricts considerably the number of possible phenomenological signatures at colliders.

This apparent limitation can be circumvented if the $SO(2)$ rotation of angle β required to perform a basis change from a generic basis where both VEV are real to a Higgs basis (see Eq. 2.31) is promoted to be a (softly broken) symmetry of the potential. In this case, any (softly broken) \mathbb{Z}_2 symmetry manifest in a given generic basis would become manifest in the related Higgs basis, and *vice versa*. Since the only matrices to commute with the generator of the $SO(2)$ symmetry, i.e. τ_2 , are the identity matrix and τ_2 itself, the only invariants are $\hat{A} + \hat{B}$ and \hat{D} . Imposing invariance of the quartic part of the potential under this $SO(2)$ (assuming the \mathbb{Z}_2 symmetry is softly broken) then reduces the total number of parameters from ten to six, such that the potential in the Higgs basis now reads

$$V_{SO(2)} = -\mu_1^2 \hat{A} - \mu_2^2 \hat{B} - \mu_3^2 \hat{C} - \mu_4^2 \hat{D} + \Lambda_1 (\hat{A} + \hat{B})^2 + \Lambda_4 \hat{D}^2 \quad . \quad (2.71)$$

Let us finally mention the \mathbb{Z}_2 symmetry can also be interpreted as a discrete subgroup of a larger continuous $U(1)$ Peccei-Quinn symmetry acting on the Higgs fields as

$$\phi_1 \rightarrow \phi_1 \quad , \quad \phi_2 \rightarrow e^{i\zeta} \phi_2 \quad (2.72)$$

where ζ is an arbitrary free phase. In this case, only the quartic form $\hat{C}^2 + \hat{D}^2$ remains invariant besides \hat{A} and \hat{B} such that the number of parameters in potential 2.70 is further reduced to six.

2.5 The MSSM scalar sector

As seen in section 2.1.1, any Supersymmetric extension of the Standard Model must contain at least two Higgs doublets with opposite hypercharges. In the simplest cases, e.g. in the MSSM, the scalar sector appears as a particular constrained 2HDM. The explicit form of the scalar potential can be obtained by considering three different types of contributions⁹ (e.g. see [1]):

⁹In order to stick to the convention used in the previous section, i.e. two $Y = +1$ doublets, an implicit replacement $\phi_2 \leftrightarrow \phi_2^\dagger$ has been performed

1. $F_i F^{i*}$ terms, where F_i are the auxiliary fields defined as $F_i \equiv \partial W / \partial A^i$ with W the superpotential and A^i a superfield. These terms give the quadratic mass terms:

$$V_F = -\mu^2(|\phi_1|^2 + |\phi_2|^2) = -\mu^2(\hat{A} + \hat{B}) \quad (2.73)$$

2. $D_a D^a$ terms, where $D^a \equiv g A_i^* (T^a)^{ij} A_j$ with T^a the generators of the gauge group, giving the quartic contributions.

$$\begin{aligned} V_D &= \frac{1}{2} \left[\frac{g_Y}{2} (|\phi_1|^2 - |\phi_2|^2) \right]^2 + \frac{1}{2} \sum_a \left[g_L (\phi_1^\dagger T^a \phi_2 + \phi_2^\dagger T^a \phi_1) \right]^2 \\ &= \frac{g_L^2}{8} \left[-4|\phi_1^\dagger \phi_2|^2 + 2|\phi_1|^2 |\phi_2|^2 + |\phi_1|^4 + |\phi_2|^4 \right] + \frac{g_Y^2}{8} [(|\phi_1|^2 - |\phi_2|^2)]^2 \\ &= \frac{g_L^2}{8} (\hat{A} + \hat{B})^2 + \frac{g_Y^2}{8} (\hat{A} - \hat{B})^2 - \frac{g_L^2}{2} (\hat{C}^2 + \hat{D}^2) \end{aligned} \quad (2.74)$$

3. SUSY soft breaking terms like $-m A_i A^{i*}$, giving additional quadratic terms

$$\begin{aligned} V_{SB} &= -m_1^2 |\phi_1|^2 - m_2^2 |\phi_2|^2 - b (\phi_1^\dagger \phi_2 + \text{h.c.}) \\ &= -m_1^2 \hat{A} - m_2^2 \hat{B} - 2b \hat{C} \end{aligned} \quad (2.75)$$

The b coefficient can in principle be complex but, in order to simplify the following notations, we explicitly choose the generic basis in such way it is real. This implies that both VEVs v_1 and v_2 are real, from (2.27).

The scalar potential of the MSSM then reads, in a generic basis where v_1 and v_2 are real,

$$\begin{aligned} V_{MSSM} &= -\tilde{m}_1^2 \hat{A} - \tilde{m}_2^2 \hat{B} - 2b \hat{C} + \frac{g_L^2}{8} (\hat{A} + \hat{B})^2 + \frac{g_Y^2}{8} (\hat{A} - \hat{B})^2 \\ &\quad - \frac{g_L^2}{2} (\hat{C}^2 + \hat{D}^2) \end{aligned} \quad (2.76)$$

with $\tilde{m}_i^2 \equiv m_i^2 + \mu^2$, or equivalently, in the Higgs basis where $v_2 = 0$,

$$\begin{aligned} V_{MSSM} &= -(\tilde{m}_1^2 c_\beta^2 + \tilde{m}_2^2 s_\beta^2 + b s_{2\beta}) \hat{\mathcal{A}} - (\tilde{m}_1^2 s_\beta^2 + \tilde{m}_2^2 c_\beta^2 - b s_{2\beta}) \hat{\mathcal{B}} \\ &\quad - (-s_{2\beta} \tilde{m}_1^2 + s_{2\beta} \tilde{m}_2^2 + 2b c_{2\beta}) \hat{\mathcal{C}} + \frac{g_L^2}{8} (\hat{\mathcal{A}}^2 + \hat{\mathcal{B}}^2) \\ &\quad + \frac{g_Y^2}{8} (c_{2\beta} (\hat{\mathcal{A}} - \hat{\mathcal{B}}) - 2s_{2\beta} \hat{\mathcal{C}})^2 \\ &\quad - \frac{g_L^2}{2} \left(\frac{s_{2\beta}}{2} (\hat{\mathcal{A}} - \hat{\mathcal{B}}) + c_{2\beta} \hat{\mathcal{C}} \right)^2 + \frac{g_L^2}{2} \hat{\mathcal{D}}^2 \end{aligned} \quad (2.77)$$

According to the definitions reviewed in section (2.4), this potential preserves CP at tree-level¹⁰ with $\delta = 0$, its quartic part is invariant under the \mathbb{Z}_2 symmetry (2.69) which is softly broken by quadratic terms and the custodial symmetry is broken due to the simultaneous presence of \hat{C} and \hat{D} terms in (2.77).

The physical spectrum of the MSSM Higgs sector is easily derived directly from (2.76) or from (2.77) using (2.38) and (2.39). Besides the three usual would-be Goldstone bosons, it contains a charged Higgs pair with squared mass

$$m_{H^\pm}^2 = \frac{2b}{\sin(2\beta)} + m_W^2 \quad (2.78)$$

and a pseudoscalar state $A^0/\sqrt{2} \equiv -(\sin\beta)\text{Im}(\phi_1^0) + (\cos\beta)\text{Im}(\phi_2^0)$ with squared mass

$$m_{A^0}^2 = m_{H^\pm}^2 - m_W^2 \quad (2.79)$$

The non degeneracy between H^\pm and A^0 is a clear signature of the breaking of the custodial symmetry in potential (2.77). The squared mass difference is proportional to m_W^2 , i.e. to g_L^2 , as can be guessed from the coefficient of the breaking term \hat{D}^2 . The two CP -even eigenstates

$$\begin{aligned} \frac{H^0}{\sqrt{2}} &\equiv \left(\text{Re}(\phi_1^0) - \frac{v_1}{\sqrt{2}}\right) \cos\alpha + \left(\text{Re}(\phi_2^0) - \frac{v_2}{\sqrt{2}}\right) \sin\alpha \\ \frac{h^0}{\sqrt{2}} &\equiv -\left(\text{Re}(\phi_1^0) - \frac{v_1}{\sqrt{2}}\right) \sin\alpha + \left(\text{Re}(\phi_2^0) - \frac{v_2}{\sqrt{2}}\right) \cos\alpha \end{aligned} \quad (2.80)$$

have squared masses

$$m_{h^0, H^0}^2 = \frac{1}{2} \left[m_{A^0}^2 + m_Z^2 \mp \sqrt{(m_{A^0}^2 + m_Z^2)^2 - 4m_Z^2 m_{A^0}^2 \cos^2 2\beta} \right] \quad (2.81)$$

and their mixing angle α is related to β through

$$\tan 2\alpha = \tan 2\beta \left(\frac{m_{A^0}^2 + m_Z^2}{m_{A^0}^2 - m_Z^2} \right) \quad (2.82)$$

Expression (2.81) leads to the tree-level mass rule

$$m_{h^0}^2 + m_{H^0}^2 = m_{Z^0}^2 + m_{A^0}^2 \quad (2.83)$$

and to a strong tree-level bound on the lightest Higgs boson mass, namely

$$m_{h^0}^2 \leq m_Z^2 \quad (2.84)$$

¹⁰Loop effects mediated dominantly by third-generation squarks may lead to sizeable violations of the tree-level CP invariance of the MSSM Higgs potential, giving rise to significant Higgs scalar-pseudoscalar transitions [95, 96]. See [40] for a recent review of the associated phenomenology.

In the limit where supersymmetry is restored, i.e. $b \rightarrow 0$ and $\tilde{m}_1^2 = \tilde{m}_2^2$, the Higgs bosons h^0 and A^0 become massless while the H^0 and the H^\pm become degenerate in mass with the Z^0 and W^\pm gauge bosons.

The tree-level MSSM scalar sector considered here is an archetypal, highly constrained 2HDM. Relations (2.78) to (2.83) are sufficient to fix all model parameters from the knowledge of m_{A^0} (i.e. the amount of SUSY breaking in the scalar sector) and $\tan\beta$. The upper bound (2.84) would suffice by itself to exclude the model when taking into account the LEP exclusion result (see section (1.4.3)). However, it is known for a long time¹¹ that this bound can be partially relaxed thanks to positive top and stop tadpoles contributions, leaving a tight, but not empty, window between 114.4 and ~ 140 GeV for m_{h^0} . Nevertheless, as seen from Figure 2.2, the saturation of

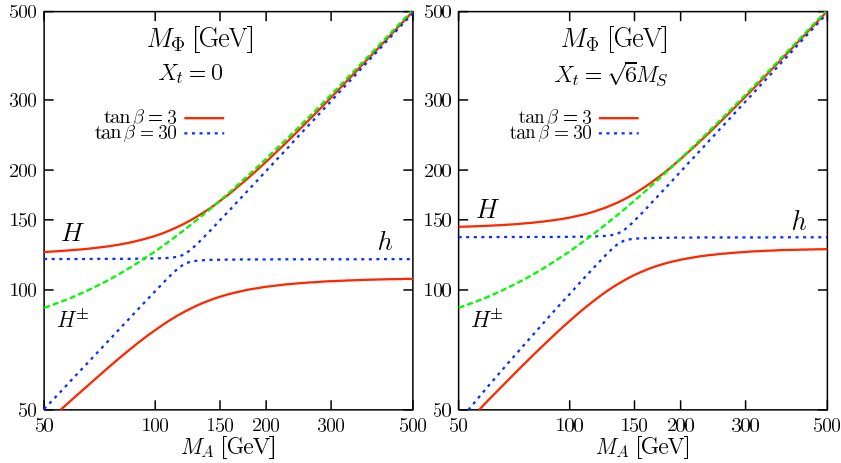


Figure 2.2: The masses of the MSSM Higgs bosons as a function of m_{A^0} for two values $\tan\beta = 3$ and 30 , in the no mixing (left) and maximal mixing (right) scenarios with $M_{SUSY} = 2$ TeV and all the other SUSY parameters set to 1 TeV. The full set of radiative corrections is included with $m_t = 178$ GeV, $m_b = 4.88$ GeV and $\alpha_s(m_Z) = 0.1172$. From Ref. [97].

the upper bound on the lightest Higgs boson mass tends to favor the decoupling limit and high $\tan\beta$ values. In this region of the parameter space, intensively studied for its experimental perspectives (see [98] for a recent overview), h^0 is light and essen-

¹¹E.g., see Ref. [97] and reference therein for a full review

tially SM-like while the other Higgs bosons are much heavier, leading to somewhat restricted possibilities for the BSM scalar sector phenomenology¹².

2.6 A twisted 2HDM

The generic two-Higgs-doublet model described in section 2.3 is not restricted by the mass relations (2.79) and (2.83), neither it suffers from the tree-level upper bound (2.84). The associated phenomenology may then be completely different, displaying unusual scalar spectrum or exotic Higgs to Higgs decays for example. However, the most general 2HDM contains fourteen parameters, among which eleven are physically relevant. This renders any global analysis of the entire parameter space much more complicated, compared for example to the MSSM scalar sector with only two degrees of freedom at tree-level.

A pragmatic approach to tackle this issue is to impose by hand global symmetries which are known to be (approximatively) present in the Standard Model or in well-motivated BSM theories, thus lowering the number of free parameters to consider in any phenomenological analysis. Even if this procedure may at first forbid interesting phenomena, like CP -violation which could be a wanted feature of the 2HDM (see section 2.1.2), it can be seen as a first step which can be further extended by introducing breaking terms as small perturbations, or as a consequence of new interactions.

Like demonstrated in section 2.4.1, implementing a generic custodial symmetry in the 2HDM restricts the number of free parameters to seven. As seen in 2.4.2, such a restricted potential is always CP invariant since the phase δ defining the CP transformation of the fields can always be aligned with the phase γ used to define the custodial transformation. From a phenomenological point of view, this leads to the degeneracy between the charged and *pseudoscalar* Higgs bosons, i.e. $m_{H^\pm}^2 = m_{A^0}^2$. Since the charged bosons are usually assumed to be rather heavy due to direct, and, even more, indirect constraints, this implies a relatively high mass for the A^0 . Typical experimental signatures in this case tend to be similar to these observed in the decoupling limit favored in the MSSM.

However, as advocated in [76], this alignment between the CP and custodial definition phases is not the only solution when the potential is further restricted. Or, by reversing the same argument, imposing simultaneously the invariance under both the CP and custodial symmetry may lead to further restrictions on potential parameters if the definition phases δ and γ are misaligned.

¹²This conclusion becomes slightly milder when higher order CP violating effects are included. They may allow, for example, the lightest Higgs boson to be lighter than the LEP bound by altering its coupling to the Z^0 boson.

A particularly interesting possibility is a “twisted” 2HDM where δ and γ are in maximal opposition, i.e. $\delta = \gamma - \pi$. The custodial invariant mixing operator \hat{C}' defined in Eq. 2.50 is then CP -odd (see Eq. 2.67) instead of being CP -even like in the $\delta = \gamma$ case. In order to restore the CP invariance of the potential, all terms linear in \hat{C}' in potential (2.51) must vanish, i.e. Λ'_6 and Λ'_8 must be set to zero. From a phenomenological point of view, this scenario is characterized by the degeneracy between charged and *scalar* Higgs bosons, i.e. $m_{H^\pm}^2 = m_{H^0}^2$, by opposition to the “usual” case described previously.

If $\delta \neq \gamma, \gamma - \pi$, \hat{C}' is not a CP eigenstate anymore such that Λ'_3 must vanish to restore the CP invariance. The resulting potential is invariant under a larger $SO(4) \times SO(4)$ symmetry which is spontaneously broken to $SO(3) \times SO(4)$. As a consequence the four components of H_2 are degenerate in mass, as seen from equations (2.52) and (2.54).

Let us emphasize that the existence of the twisted scenario in the 2HDM, and more generically the interpretation of the possible interplay between the custodial and CP symmetries in terms of aligned/misaligned phases, is a non trivial result. Phenomenological studies of the $\rho \approx 1$ constraint have emphasized vanishing contributions in the $m_{H^\pm}^2 \approx m_{H^0}^2$ limit (see [99] or more recently [75] and [71]) but did not interpret this result in terms of symmetries. The interplay between the CP and custodial symmetry in 2HDM has also been discussed in [93], but the second CP conserving custodial scenario found by the authors is in fact physically indistinguishable from the “usual” case since, according to their own conclusion, H^0 is redefined as CP odd.

One genuine feature of the twisted potential (2.87) is the presence of an *accidental* \mathbb{Z}_2 symmetry acting in the Higgs basis where $\delta = 0$ as

$$H_1 \rightarrow H_1 \quad , \quad H_2 \rightarrow -H_2 \quad . \quad (2.85)$$

In the Higgs basis where $\langle H_2 \rangle = 0$, this discrete symmetry is left unbroken and could advantageously supersede the CP invariance required to distinguish the different custodial symmetry realizations, i.e. the different values of γ . For illustration, it would nicely reconcile two apparent features of the electroweak interactions, namely natural flavor conservation and explicit CP -violation in the Yukawa sector [100], if all fermionic fields are even under \mathbb{Z}_2 . Where this is the case, the lightest neutral component of H_2 would be a candidate for cold dark matter, as mentioned in section 2.1.2.

In the present work, we further assume the presence of an additional softly-broken $SO(2)$ symmetry which generalize the \mathbb{Z}_2 symmetry accidentally present in the Higgs basis to all generic basis with real VEVs (see section 2.4.3). The full scalar potential of our “twisted model” then reads, in the Higgs basis

$$V_{\text{twisted}} = -\mu_1^2 \hat{A} - \mu_2^2 \hat{B} + \Lambda_S (\hat{A} + \hat{B})^2 + \Lambda_{AS} \hat{D}^2 \quad (2.86)$$

when the phase convention for H_2 is fixed such that $\delta = 0$ in (2.65). In a generic basis where both doublets have real VEVs, the same potential reads

$$V_{\text{twisted}} = -m_1^2 \hat{A} - m_2^2 \hat{B} - m_3^2 \hat{C} + \Lambda_S (\hat{A} + \hat{B})^2 + \Lambda_{AS} \hat{D}^2 \quad . \quad (2.87)$$

The physical spectrum is straightforward to determine. It contains a CP -even SM-like Higgs boson $h^0 \equiv \sqrt{2}(\text{Re}(H_1) - v/\sqrt{2})$ with squared mass

$$m_{h^0}^2 = 2\Lambda_S v^2 \quad , \quad (2.88)$$

a pair of charged Higgs bosons and a CP -even scalar¹³ $H^0 \equiv -\sqrt{2}\text{Re}(H_2)$ forming a triplet under the twisted custodial symmetry

$$m_T^2 \equiv m_{H^\pm}^2 = m_{H^0}^2 = \frac{m_3^2}{\sin(2\beta)} \quad (2.89)$$

and pseudoscalar state $A^0 = \sqrt{2}\text{Im}(H_2)$, singlet under the custodial symmetry

$$m_{A^0}^2 = m_{H^\pm}^2 + \frac{\Lambda_{AS} v^2}{2} \quad . \quad (2.90)$$

Since h^0 remains the only massive Higgs boson in the limit of an exact $SO(8)$ symmetry ($\Lambda_{AS}, m_3 \rightarrow 0$), one may expect the unusual hierarchy $m_{A^0}, m_{H^0}, m_{H^\pm} \ll m_{h^0}$. The pseudoscalar state A^0 may be much lighter than the degenerate triplet (if $\Lambda_{AS} < 0$), but its mass is not protected by any additional approximate symmetry, such that $m_{A^0} \approx 0$ is not a natural feature of this model.

Regarding Yukawa couplings, the presence of a softly-broken \mathbb{Z}_2 symmetry allows to define type I and type II models, each of them displaying completely different phenomenologies as detailed in the next chapters. As already mentioned in section 2.4.3, in a type I model, all right handed fermions are defined as even under the new parity, such that only ϕ_1 can couple to them. In a type II model, the right handed up-type quarks are \mathbb{Z}_2 -odd and get their mass through their Yukawa interactions with ϕ_2 , while the other Yukawa couplings remain identical to the type I case.

A complete list of Feynman rules for the twisted 2HDM (type I and type II) is available in Appendix A. All bosonic couplings are expressed in terms of the three free parameters of the potential which are conveniently chosen to be m_{h^0} , m_T and m_{A^0} , while all the Yukawa couplings are expressed in term of $\tan \beta$. A genuine feature of the model appearing in these expressions is that h^0 shares all the SM Higgs coupling to SM particles, and, contrary to what happen in more general 2HDMs, the couplings of H^0 to a pair of SM gauge bosons exactly vanish¹⁴. Because of the presence of an

¹³The minus sign here is conventional. It corresponds to an unphysical $\gamma \rightarrow \gamma + 2\pi$ and $\delta \rightarrow \delta + 2\pi$ redefinition of one of the custodial and CP symmetries eigenstates in (2.55) and (2.66). This specific choice allows us to recover definitions of h^0 and H^0 similar to those obtained in the MSSM when $\beta - \alpha = \pi/2$, regarding the particular definition of α in (2.80).

¹⁴This is related to the existence of two equivalent definitions of the CP transformation of the fields in some limit of the potential parameter, like explained in section 2.4.2

accidental \mathbb{Z}_2 symmetry in the potential, the new bosons belonging to H_2 , i.e. H^\pm , H^0 and A^0 , also always come in pairs in all three- and four-bosons vertices.

Chapter 3

Constraints on the twisted 2HDM

“We live on an island surrounded by a sea of ignorance. As our island of knowledge grows, so does the shore of our ignorance.”

John A. Wheeler (1911 - 2008)

This chapter is dedicated to an overview of the theoretical, indirect and direct constraints which may restrict the parameter space of the twisted 2HDM introduced in section 2.6. Since in this scenario, the CP -even Higgs boson h^0 displays exactly the same couplings to the SM particles as the SM Higgs boson, most of these constraints come from the phenomenological implications of the presence of the new scalar states, A^0 , H^0 and H^\pm .

3.1 Theoretical constraints

3.1.1 Vacuum stability and minimum constraints

The vacuum stability constraints come from the requirement of a positive potential for large classical values of the fields in an arbitrary direction in the (ϕ_1, ϕ_2) plane. These constraints can be obtained by considering only the quartic terms of the potential [101,

89]. If one defines the classical combinations $x_1 \equiv \phi_1^\dagger \phi_1$ and $x_2 \equiv \phi_2^\dagger \phi_2$, then $\phi_1^\dagger \phi_2 = c\sqrt{x_1 x_2} e^{i\alpha}$ with $c < 0$ thanks to the Cauchy-Schwartz inequality.

From $x_1, x_2 > 0$ one can trivially derive

$$\Lambda_S > 0 \quad (3.1)$$

while the condition

$$4\Lambda_S > |\Lambda_{AS}| \quad \text{if} \quad \Lambda_{AS} < 0 \quad (3.2)$$

is obtained in the limit where $c = \pm 1$. In terms of masses, these conditions are equivalent to

$$m_{h^0}^2 > 0 \quad \text{and} \quad m_{h^0}^2 > m_T^2 - m_{A^0}^2 \quad . \quad (3.3)$$

Since condition (2.26) describes *extrema* of the potential, but not necessarily *minima*, an additional constraint should hold on the matrix of second derivatives of the potential. The eigenvalues of this matrix being directly related to the squared masses of physical fields, the minimum hypothesis is enforced by requiring

$$m_{h^0, H^0, A^0, H^\pm}^2 > 0 \quad . \quad (3.4)$$

Finally, the minimum found with the *local* conditions mentioned above is also *global* as can be derived explicitly by considering equations 2.27 together with the expression of the twisted 2HDM potential 2.87. More generally, this may be related to the simultaneous presence of the CP and \mathbb{Z}_2 symmetries in the Higgs basis, e.g. see [102].

3.1.2 Unitarity and perturbativity constraints

The unitarity constraints arising in a two-Higgs-doublet model due to the presence of additional scalar-scalar scattering amplitudes have been worked out for both CP conserving and CP violating potentials [103, 104]. They can be advantageously summarised as

$$|\Lambda_{YI^3}^{\mathbb{Z}_2}| < 8\pi \quad (3.5)$$

where $|\Lambda_{YI^3}^{\mathbb{Z}_2}|$ are the eigenvalues of the high energy scattering matrix for different quantum numbers of the initial state: total hypercharge Y , weak isospin I^3 and \mathbb{Z}_2 parity.

In the twisted scenario (2.87), the relevant contributions are

$$\begin{aligned}
\Lambda_{21}^{\text{even}} &= 2\Lambda_S \pm \frac{\Lambda_{AS}}{2} \\
\Lambda_{00}^{\text{even}} &= 6\Lambda_S \pm \left(4\Lambda_S + \frac{\Lambda_{AS}}{2}\right) \\
\Lambda_{00}^{\text{odd}} &= 2\Lambda_S + \Lambda_{AS} \pm \frac{3}{2}\Lambda_{AS}
\end{aligned} \tag{3.6}$$

Using relations (2.88) and (2.90), constraints (3.5) restrict the possible values of the scalar masses. In particular, in the limit where all scalar masses are small except one, namely m_S , one has

$$m_S \lesssim 550 \text{ GeV} \quad . \tag{3.7}$$

If all masses are non negligible, the unitarity requirement may help to restrict, for example, the allowed region in the (m_{A^0}, m_T) plane for different values of m_{h^0} , see Figure 3.1.

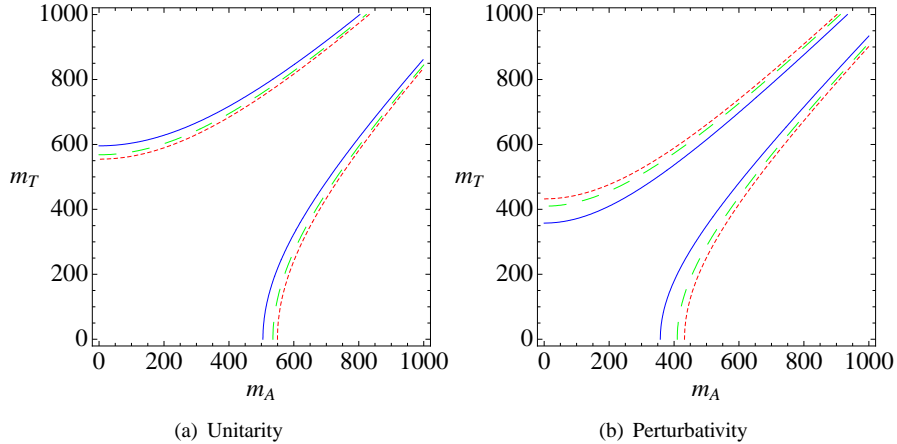


Figure 3.1: Unitarity and perturbativity constraints in the (m_{A^0}, m_T) plane for the twisted 2HDM scenario. Dotted red lines are limits for $m_{h^0} = 120$ GeV, dashed green lines for $m_{h^0} = 300$ GeV and plain blue lines for $m_{h^0} = 500$ GeV. The allowed regions lie between these lines.

Perturbativity constraints may be much stronger than unitarity limits and should in general be taken into account. In the present work, we assume the theory satisfies the perturbative requirement if all the dimensionless combinations of parameters appearing in the three- and four- scalar vertices of Appendix A are bounded by 4π , such that

the effective parameter of perturbation theory is smaller than one. In terms of scalar masses, the resulting bounds are shown on Figure 3.1.

The perturbativity requirement also restricts the allowed values for the Yukawa couplings to fermions, but it is in general a much weaker restriction than precision electroweak tests. In the context of the present work, we restrict the Yukawa coupling of all physical scalar bosons to be smaller or equal to the top Yukawa coupling in the SM, i.e. $\tan \beta \lesssim 1$ in type I models and $\tan \beta \lesssim m_t/m_b$ in type II models.

Let us emphasize that our treatment of the perturbativity constraint is not necessarily the most generic one. As advocated in [105], a more robust limit could be, for example, obtained by imposing that the perturbative expansion of the β -functions appearing in the model parameters RGEs remains consistent, i.e. that any higher loop order contribution remains smaller than any lower loop contribution.

Nevertheless, this method implies the complex calculation of a large set of higher order corrections and gives anyway results similar to those obtained with a simple 4π bound for well-known models like the SM or the MSSM. From a more pragmatic point of view, the perturbativity bound should also be seen more as a somewhat fuzzy limit for our perturbative approach, above which non-perturbative effects due for example to the presence of very large resonances play a non negligible role, than as a strict theoretical restriction.

3.2 Indirect constraints

3.2.1 Electroweak precision parameters

The ρ parameter introduced in section 1.4.2 is a good measurement of the breaking of the *vectorial* part of the $SU(2)_L$ symmetry. In particular, it is highly sensible to the presence of heavy non-degenerate doublets transforming under this symmetry. Nevertheless, it is also important to quantify the effects due to the presence of heavy degenerate doublets contributing for example to the breaking of the *axial* part of $SU(2)_L$.

The following three parameters are necessary¹ to describe all the one-loop BSM electroweak effects [108]:

$$\begin{aligned}\alpha T &= \frac{1}{m_W^2} (\Pi^{WW}(0) - c_W^2 \Pi^{ZZ}(0)) = \Delta\rho, \\ \alpha S &= \frac{4s_W^2 c_W^2}{m_Z^2} \left(\Delta\Pi^{ZZ}(m_Z^2) - \frac{c_W^2 - s_W^2}{s_W c_W} \Delta\Pi^{\gamma Z}(m_Z^2) - \Delta\Pi^{\gamma\gamma}(m_Z^2) \right), \\ \alpha(S+U) &= 4s_W^2 \left(\frac{\Delta\Pi^{WW}(m_W^2)}{m_W^2} - \frac{c_W}{s_W} \frac{\Delta\Pi^{\gamma Z}(m_Z^2)}{m_Z^2} - \frac{\Delta\Pi^{\gamma\gamma}(m_Z^2)}{m_Z^2} \right)\end{aligned}$$

where $\Delta\Pi(k^2) \equiv \Pi(k^2) - \Pi(0)$. The T parameter is a simple redefinition of ρ , i.e. it is proportional to the breaking of the vectorial part of $SU(2)_L$. The S parameter is associated to the difference between the self-energy of the Z^0 boson at $k^2 = m_Z^2$ and $k^2 = 0$. The $S + U$ parameter is defined in the same way for the W^\pm bosons. These two last parameters reflect the breaking of the axial part of $SU(2)_L$ by mass terms. S , T and U are defined with an α factor factorized, and with all SM contributions (including those associated with a Higgs boson) explicitly removed. They are then expected to be of order of unity in the presence of new physics and zero otherwise. The current experimental situation for these parameters is partially summarised on Figure 3.2 and the SM Higgs boson contribution is visible on Figure 3.3.

The T parameter

The total contribution of new scalar states to the T parameter in the context of the most generic multi-Higgs-doublet model has been computed recently in [109]. In the context of the present work, we are only interested in the restricted expression of these corrections in the framework of a simple CP conserving 2HDM. The result is known for a long time in the limit where all scalar squared masses are bigger than m_Z^2 (see [99, 24] or [29] for a review of the calculation). If one of the scalar is lighter than m_Z , however, the exact expression obtained in [110] and reported in [111] gives a more

¹But they may be not sufficient. Strictly speaking, three additional parameters, namely V , W and X , are needed if the new physics scale is comparable with m_Z [106]. However, the explicit expressions obtained in [107] for these parameters in the generic 2HDM show that they only contain subleading contributions and that they are in general dominated by at least one of the usual oblique parameters.

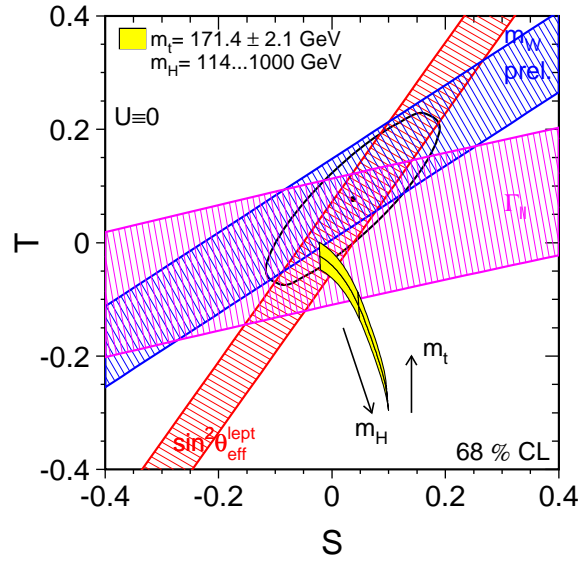


Figure 3.2: Current experimental constraints on the S and T precision electroweak parameters (assuming $U = 0$) from [30]. All limits are at 1σ and the $(S, T) = (0, 0)$ SM reference point corresponds to $\alpha_s=0.118$, $m_Z=91.1875$ GeV, $m_t=175$ GeV and $m_{t,0}=150$ GeV. Since the reference top quark mass does not belong to the experimental interval anymore, the yellow band does not include $(0, 0)$.

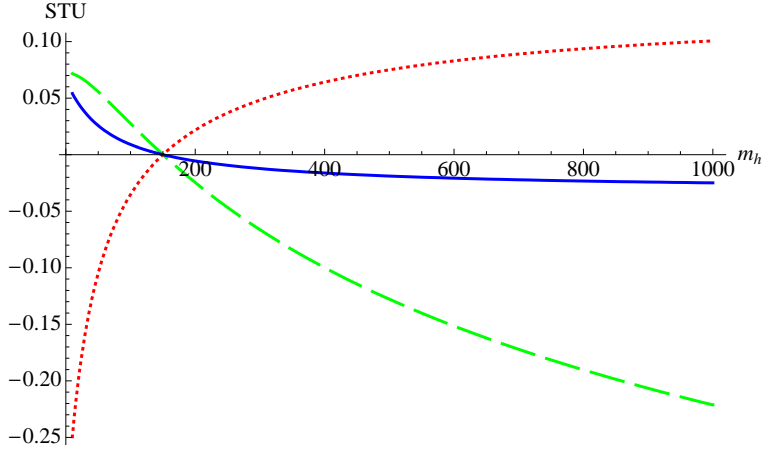


Figure 3.3: Contribution of the SM Higgs boson to the S (dotted red), T (dashed green) and U (plain blue) electroweak oblique parameters. The reference point is set as on Fig. 3.2.

precise prediction. It reads

$$\begin{aligned} \Delta T = & \frac{1}{16\pi \sin^2 \theta_W m_W^2} \{ F(m_{H^\pm}^2, m_{A^0}^2) \\ & + \sin^2(\beta - \alpha) [F(m_{H^\pm}^2, m_{H^0}^2) - F(m_{A^0}^2, m_{H^0}^2)] \\ & + \cos^2(\beta - \alpha) [F(m_{H^\pm}^2, m_{h^0}^2) - F(m_{A^0}^2, m_{h^0}^2) + F(m_W^2, m_{H^0}^2) \\ & - F(m_W^2, m_{h^0}^2) - F(m_Z^2, m_{H^0}^2) + F(m_Z^2, m_{h^0}^2) \\ & + 4m_Z^2 \overline{B}_0(m_Z^2, m_{H^0}^2, m_{h^0}^2) - 4m_W^2 \overline{B}_0(m_W^2, m_{H^0}^2, m_{h^0}^2)] \} \quad (3.8) \end{aligned}$$

where

$$F(m_1^2, m_2^2) = \frac{m_1^2 + m_2^2}{2} - \frac{m_1^2 m_2^2}{m_1^2 - m_2^2} \ln \frac{m_1^2}{m_2^2} . \quad (3.9)$$

and

$$\overline{B}_0(m_1^2, m_2^2, m_3^2) = \frac{m_1^2 \log m_1^2 - m_3^2 \log m_3^2}{m_1^2 - m_3^2} - \frac{m_1^2 \log m_1^2 - m_2^2 \log m_2^2}{m_1^2 - m_2^2} \quad (3.10)$$

In this expression (and in all the forthcoming ones), the SM Higgs correction with reference choice $(m_{h^0}^{SM})_{\text{ref}} = m_{h^0}$ has been explicitly subtracted.

The numerical result of this calculation is shown on Figure 3.4 as a function of m_{H^\pm} for different values of $(\beta - \alpha)$ and for fixed values of all other scalar masses. One can

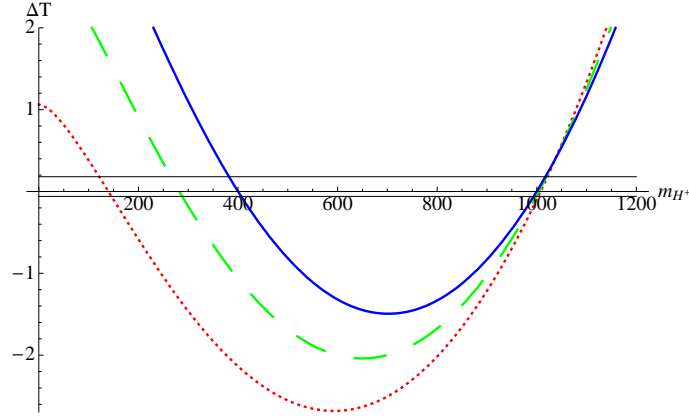


Figure 3.4: ΔT correction in a CP conserving 2HDM as defined in (3.8) with respect to the charged Higgs pair mass (in GeV), for different values of $(\beta - \alpha)$: 0 (dotted red), $\pi/4$ (dashed green) and $\pi/2$ (plain blue). The other scalars masses are fixed to $m_{h^0} = 150$ GeV, $m_{H^0} = 400$ GeV and $m_{A^0} = 1$ TeV. The thin horizontal black lines shows the 2σ limits on ΔT (assuming $\Delta S = 0$) from [30].

easily distinguish four situations where ΔT is close to zero:

1. When $m_{H^\pm} \approx m_{A^0}$, whatever the value of the other parameters
2. When $m_{H^\pm} \approx m_{H^0}$ and $\beta - \alpha = \pi/2$
3. When $m_{H^\pm} \approx m_{h^0}$ and $\beta - \alpha = 0$
4. A continuum of solutions where $m_{H^\pm} \in]m_{h^0}, m_{H^0}[$ and $\beta - \alpha \in]0, \pi/2[$

The first possibility corresponds to the “usual” custodial scenario while the following ones correspond to the “twisted” situation described in the previous chapter. The presence of two realisations of this last possibility, $m_{H^\pm} = m_{h^0}$ and $m_{H^\pm} = m_{H^0}$, is easily understood as an interchange in the definition of h^0 and H^0 (equivalent to a $\pi/2$ shift in α), see Eq. (2.80). The existence of a continuum of solutions between these two extreme possibilities corresponds to cases where the state S^3 belonging to the custodial triplet (see Eq. 2.53) is not a mass eigenstate but a mixture of h^0 and H^0 . These results can also be verified directly by considering the analytic expression (3.8) and the symmetry properties of the function $F(m_1^2, m_2^2)$, namely $F(m_1^2, m_2^2) = F(m_2^2, m_1^2)$ and $F(m^2, m^2) = 0$.

An interesting possibility in the framework of the twisted 2HDM arises when the pseudoscalar state A^0 is (moderately) light while all the other scalars are heavy (\gg

100 GeV). In this case, a slight deviation from the degeneracy $m_{H^\pm} = m_{H^0}$, due to either loop corrections² or to the presence of small custodial breaking terms in the potential, could compensate for large logarithmic contributions involving m_{h^0} . As shown in [75], this can be seen directly from the expression of the first order approximation of ΔT in the $m_{H^\pm} \approx m_{H^0}$ region:

$$\Delta T \approx \frac{1}{16\pi m_W^2 \cos^2 \theta_W} \times \left\{ \cot^2 \theta_W \frac{m_{H^\pm}^2 - m_{H^0}^2}{2} - 3m_W^2 \left[\log \frac{m_{h^0}^2}{m_W^2} + \frac{1}{\sin^2 \theta_W} \log \frac{m_W^2}{m_Z^2} + \frac{1}{6} \right] \right\} . \quad (3.11)$$

An estimate of the amount of breaking required for a vanishing T as a function of the h^0 Higgs mass can be found on Fig. 3.5.

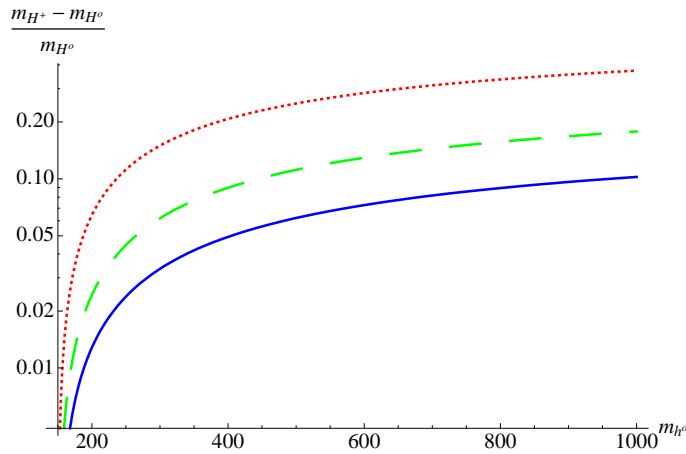


Figure 3.5: Relative mass difference $(m_{H^\pm} - m_{H^0})/m_{H^0}$ required to achieve $\Delta T = 0$ with respect to the SM-like Higgs boson mass m_{h^0} (in GeV) in the twisted 2HDM scenario. The dotted red, dashed green and plain blue lines correspond respectively to $m_{H^0}=200, 300$ and 400 GeV. The A^0 mass is fixed at 100 GeV but does not affect sizeably the results if $m_{A^0} \ll m_{h^0}, m_T$.

The S and U parameter

Contrary to the T parameter, the S and U parameters can only depend logarithmically on the mass of the new scalar particles. The exact one loop additional contributions in

²A naive estimation involving only bosonic corrections gives the right sign for the mass difference.

a generic CP conserving 2HDM read [110, 111]

$$\begin{aligned}
\Delta S &= \frac{1}{\pi m_Z^2} \left\{ \sin^2(\beta - \alpha) \mathcal{B}_{22}(m_Z^2; m_{H^0}^2, m_{A^0}^2) - \mathcal{B}_{22}(m_Z^2; m_{H^\pm}^2, m_{H^\pm}^2) \right. \\
&\quad + \cos^2(\beta - \alpha) \left[\mathcal{B}_{22}(m_Z^2; m_{h^0}^2, m_{A^0}^2) + \mathcal{B}_{22}(m_Z^2; m_Z^2, m_{H^0}^2) \right. \\
&\quad \left. \left. - \mathcal{B}_{22}(m_Z^2; m_Z^2, m_{h^0}^2) - m_Z^2 \mathcal{B}_0(m_Z^2; m_Z^2, m_{H^0}^2) + m_Z^2 \mathcal{B}_0(m_Z^2; m_Z^2, m_{h^0}^2) \right] \right\} \\
\Delta U &= -\Delta S + \frac{1}{\pi m_Z^2} \left\{ \mathcal{B}_{22}(m_W^2; m_{A^0}^2, m_{H^\pm}^2) - 2\mathcal{B}_{22}(m_W^2; m_{H^\pm}^2, m_{H^\pm}^2) \right. \\
&\quad + \sin^2(\beta - \alpha) \mathcal{B}_{22}(m_W^2; m_{H^0}^2, m_{H^\pm}^2) + \cos^2(\beta - \alpha) \left[\mathcal{B}_{22}(m_W^2; m_{h^0}^2, m_{H^\pm}^2) \right. \\
&\quad + \mathcal{B}_{22}(m_W^2; m_W^2, m_{H^0}^2) - \mathcal{B}_{22}(m_W^2; m_W^2, m_{h^0}^2) \\
&\quad \left. \left. - m_W^2 \mathcal{B}_0(m_W^2; m_W^2, m_{H^0}^2) + m_W^2 \mathcal{B}_0(m_W^2; m_W^2, m_{h^0}^2) \right] \right\} \quad (3.12)
\end{aligned}$$

where

$$\mathcal{B}_0(q^2; m_1^2, m_2^2) = 1 + \frac{1}{2} \left[\frac{x_1 + x_2}{x_1 - x_2} - (x_1 - x_2) \right] \log \frac{x_1}{x_2} + \frac{1}{2} f(x_1, x_2) \quad , \quad (3.13)$$

$$\begin{aligned}
\mathcal{B}_{22}(q^2; m_1^2, m_2^2) &= \frac{q^2}{24} \left\{ 2 \log q^2 + \log(x_1 x_2) + [(x_1 - x_2)^3 - 3(x_1^2 - x_2^2) \right. \\
&\quad + 3(x_1 - x_2)^2] \log \frac{x_1}{x_2} - \left[2(x_1 - x_2)^2 - 8(x_1 + x_2) + \frac{10}{3} \right] \\
&\quad - [(x_1 - x_2)^2 - 2(x_1 + x_2) + 1] f(x_1, x_2) \\
&\quad \left. - 6F(x_1, x_2) \right\} \quad , \quad (3.14)
\end{aligned}$$

$$f(x_1, x_2) = \begin{cases} -2\sqrt{\Delta} \left[\arctan \frac{x_1 - x_2 + 1}{\sqrt{\Delta}} - \arctan \frac{x_1 - x_2 - 1}{\sqrt{\Delta}} \right], & \Delta > 0 \\ 0 & \Delta = 0 \\ \sqrt{-\Delta} \log \frac{x_1 + x_2 - 1 + \sqrt{-\Delta}}{x_1 + x_2 - 1 - \sqrt{-\Delta}} & \Delta < 0 \end{cases} \quad (3.15)$$

$$\Delta \equiv 2(x_1 + x_2) - (x_1 - x_2)^2 - 1 \quad , \quad (3.16)$$

and $x_i \equiv m_i^2/q^2$.

The numerical results for these contributions are shown on Figure 3.6. By comparing these results with the SM contribution shown on Figure 3.3, one can easily see that scenarios with a light pseudoscalar and a heavy degenerate triplet are favoured by both S and U parameters. Indeed, in this region of the parameter space, the 2HDM contribution has an opposite sign compare to the SM one. For sufficiently small pseudoscalar masses (and large triplet masses), this extra contribution could even partially compensate for a large positive contribution to the S parameter due to an heavy (≈ 300 GeV)

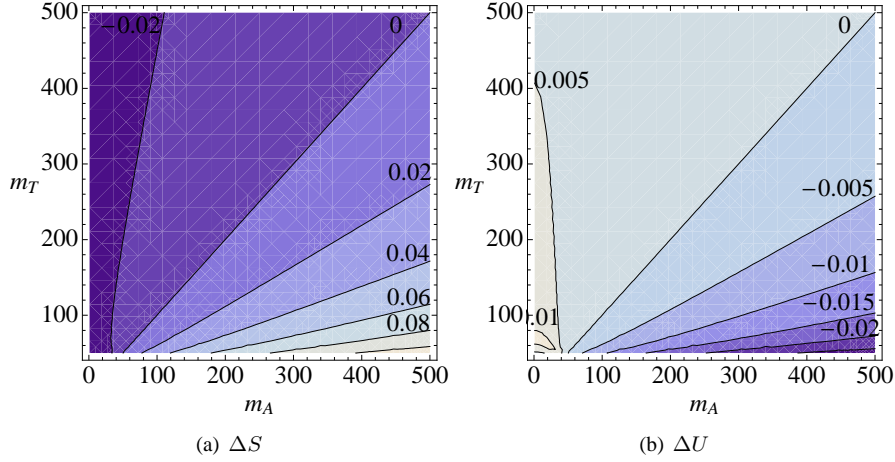


Figure 3.6: ΔS and ΔU parameters in a twisted 2HDM ($\beta - \alpha = \pi/2$, $m_{H^0} \approx m_{H^\pm}$) as a function of m_{A^0} and m_T (in GeV). The reference point is fixed as on Fig. 3.2.

SM Higgs. *A contrario*, scenarios with a very heavy pseudoscalar and a light triplet are disfavoured or even excluded (depending on the actual value of the T parameter) by the upper experimental bounds on S .

3.2.2 Bottom quark physics

The $\bar{B} \rightarrow X_s \gamma$ decay

The $\bar{B} \rightarrow X_s \gamma$ branching rate was early found to put stringent bound on the charged Higgs boson masses. In the generic 2HDM, and at leading logarithmic order (LO), it is given by (in units of the branching ratio for the semileptonic b decay) [112]:

$$\frac{\text{BR}(b \rightarrow s\gamma)}{\text{BR}(b \rightarrow ce\bar{\nu})} = \frac{6\alpha}{\pi} \frac{\left[\eta^{\frac{16}{23}} A_\gamma + \frac{8}{3} (\eta^{\frac{14}{23}} - \eta^{\frac{16}{23}}) A_g + C \right]^2}{I(m_c/m_b) \left[1 - \frac{2}{3\pi} \alpha_s(m_b) f(m_c/m_b) \right]} \quad (3.17)$$

where $\eta = \alpha_s(m_Z)/\alpha_s(m_b)$, I is a phase factor, f is a QCD correction factor for the semileptonic process ($f(m_c/m_b) = 2.41$), and C is a coefficient coming from operator mixing in the leading logarithmic QCD corrections ($C \simeq -0.177$). Finally A_γ and A_g are the coefficients of the effective operators $\bar{s}_L \sigma^{\mu\nu} b_R F_{\mu\nu}$ and $\bar{s}_L \sigma^{\mu\nu} T^a b_R G_{\mu\nu}^a$.

The contributions to $A_{\gamma,g}$ from W and charged Higgs bosons have been computed respectively in [113] and [114, 115]. They read

$$\begin{aligned} A_{\gamma,g}^W &= \frac{3}{2} \frac{m_t^2}{m_W^2} f_{\gamma,g}^{(1)} \left(\frac{m_t^2}{m_W^2} \right) \\ A_{\gamma,g}^H &= \frac{1}{2} \frac{m_t^2}{m_{H^\pm}^2} \left[|Y|^2 f_{\gamma,g}^{(1)} \left(\frac{m_t^2}{m_{H^\pm}^2} \right) + XY^* f_{\gamma,g}^{(2)} \left(\frac{m_t^2}{m_{H^\pm}^2} \right) \right] \end{aligned} \quad (3.18)$$

where X and Y are the couplings of the positively charged Higgs boson to the $\bar{u}_L d_R$ and $\bar{u}_R d_L$ leptonic currents (discarding additional mass and CKM factors). In the type I and type II models considered here (see Appendix A), one has

$$\text{Type I} : \quad X = -\tan\beta \quad Y = \tan\beta \quad (3.19)$$

$$\text{Type II} : \quad X = \tan\beta \quad Y = \cot\beta \quad (3.20)$$

The Inami-Lim functions f appearing in (3.18) read

$$\begin{aligned} f_\gamma^{(1)} &= \frac{(7 - 5x - 8x^2)}{36(x-1)^3} + \frac{x(3x-2)}{6(x-1)^4} \log x \\ f_\gamma^{(2)} &= \frac{(3-5x)}{6(x-1)^2} + \frac{(3x-2)}{3(x-1)^3} \log x \\ f_g^{(1)} &= \frac{(2+5x-x^2)}{12(x-1)^3} - \frac{x}{2(x-1)^4} \log x \\ f_g^{(2)} &= \frac{(3-x)}{2(x-1)^2} - \frac{1}{(x-1)^3} \log x \end{aligned} \quad (3.21)$$

The numerical results for the LO contributions are displayed on Figure 3.7 as exclusion limits in the $(\tan\beta, m_{H^\pm})$ plane, both for type I and type II models, taking into account the world average of the experimental value by the Heavy Flavor Averaging Group [116]:

$$\text{BR}(\bar{B} \rightarrow X_s \gamma) = (3.55 \pm 0.24_{-0.10}^{+0.09} \pm 0.03) \times 10^{-4} \quad (3.22)$$

On these plots, the LO contribution is scaled to fit the NNLO SM prediction [117]

$$\text{BR}(\bar{B} \rightarrow X_s \gamma) = (3.15 \pm 0.23) \times 10^{-4} \quad (3.23)$$

in the decoupling limit $m_{H^\pm} \rightarrow \infty$ and the theoretical error associated to this value is added in quadrature to the experimental error. As expected, the small $\tan\beta$ region for a type I 2HDM is left unconstrained since, in this case, the charged Higgs bosons

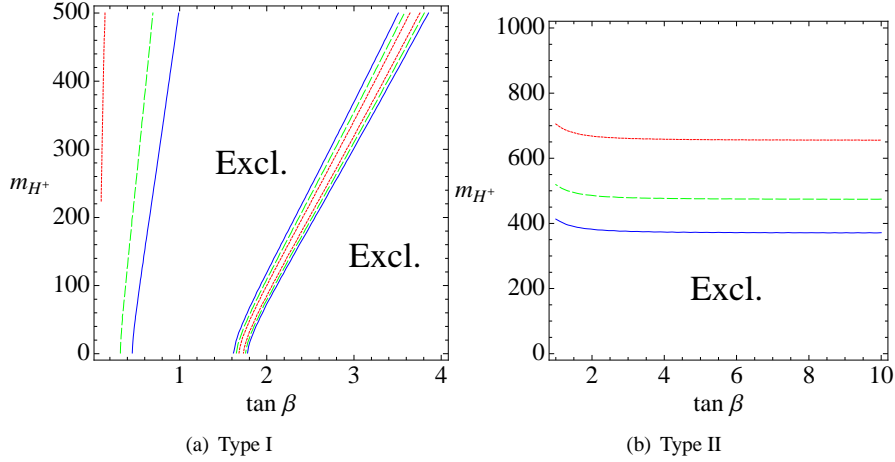


Figure 3.7: Leading order $b \rightarrow s\gamma$ bounds on the charged Higgs mass (in GeV) with respect to $\tan\beta$ in (a) type I and (b) type II scenarios, at one (dotted red), two (dashed green) and three (plain blue) standard deviations.

decouple from fermions. For larger values of $\tan\beta$, only a very small region of the parameter space survives the constraint. In type II models, the lower bound on the charged Higgs mass ($\gtrsim 500$ GeV at 95% CL) is essentially independent of $\tan\beta$ as soon as $\tan\beta > 2$, due to the identity $XY^* = 1$.

The SM leading order prediction of the $\overline{B} \rightarrow X_s\gamma$ branching suffers from large uncertainties which can be partially reduced by computing the main NLO and NNLO corrections. For the 2HDM, an estimation of the NLO corrections in Ref. [118] shows a sizeable effect (see Figure 3.8) which is sufficient to drastically reduce the lower bound obtained at LO. The current status for a type II model is summarised in [117]. The 95% (99%) lower bound amounts to around 295 (230) GeV and stays practically constant down to $\tan\beta \simeq 2$. Experimental results may even be interpreted as favouring a charged Higgs mass of around 650 GeV. Type I scenarios at low $\tan\beta$ values are close to the decoupling limit, such that the new physics corrections are generally small in magnitude (but of opposite sign compare to type II) and the NLO effects are not relevant (e.g. see Ref. [119] for a discussion). At higher $\tan\beta$ values, the strong coupling regime is quickly reached and even the NLO prediction are, at times, ill-defined (i.e. highly scale dependent) in this region. In the following we only consider the $\tan\beta \lesssim 0.5$ region and discard the open possibility for high $\tan\beta$ values.

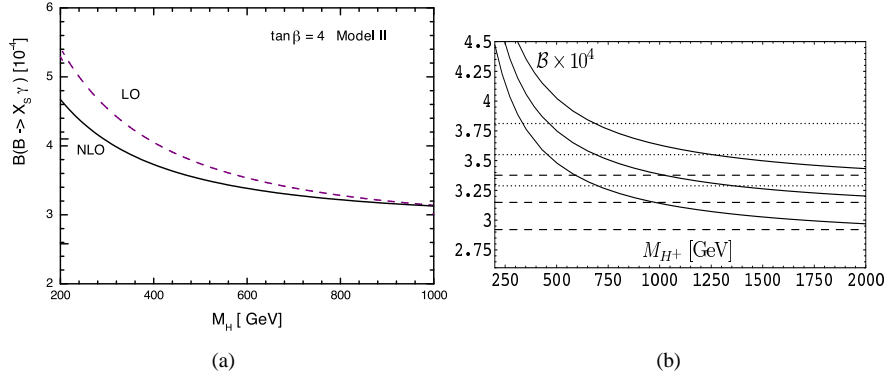


Figure 3.8: (a) Comparison of the LO and NLO predictions for the $\bar{B} \rightarrow X_s \gamma$ branching rate as a function of the charged Higgs mass in a type II model ($\tan\beta = 4$), adapted from Ref. [119]. (b) Same figure for $\tan\beta = 2$, compared to the best SM NNLO prediction (dashed lines) and experimental measurement (dotted lines), from Ref. [117].

The $B \rightarrow \tau\nu_\tau$ and $B \rightarrow D\tau\nu_\tau$ decays

If the charged Higgs bosons couple strongly enough to the $\bar{b}c$ or $\bar{b}u$ quark currents, and at the same time to the $\tau\bar{\nu}_\tau$ leptonic current (i.e., in type II scenarios with large $\tan\beta$), they could sizeably affect the $B \rightarrow \tau\nu_\tau$ and $B \rightarrow D\tau\nu_\tau$ branching ratios.

The normalised³ branching ratio

$$R^{\text{exp}} \equiv \frac{\text{BR}(B \rightarrow D\tau\nu_\tau)}{\text{BR}(B \rightarrow D\ell\nu_\ell)} = (41.6 \pm 11.7 \pm 5.2)\% \quad (3.24)$$

recently measured by the BaBar collaboration [120] depends on the effective coupling constant $g_S \equiv m_B^2 \tan\beta^2 / m_{H^\pm}^2$ as on Figure 3.9. Translating the 2σ conservative bound $g_S \lesssim 1.5$ extracted from this plot as a bound on the 2HDM type II parameter space, one gets

$$\tan\beta \lesssim 0.23 \text{ GeV}^{-1} \times m_{H^\pm} \quad . \quad (3.25)$$

Regarding the lower bound on m_{H^\pm} from the $b \rightarrow s\gamma$ process, this last constraint can only be relevant in the very high $\tan\beta$ region ($\tan\beta \gtrsim 70$) which is already discarded by the requirement of perturbativity for the Yukawa couplings.

³The normalization reduces the dependence on the vector form factor and thus tames the main theoretical uncertainties.

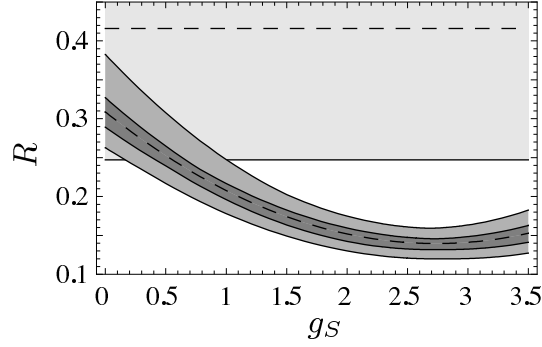


Figure 3.9: R as a function of g_S . The light gray band shows the experimental value (with one sigma errors). The gray and dark gray bands show the theoretical prediction, with and without systematic uncertainties on the form factors. From Ref. [121].

A similar bound can be obtained from the rare process $B \rightarrow \tau\nu_\tau$. Considering the relative importance of the recent experimental result from Belle [122] compared to the best SM prediction

$$\frac{\text{BR}(B \rightarrow \tau\nu_\tau)}{\text{BR}(B \rightarrow \tau\nu_\tau)_{SM}} = 1.13 \pm 0.44 \quad (3.26)$$

where only the experimental error has been considered, and the theoretical prediction for this ratio in a 2HDM type II model (e.g. see [123] for a review of the calculation in the Minimal Flavour Violation hypothesis framework):

$$\frac{\text{BR}(B \rightarrow \tau\nu_\tau)}{\text{BR}(B \rightarrow \tau\nu_\tau)_{SM}} = (1 - g_S^2)^2 \quad (3.27)$$

one gets

$$\tan\beta \lesssim 0.13 \text{ GeV}^{-1} \times m_{H^\pm} \quad . \quad (3.28)$$

Assuming $m_{H^\pm} \gtrsim 300$, this constrain may restrict significantly the $\tan\beta \gtrsim 40$ region.

Let us however emphasise that this bound should be considered very carefully: the $B \rightarrow \tau\nu_\tau$ signal “evidence” in the BaBar experiment [124] is still statistically lower than then one obtained by the Belle collaboration, and the large uncertainties associated with the theoretical result from lattice calculations could be highly underestimated.

The $B_0 - \overline{B}_0$ mixing

The virtual effects of the charged Higgs bosons on the $B_d - \overline{B}_d$ oscillations⁴ are described at leading order using the expression

$$\Delta m_B \equiv |M_{B_L} - M_{B_s}| = \frac{f_B^2 B_B m_B |V_{td}|^2 |V_{tb}|^2 m_t^2}{48\pi^2 v^4} (I_{WW} + I_{WH} + I_{HH}) \quad (3.29)$$

obtained in [126]. The mass, decay constant and bag parameter of the B meson are denoted by m_B , f_B and B_B , respectively. The Inami-Lim functions read

$$\begin{aligned} I_{WW} &= 1 + \frac{9}{1-y_W} - \frac{6}{(1-y_W)^2} - \frac{6}{y_W} \left(\frac{y_W}{1-y_W} \right) \log y_W \\ I_{WH} &= |Y|^2 y_H \left(\frac{(2x-8) \log y_H}{(1-x)(1-y_H)^2} + \frac{6x \log y_W}{(1-x)(1-y_W)^2} \right. \\ &\quad \left. - \frac{8-2y_W}{(1-y_W)(1-y_H)} \right) \\ I_{HH} &= |Y|^4 y_H \left(\frac{1+y_H}{(1-y_H)^2} + \frac{2y_H \log y_H}{(1-y_H)^3} \right) \end{aligned} \quad (3.30)$$

with $y_{W,H} \equiv m_t^2/m_{W,H^\pm}^2$, $x \equiv m_{H^\pm}^2/m_W^2$ and where I_{WH} and I_{HH} correspond to the contributions proportional to diagrams with the exchange of one or two charged Higgs bosons.

Like for $b \rightarrow s\gamma$, and in order to avoid discussing the actual choice of the SM parameters values entering this expression (some of them being actually poorly known), we normalise the overall factor to recover the most recent SM prediction from lattice simulations [127]

$$\Delta m_B^{SM} = 0.69 \pm 0.15 \text{ ps}^{-1} \quad (3.31)$$

in the limit where $I_{WH}, I_{HH} \rightarrow 0$, corresponding to $m_{H^\pm} \rightarrow \infty$. Let us however stress that the error associated to this indirect SM prediction is likely to be optimistic, leading to an overestimation of the actual constraints.

The numerical results for the LO contributions are displayed on Figure 3.10. The central value is fixed to the world average [5]

$$\Delta M_B^{exp} = 0.507 \pm 0.005 \text{ ps}^{-1} \quad (3.32)$$

⁴The $B_s - \overline{B}_s$ mixing could also be considered here, but the high degree of correlation between the theoretical errors associated to these two quantities lowers its interest to constrain New Physics, e.g. see Ref. [125].

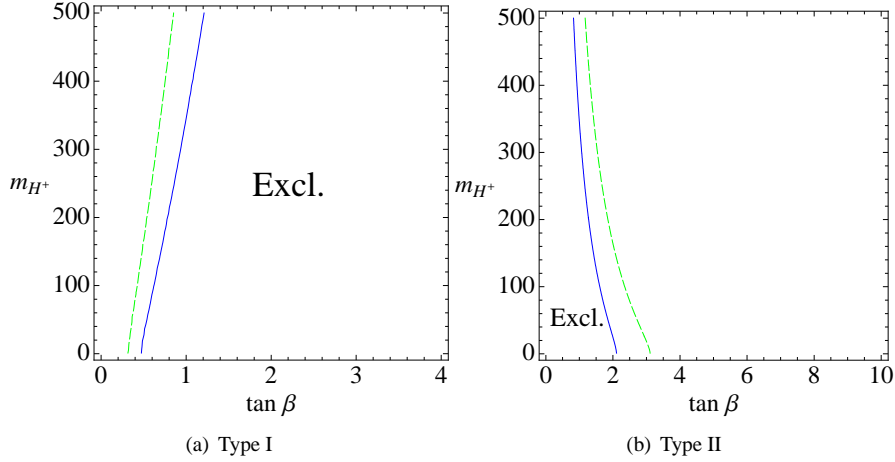


Figure 3.10: Leading order bounds on the charged Higgs mass (in GeV) from the $B_0 - \overline{B}_0$ mixing measurement, with respect to $\tan\beta$ in (a) type I and (b) type II scenarios, at two (dashed green) and three (plain blue) standard deviations. There are no 1σ limits on these figures due to the slight discrepancy between the SM prediction (3.31) and the current experimental measurement (3.32).

and, regarding the impressive experimental precision associated to this measurement, the quoted error is largely dominated by the theoretical uncertainty in (3.31). For type I scenarios, the $\tan\beta \lesssim 0.5 - 1$ constraint obtained on the whole range of charged Higgs masses is similar to the one obtained from the $b \rightarrow s\gamma$ process (see Figure 3.7). In case of type II 2HDMs, the $\tan\beta < 2$ region is excluded at more than 95% CL, almost independently of m_{H^\pm} .

The NLO QCD corrections to (3.29) have been discussed in [128]. They modify both the overall coefficient, making it dependent on Y and m_{H^\pm} , and the functions I . Like in the $b \rightarrow s\gamma$ case, inclusion of $\mathcal{O}(\alpha_s)$ QCD corrections reduces the sensitivity of Δm_B to charged Higgs contributions and slightly weakens the above constraints.

The $Zb\overline{b}$ vertex

Radiative loop corrections to the $Z \rightarrow b\overline{b}$ process involving new charged and neutral scalars (see Figure 3.11) may give sizeable contributions to the observable hadronic branching ratio of Z bosons to $b\overline{b}$

$$R_b \equiv \frac{\Gamma(Z \rightarrow b\overline{b})}{\Gamma(Z \rightarrow \text{hadrons})} \quad (3.33)$$

and to the b quark asymmetry

$$A_b = \frac{g_L^2 - g_R^2}{g_L^2 + g_R^2} \quad (3.34)$$

where g_L and g_R are the left and right handed couplings of Z to b quarks.

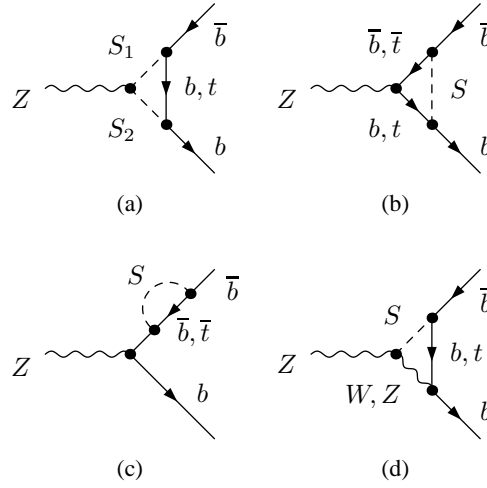


Figure 3.11: Four types of one scalar loop contributions to the $Zb\bar{b}$ vertex. S may stand for a neutral or a charged scalar.

The corrections to g_L and g_R defined as

$$\delta g_{L,R} = g_{L,R}^{\text{true}} - g_{L,R}^{SM} \quad (3.35)$$

have been derived in great detail in [129] in the context of CP conserving 2HDMs. They can be related at first order to the corrections to R_b and A_b through

$$\begin{aligned} \delta R_b &= -0.7788 \delta g_L + 0.1410 \delta g_R \\ \delta A_b &= -0.2984 \delta g_L - 1.623 \delta g_R \end{aligned} \quad (3.36)$$

such that δR_b (δA_b) is mainly dominated by the δg_L (δg_R) correction. The latest experimental values [5]

$$\begin{aligned} R_b &= 0.21629 \pm 0.00066 \\ A_b &= 0.923 \pm 0.020 \end{aligned} \quad (3.37)$$

agree at less than one standard deviation with the SM prediction

$$\begin{aligned} R_b &= 0.21578 \pm 0.00010 \\ A_b &= 0.9347 \pm 0.0001 \end{aligned} \quad (3.38)$$

for which the theoretical error is nearly one order of magnitude smaller than the experimental one and can be safely neglected.

The contributions of diagrams 3.11(a), 3.11(b) and 3.11(c) for the neutral scalar states read, in a twisted 2HDM,

$$\delta g_{R,L}(a) = \pm \frac{1}{16\pi^2} \frac{e}{s_W c_W} \left(\frac{\sqrt{2} m_b \tan \beta}{v} \right)^2 C_{24}(m_b^2, m_{H^0}^2, m_{A^0}^2) \quad (3.39)$$

$$\begin{aligned} \delta g_{R,L}(b) &= -\frac{1}{16\pi^2} g_{Zb\bar{b}}^{L,R} \left(\frac{\sqrt{2} m_b}{v} \right)^2 [C_{234}(m_{h^0}^2, m_b^2, m_b^2) \\ &\quad + \tan^2 \beta (C_{234}(m_{H^0}^2, m_b^2, m_b^2) + C_{234}(m_{A^0}^2, m_b^2, m_b^2))] \end{aligned} \quad (3.40)$$

$$\begin{aligned} \delta g_{R,L}(c) &= -\frac{1}{16\pi^2} g_{Zb\bar{b}}^{L,R} \left(\frac{\sqrt{2} m_b}{v} \right)^2 [B_1(m_b^2; m_b^2, m_{h^0}^2) \\ &\quad + \tan^2 \beta (B_1(m_b^2; m_b^2, m_{H^0}^2) + B_1(m_b^2; m_b^2, m_{A^0}^2))] \end{aligned} \quad (3.41)$$

where

$$C_{234} \equiv -2C_{24} + \frac{1}{2} - m_Z^2 (C_{22} - C_{23}) \quad . \quad (3.42)$$

The B_i and C_{ij} functions correspond respectively to the two- and three-point 't Hooft-Passarino-Veltman one-loop integrals and are defined like in Appendix F of Ref. [129]. The $Zb\bar{b}$ SM tree-level couplings are given by

$$g_{Zb\bar{b}}^L = \frac{e}{s_W c_W} \left(-\frac{1}{2} + \frac{1}{3} s_W^2 \right) \quad (3.43)$$

$$g_{Zb\bar{b}}^R = \frac{e}{s_W c_W} \left(\frac{1}{3} s_W^2 \right) \quad . \quad (3.44)$$

We neglect the contribution associated to the diagrams 3.11(d) which is suppressed by a factor m_b/m_Z compare to the other ones.

The same contributions, but for the charged scalar states, can be simplified to

$$\delta g_L = \frac{1}{16\pi^2} \left(\frac{\sqrt{2}m_t}{v} Y \right)^2 \frac{e}{2s_W c_W} \left[\frac{R}{R-1} - \frac{R \log R}{(R-1)^2} \right] \quad (3.45)$$

$$\delta g_R = \frac{1}{16\pi^2} \left(\frac{\sqrt{2}m_b}{v} X \right)^2 \frac{e}{2s_W c_W} \left[\frac{R}{R-1} - \frac{R \log R}{(R-1)^2} \right] \quad (3.46)$$

where $R \equiv m_t^2/m_{H^\pm}^2$. Summing all these contributions with the SM predictions (3.38), and requiring the result to be compatible with the experimental measurements (3.38) allows us to put constraints on the twisted 2HDM parameter space.

Since all coefficients in (3.36) are $\mathcal{O}(1)$, corrections to R_b and A_b are typically expected to have similar magnitudes. However, the high experimental precision associated with the R_b measurement makes it much more discriminating than A_b on the whole parameter space, as shown by an explicit numerical analysis. In type I models, the only relevant contribution is the charged Higgs correction to δg_L since all the other ones are suppressed by m_b/v . But the typical bound extracted in this case, $\tan \beta \lesssim 1$, is not relevant when compared to the one coming from the $B_0 - \bar{B}_0$ measurement.

The situation is more interesting in type II models where the neutral scalar contributions are potentially sizeable. The corrections associated to diagrams 3.11(b) and 3.11(c) are similar to those involving the SM Higgs boson, but scaled by $\tan^2 \beta$. Despite this additional factor, they only become relevant for $\tan \beta \gtrsim 50$, i.e. above the perturbativity limit. The amplitude of diagram 3.11(a) vanishes if $S_1 = S_2$ because of the CP symmetry. But if S_1 and S_2 are different particles (with opposite CP parities), it grows with the mass difference ($m_{S_1} - m_{S_2}$).

In the type II twisted 2HDM, this restricts the allowed region in the (m_{A^0}, m_{H^0}) plane as illustrated on Figure 3.12. Since the (H^0, H^\pm) triplet is forced to be rather heavy by the B physics constraints previously reviewed, the mass of the pseudoscalar A^0 is bounded from below. For $\tan \beta = 50$ and $m_{H^\pm} > 300$ GeV, for example, this bound is approximatively $m_{A^0} > 60$ GeV at 95% CL. Note that this bound is somewhat lower than the one obtained in [129] ($m_{A^0} > 100$ GeV). At the time of this work, the experimental value of R_b was indeed sizeably bigger, leaving less room for negative contributions from new physics.

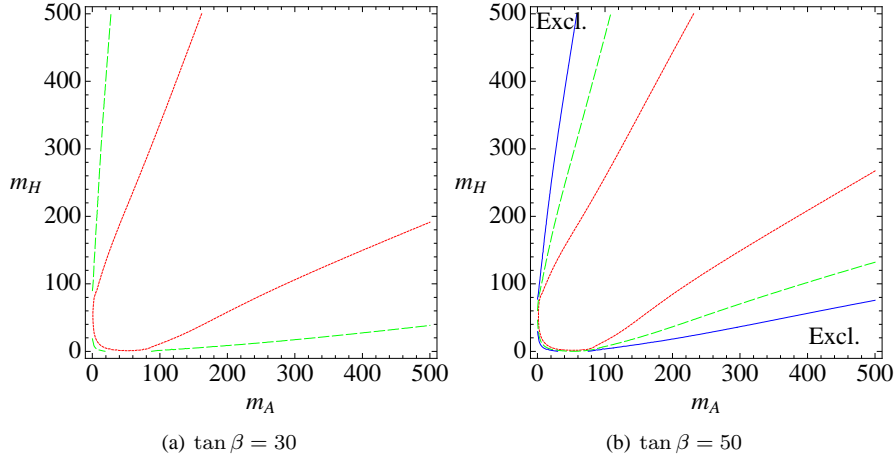


Figure 3.12: Constraints at 1σ (dotted red), 2σ (dashed green) and 3σ (plain blue) on the twisted 2HDM type II parameter space from the R_b measurement, for two $\tan\beta$ hypothesis.

3.2.3 The muon anomalous magnetic moment

The anomalous magnetic moment of the muon

$$a_\mu \equiv \frac{g - 2}{2} \quad (3.47)$$

is known to be a particularly sensible quantity when trying to detect indirectly the presence of specific types of Beyond the Standard Model new physics. A recent prediction, incorporating the $e^+e^- \rightarrow \pi\pi$ data obtained by CMD-2, KLOE and SND, gives [130]

$$a_\mu^{\text{th,SM}} = (11659180.4 \pm 5.1) \times 10^{-10} \quad (3.48)$$

which must be compared to the latest experimental measurement from the Brookhaven experiment [131]

$$a_\mu^{\text{exp}} = (11659208.0 \pm 6.3) \times 10^{-10} \quad (3.49)$$

The 3.4σ deviation between these two values

$$\Delta a_\mu \equiv a_\mu^{\text{exp}} - a_\mu^{\text{th,SM}} = (276 \pm 81) \times 10^{-11} \quad (3.50)$$

may be optimistically interpreted as a signal of new physics, or, at least, as a valuable constraint. Due to the small mass of the muon, this constraint is only relevant for

Higgs physics when the coupling of the Higgs field to leptons is increased compare to its SM value. In the twisted 2HDM considered here, this corresponds to the type II scenario for Yukawa couplings, for which the one- and two-loops contributions are reported in [132].

The relevant one-loop diagrams are presented in Figure 3.13(a) and 3.13(b). The

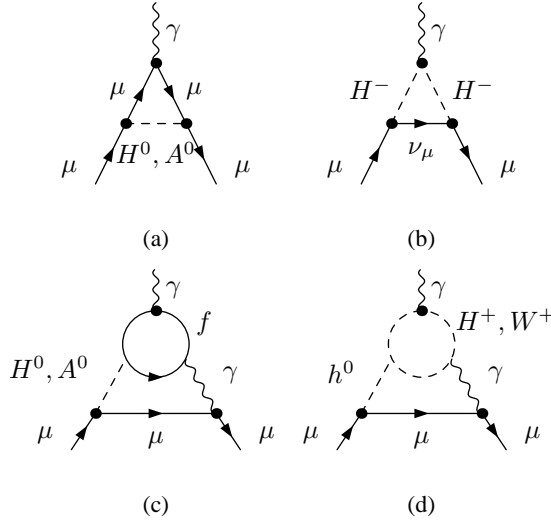


Figure 3.13: One-loop contribution to a_μ due to (a) neutral (pseudo-)scalars and (b) charged Higgs boson exchange. Two-loop contributions to a_μ from (c) a light (pseudo-) scalar with a fermionic loop or (d) from a light scalar with a charged boson loop.

associated contributions are

$$a_\mu^S|_{1\text{-loop}} = \frac{g^2 m_\mu^2 \tan^2 \beta}{32\pi^2 m_W^2} L_S \left(\frac{m_\mu^2}{m_S^2} \right) \quad (3.51)$$

where the loop integrals L_S are given by

$$\begin{aligned} L_{H^0}(z) &= z \int_0^1 dx \frac{x^2(2-x)}{x^2z + (1-x)} \\ L_{A^0}(z) &= z \int_0^1 dx \frac{-x^3}{x^2z + (1-x)} \\ L_{H^\pm}(z) &= z \int_0^1 dx \frac{-x(1-x)}{(x-1)z + 1} . \end{aligned} \quad (3.52)$$

At one loop, the scalar contribution $a_\mu^{H^0}$ is positive whereas the pseudoscalar and the charged Higgs boson give negative contributions. Each contribution reaches its extremum at small masses and vanishes like $m_\mu^2/m_S^2 \log(m_S^2/m_\mu^2)$ at large masses. The absolute magnitude of each type of contribution is shown on Figure 3.14(a) for $\tan\beta = 1$. The total one loop correction is dominated by the neutral contributions

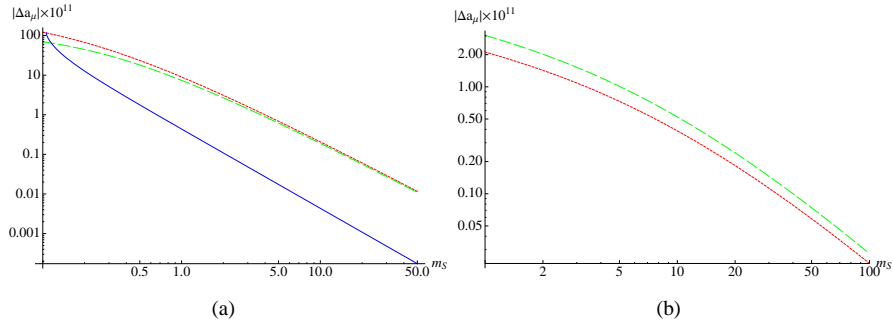


Figure 3.14: (a) Absolute value of the one loop contribution to a_μ from a neutral scalar H^0 (dotted red), a pseudoscalar A^0 (dashed green) and a charged Higgs boson (plain blue). The neutral scalars contribution is positive while the other ones are negative. $\tan\beta$ is fixed to 1. (b) Same for the two loops contributions from a neutral scalar H^0 (dotted red) and a pseudoscalar A^0 (dashed green). At two loops, the neutral scalars contribution is negative while the pseudoscalar one is positive. Only the b , τ and μ fermion loops are included.

for masses above 0.2 GeV. Solving at one loop the a_μ theory/experiment discrepancy within the twisted 2HDM with a moderate $\tan\beta$ would require a very light ($\lesssim 10$ GeV) scalar H^0 . We discard this open possibility in the forthcoming analysis since the coupling of such a very light (pseudo-)scalar to the bottom quark is strongly constrained (i.e. $\tan\beta \lesssim 1$) by the measurement of the Wilczek process $\Upsilon \rightarrow H^0\gamma \rightarrow \tau^+\tau^-\gamma$ in low energy e^+e^- experiments like CLEO [133].

The situation is quite different when considering the principal two-loop contributions shown in Figure 3.13(c) (the correction involving a W^\pm/H^\pm loop, shown on Figure 3.13(d) is not relevant in the twisted 2HDM due to the reduced coupling of h^0 to muons). The associated formulae is⁵

$$a_\mu^S|_{2\text{-loop}} = \frac{g^2 m_\mu^2 \tan^2 \beta}{32\pi^2 m_W^2} \frac{e^2}{2\pi^2} \sum_f \xi_f \tilde{L}_S \left(\frac{m_f^2}{m_S^2} \right) \quad (3.53)$$

⁵We corrected a missing factor 2π in Eq. (7) of Ref. [132] compared to the original calculation in Ref. [134].

where the sum over f runs over b , τ and μ . The up-type quarks contributions are suppressed by an additional factor $1/\tan^2\beta$ in type II models and can only contribute significantly for $m_S \approx m_t$. The additional charge/color factor ξ_f is given by $\xi_b = 3 \times (-1/3)^2$ for the bottom quark and $\xi_{\tau,\mu} = 1$ for the leptons. The two-loops integrals \tilde{L}_S read

$$\begin{aligned}\tilde{L}_{H^0}(z) &= \frac{z}{2} \int_0^1 dx \frac{-(1-2x(1-x))}{x(1-x)-z} \log \frac{x(1-x)}{z} \\ \tilde{L}_{A^0}(z) &= \frac{z}{2} \int_0^1 dx \frac{1}{x(1-x)-z} \log \frac{x(1-x)}{z}\end{aligned}\quad (3.54)$$

and the scalar contribution is now negative whereas the pseudoscalar one is positive. The total two-loop contributions can be seen in Figure 3.14(b). By comparing with Figure 3.14(a), one sees that these two-loops corrections are dominant for $m_S \gtrsim 10$ GeV (they cancel against the one-loop part for $m_S \approx 5$ GeV). Due to the opposite sign in the scalar and pseudoscalar contributions, solving the a_μ theory/experiment discrepancy within the twisted 2HDM with a moderate $\tan\beta$ in this region would require a light *pseudoscalar* ($20 \lesssim m_{A^0} \lesssim 100$ GeV). If $\tan\beta \approx 30$, a perfect agreement can even be reached for $m_{A^0} \approx 20$ GeV. A larger $\tan\beta$ value would require an heavier pseudoscalar and *vice versa*.

3.3 Direct constraints from collider experiments

3.3.1 The LEP experiment

Searches for h^0

The LEP searches for a SM Higgs boson in the standard decay modes $h^0 \rightarrow b\bar{b}$ and $h^0 \rightarrow \tau^+\tau^-$ and the associated limit have been already reviewed in section 1.4.3. In the context of models with an extended scalar sector, h^0 may also decay, possibly dominantly, in a pair of lighter Higgs bosons. Since such a light object has escaped the LEP searches, it must either have a reduced coupling to ZZ or unusual decay properties. In the context of the twisted 2HDM, both A^0 and H^0 could satisfy this requirement thanks to the vanishing ZZA^0 and ZZH^0 vertices. However, H^0 is degenerate in mass with H^\pm and the possibility of a light (i.e. $\lesssim 100$ GeV) charged Higgs boson is strongly disfavoured by both direct and indirect measurements. We then focus on the light A^0 hypothesis in the following.

Constraints on the $h^0 \rightarrow A^0A^0$ decay mode from LEP data have been considered in the framework of the NMSSM (see [40] and reference therein). If $m_{A^0} > 2m_b$

(like assumed to avoid Υ constraints and any unnatural fine tuning of relation (2.90)), it has been first thought that this decay could explain the simultaneous excesses observed in the $Z2b$ [33] and $Z4b$ [135] final states by adjusting m_{h^0} , $\text{BR}(h^0 \rightarrow A^0 A^0)$, $\text{BR}(h^0 \rightarrow b\bar{b})$ and $\text{BR}(A^0 \rightarrow b\bar{b})$. However, the $Z4b$ excess tends to favour slightly higher masses for h^0 (in the 105-110 GeV region) compare to the main $Z2b$ excess (in the 100 GeV region), decreasing the significance of a global fit. Even if this issue could be investigated more deeply, especially using a model independent approach, we stick to the conservative SM bound $m_{h^0} > 114.4$ GeV for the forthcoming phenomenological analysis.

Searches for H^0 and A^0

The model independent searches for the $e^+e^- \rightarrow Z^* \rightarrow H^0 A^0$ pair production process at LEP, in the $4b$, $2b2\tau$ and 4τ channels, put the tightest constraint on the twisted 2HDM mass spectrum, in particular for type I models where indirect constraints from B physics are less relevant and a light triplet (H^\pm, H^0) is allowed. The final result from [135] is shown on Figure 3.15.

Taking into account the approximate values for $\text{BR}(H^0, A^0 \rightarrow b\bar{b})$ and $\text{BR}(H^0, A^0 \rightarrow \tau^+\tau^-)$ quoted in section 4.1, the limit can be fixed to $m_{A^0} + m_{H^0} \gtrsim 170$ GeV for $m_{A^0} \approx m_{H^0}$. If A^0 is very light, $m_{A^0} \lesssim 30$ GeV, a slight loss of efficiency in the $4b$ and $2b2\tau$ analysis allows for a lighter H^0 , $m_{H^0} \gtrsim 130$ GeV.

If $m_{H^0} \gtrsim m_Z + m_{A^0}$, the scalar boson H^0 could also decay to ZA^0 (see section 4.3 for a more in-depth review), thus reducing dramatically the branching ratio of $H^0 \rightarrow \tau^+\tau^-, b\bar{b}$. The final state signatures associated to this possibility (namely $Zb\bar{b}b\bar{b}$, $Zb\bar{b}\tau^+\tau^-$ and $Z\tau^+\tau^-\tau^+\tau^-$) would mimic the $h^0 \rightarrow A^0 A^0$ process described previously, but with a different kinematical structure⁶. In the absence of any dedicated experimental study (to our knowledge) for this open possibility, we adopt a conservative approach and restrict the model using the (m_{H^0}, m_{A^0}) limits already mentioned.

Another strong constraint in the low m_{A^0} region for type II models can be deduced from searches for the Yukawa process $e^+e^- \rightarrow b\bar{b}A^0$ with $A^0 \rightarrow \tau^+\tau^-, b\bar{b}$. The result for each mode is shown on Figure 3.16. Due to the reduced branching ratio for $A^0 \rightarrow \tau^+\tau^-$, the $A^0 \rightarrow b\bar{b}$ mode is the more restrictive in the $m_{A^0} > 2m_b$ region. The limit is $\tan\beta \lesssim 20$ for $m_{A^0} \simeq 10$ GeV and becomes quickly less relevant for higher masses due to the smaller production cross section.

⁶In this case, the decay products of the Z boson and the two *softer* b -jets should be used to reconstruct the H^0 mass.

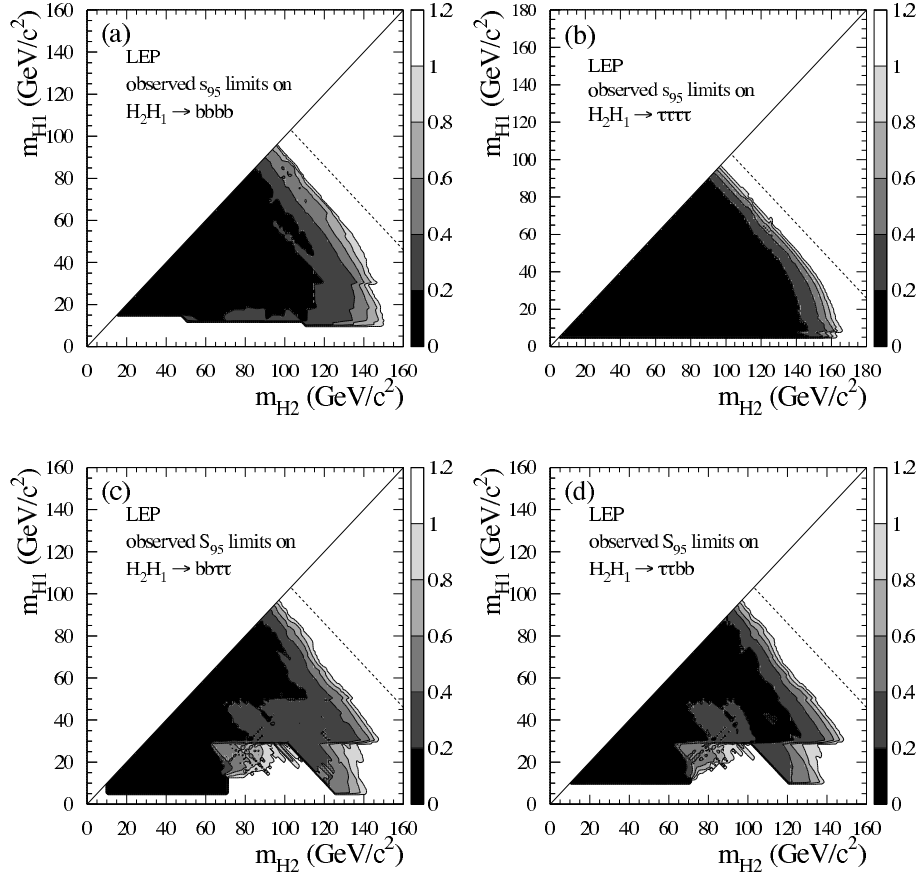


Figure 3.15: Largest relative cross section for $e^+e^- \rightarrow Z^* \rightarrow H^0 A^0$ compatible with data, at the 95% CL, projected on the (m_{H^0}, m_{A^0}) plane ($H_2 = H^0$ and $H_1 = A^0$). The reference cross section is equal to the twisted 2HDM prediction for the production of the H^0, A^0 pair. In plot (a) both Higgs bosons are assumed to decay exclusively to $b\bar{b}$ and in plot (b) exclusively to $\tau^+\tau^-$. In plot (c) the H^0 boson is assumed to decay exclusively to $b\bar{b}$ and the A^0 boson exclusively to $\tau^+\tau^-$ and in plot (d) the A^0 boson is assumed to decay exclusively to $b\bar{b}$ and the H^0 boson exclusively to $\tau^+\tau^-$. The dashed lines represent the approximative kinematic limits of the processes. From Ref. [135].

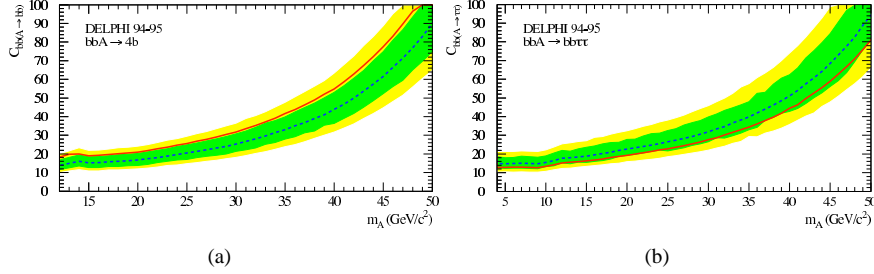


Figure 3.16: (a) Observed upper limit (in red) on $C_{bb(A\to bb)} \equiv \tan\beta\sqrt{\text{BR}(A^0 \to b\bar{b})}$ compare to the SM expectation at 68.3% (green) and 95.0% (yellow) CL. The excess observed in the data translates into an exclusion slightly weaker than expected. (b) Same for $A^0 \to \tau^+\tau^-$. From the DELPHI collaboration note [136].

Finally, the loop decay $Z \to A^0\gamma$ (through a t quark loop in type I models, or through b and τ loops in type II models) can also be used to constrain the A^0 mass. However, an extensive analysis of this channel [137] has shown that the LEP measurement sensitivity (of order 10^{-6} for the associated branching ratio) was not sufficient to put a tighter lower bound on m_{A^0} than the one obtained using the Yukawa process $e^+e^- \to b\bar{b}A^0$ in type II models, see Figure 3.17. This type II model result can easily be extrapolated to type I models, which appear to be even less constrained.

Searches for H^\pm

Results for charged Higgs boson searches at LEP in the general 2HDM (type I and type II) by the DELPHI collaboration are available in Ref. [138]. In addition to the usual fermionic decays $H^+ \to \tau^+\nu_\tau$ and $H^+ \to c\bar{s}$, the possibility for a charged Higgs boson produced in pair in $e^+e^- \to Z^* \to H^+H^-$ to decay into $W^{+(*)}A^0$ has also been taken into account. The existence of a charged Higgs boson with mass lower than 76.7 GeV (type I) or 74.4 GeV (type II) is excluded at the 95% CL, for a wide range of the model parameter.

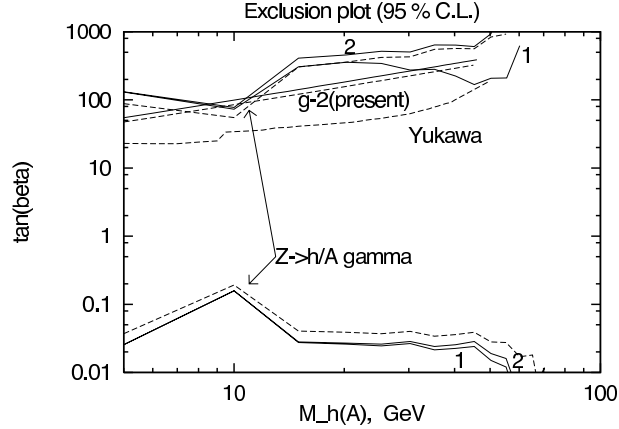


Figure 3.17: Constraint on the $(m_{A^0}, \tan\beta)$ parameter space from the $Z \rightarrow A^0\gamma$ decay in type II models (lower and upper dashed line). The same limits for a CP -even Higgs boson (plain lines) and those obtained from the Yukawa process and the $(g - 2)$ measurement (labelled upper dashed lines) are shown for comparison. From Ref. [137].

3.3.2 The Tevatron experiment

Searches for h^0

As for the LEP limit, searches for a SM Higgs boson h^0 at the Tevatron are already described in 1.4.4 and we focus here on the $h^0 \rightarrow A^0 A^0$ exotic decay, with $A^0 \rightarrow b\bar{b}, \tau^+\tau^-$.

The case of direct production of h^0 through its effective coupling to gluons, followed by the decays $h^0 \rightarrow A^0 A^0 \rightarrow b\bar{b}b\bar{b}$ has been covered in Ref. [139]. As expected, the $4b$ QCD background overwhelms the signal and a discovery can only be achieved if the h^0 production is enhanced by one order of magnitude (e.g. in the large $\tan\beta$ limit). The same process where one of the A^0 decays into $\tau^+\tau^-$ instead of $b\bar{b}$ would provide a cleaner signature but with a reduced cross section due to the small $A^0 \rightarrow \tau^+\tau^-$ branching ratio. The conclusion regarding the feasibility of this analysis at the Tevatron is then expected to be also negative, but, to our knowledge, this naive guess has not yet been confirmed by a real analysis.

The associated production of h^0 with a vector boson $V = W, Z$ being the second strongest production mechanism at the Tevatron, it is also natural to consider the exotic decay $h^0 \rightarrow A^0 A^0$ in this framework. Detailed studies (see [140], [141] and the

references therein for a complete overview) of both the $Vb\bar{b}\tau^+\tau^-$ and $Vb\bar{b}b\bar{b}$ final states have shown their potential interest in the future, but the associated statistical significance is too small to constrain the model parameters with the currently available integrated luminosity.

Searches for H^0 and A^0

Searches for the H^0 and A^0 bosons at the Tevatron experiment take place for production in association with b quarks, or in gluon fusion involving a b quark loop, and decays to $b\bar{b}$ and $\tau^+\tau^-$ final states. Since most analysis are oriented towards the MSSM Higgs bosons discovery, they focus (to our knowledge) exclusively on the $m_S \gtrsim 70$ GeV mass region. Exclusion regions for Run I and Run II are visible in Figure 3.18 for specific MSSM scenarios. We translate them as a conservative $\tan\beta > 35$ bound on the whole $m_{A^0, H^0} > 70$ GeV mass range.

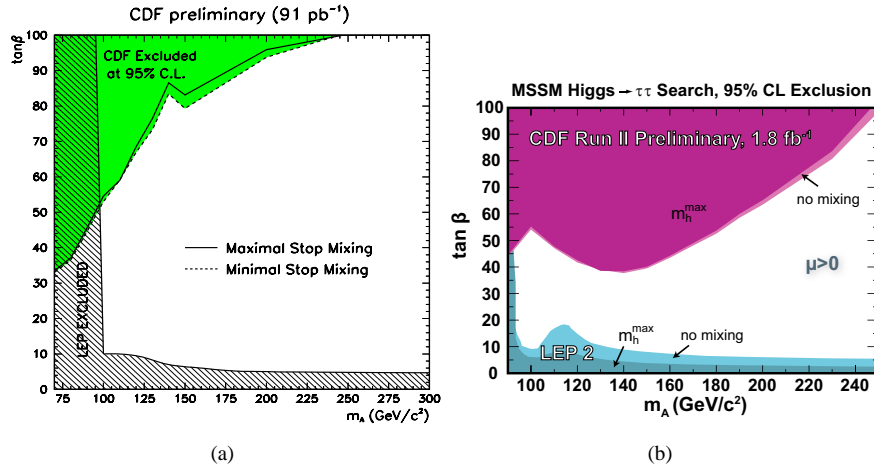


Figure 3.18: (a) 95% CL bounds on $\tan\beta$ with respects to m_{A^0} from the $b\bar{b}A^0 \rightarrow b\bar{b}b\bar{b}$ process at Tevatron, Run I. From Ref. [142]. (b) Same for the $b\bar{b}A^0 \rightarrow b\bar{b}\tau^+\tau^-$ process at Tevatron, Run II. From Ref. [143].

Another interesting possibility to produce a light A^0 boson at the Tevatron is the charged Higgs associated production $p\bar{p} \rightarrow W^{\pm*} \rightarrow H^{\pm}A^0$ proposed in [144], where the charged Higgs may further decay to $W^{\pm}A^0$. For the most favourable mass scenarios ($m_{A^0} < 20$ GeV, $m_{H^{\pm}} < 90$ GeV), the associated cross sections can be larger

than 500 fb and this mechanism could be detected in the $W4b$ final state. However, to our knowledge, this hypothesis has not yet been tested experimentally.

Searches for H^\pm

If $m_{H^\pm} < m_t$, a top quark could decay significantly often to H^+b . This possibility has been considered by the Tevatron experiments for various charged Higgs decay hypothesis, namely $\tau^+\nu_\tau$, $c\bar{s}$, $t^*\bar{b}$ and W^+A^0 . The result is shown on Figure 3.19 as a 95% CL upper bound on the $t \rightarrow H^+b$ branching ratio ($\lesssim 0.5$ for the whole H^+ mass range) and as an excluded region in the MSSM ($m_{H^\pm}, \tan\beta$) parameter space.

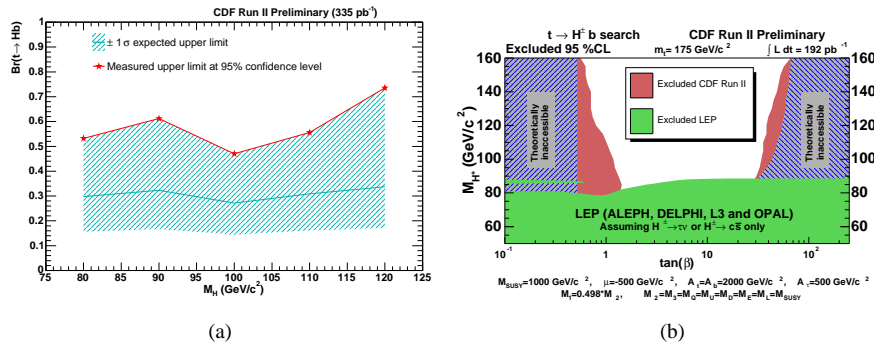


Figure 3.19: (a) Observed 95% CL upper bound on the $t \rightarrow H^+b$ branching ratio with respect to the charged Higgs mass hypothesis and the $\pm 1\sigma$ SM expectation. A small excess observed in the data translates into an exclusion weaker than expected. From Ref. [145]. (b) The same bound translated onto the MSSM ($m_{H^\pm}, \tan\beta$) parameter space. From Ref. [146]

3.4 Summary

All the relevant constraints introduced in the previous sections are summarised in Table 3.1. Only the most stringent bounds are presented, and some of them could be strongly correlated with the others. Like already emphasised in the introduction of this work, let us again stress these constraints have been derived with the implicit assumption that all BSM contribution beyond the minimal twisted 2HDM are negligible.

Type I & II	$m_{h^0} < 500 \text{ GeV}$	Unitarity
	$m_T^2 - m_{A^0}^2 < (400 \text{ GeV})^2$	Perturbativity
	$m_{H^\pm} = m_{H^0} + \epsilon$	$\Delta T \approx 0$, if $m_{h^0} > 250 \text{ GeV}$
	$m_{A^0} \ll m_T$	$\Delta S \approx 0$, if $m_{h^0} > 250 \text{ GeV}$
	$m_{h^0} > 114.4 \text{ GeV}$	LEP bound on the SM Higgs
Type I	$m_T \gtrsim 130 \text{ GeV}$	LEP $Z \rightarrow H^0 A^0$ ($m_{A^0} < 30 \text{ GeV}$)
	$m_T \gtrsim 170 \text{ GeV} - m_{A^0}$	LEP $Z \rightarrow H^0 A^0$ ($m_{A^0} > 30 \text{ GeV}$)
	$m_{A^0} > 10 \text{ GeV}$	No fine tuning in (2.90)
	$\tan \beta \lesssim 0.4$	$b \rightarrow s\gamma$ and $B_0 - \bar{B}_0$ mixing
Type II	$m_T > 295 \text{ GeV}$	$b \rightarrow s\gamma$
	$m_{A^0} \gtrsim 30 \text{ GeV}$	R_b (correlated with m_T)
	$m_{A^0} \lesssim 100 \text{ GeV}$	Favoured by a_μ
	$\tan \beta \gtrsim 5$	$B_0 - \bar{B}_0$ mixing
	$\tan \beta \lesssim 35$	$B \rightarrow \tau\nu_\tau$ and LEP $bbA \rightarrow 4b$

Table 3.1: Summary of the relevant constraints for the twisted 2HDM.

They appear more as reasonable choices when trying to restrict the parameter space for the phenomenological study of collider signatures presented in Chapter 4, than as really strict bounds.

Typical spectra for the MSSM scalar sector (SPS 1a, see [147]), the type I and type II twisted 2HDMs are shown in Figure 3.20. One can clearly foresee qualitative differences for the typical phenomenology associated with these models. The (constrained) MSSM Higgs phenomenology in the low mass region is very similar to what can be expected in the SM. The proof of the existence of enlarged scalar sector at the LHC will have to rely on the direct detection of the heavy states H^\pm , H^0 and A^0 , which may require a high luminosity ($\sim 100 \text{ fb}^{-1}$, depending on $\tan \beta$). The same conclusion also holds for most of the “usual” 2HDM scenarios considered in the literature, where the nearly degenerate custodial triplet (H^\pm , A^0) is forced to be relatively heavy by strong B physics constraints.

The situation could be completely different in a twisted 2HDM due to an inverted spectrum. In type I scenarios, namely when only one Higgs doublet gives their mass to all fermions, the reduced Yukawa coupling of the charged Higgs allows for a moderately light custodial triplet (H^\pm , H^0). A small mass splitting inside this triplet and the presence of a light pseudoscalar A^0 can help a rather heavy SM Higgs ($m_{h^0} \approx 300 \text{ GeV}$) to pass the electroweak precision tests (see section 3.2.1). If $m_{h^0} > 2m_T$, many exotic scalar decays can be kinematically allowed ($h^0 \rightarrow H^+ H^-$, $h^0 \rightarrow H^0 H^0$, ...) giving rise to interesting new possibilities of collider signatures.

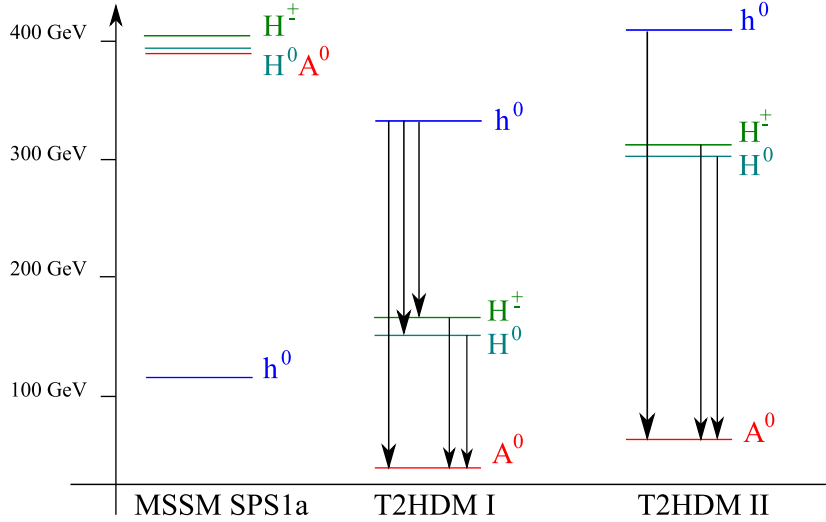


Figure 3.20: Illustrative spectra for the MSSM scalar sector (Snowmass Points and Slopes 1a [147]) and the type I and type II twisted 2HDMs. The different decay possibilities (e.g. $h^0 \rightarrow A^0 A^0$, $H^\pm \rightarrow W^\pm A^0$, ...) are symbolised by arrows.

In type II scenarios, namely when the first Higgs doublet couples to up-type right handed fermions and the second one couples to down-type right handed fermions, the custodial triplet mass is constrained to be larger due to the $b \rightarrow s\gamma$ bound on the charged Higgs mass. A reduced mass splitting inside this heavy triplet can then suffice to allow for a very heavy SM Higgs ($m_{h^0} \approx 400$ GeV). The electroweak oblique parameter S together with the available data for the muon anomalous magnetic moment favour the presence of light pseudoscalar in this case but its mass is bounded by below ($m_{A^0} > 30$ GeV) due to the LEP direct searches and the R_b measurement. Even if the $m_{h^0} > 2m_T$ condition is hardly satisfied in this context due to unitarity and perturbativity constraints on m_{h^0} , unusual decays for H^0 and H^\pm remain an interesting open possibility.

To conclude, it should be noted that none of the two types of scenarios considered here is clearly favoured compared to the other. Type I scenarios can almost trivially satisfy all the reviewed constraints since, besides the possibility of invisible decays of the h^0 boson, they display almost the same phenomenology as the Standard Model in the decoupling regime $\tan\beta \approx 0$ (which is formally equivalent to an Inert Doublet Model). On the other hand, in type II scenarios, the new scalar particles never completely decouple from the Standard Model fermions since both the $\tan\beta \rightarrow 0$ and $\tan\beta \rightarrow \infty$ limits correspond to large Yukawa couplings. This implies strong constraints from

precision B physics measurements, in particular on the charged Higgs mass. But this apparently more restricted aspect of type II scenarios is tempered by the possibility to explain the measured a_μ value, which remains one of the rare experimental hint in favour of BSM physics, and by a potentially greater theoretical interest when trying to interpret the observed fermion mass hierarchy.

Chapter 4

Phenomenology at the LHC

“The true method of knowledge is experiment.”

William Blake (1757-1827)

This last chapter is dedicated to an overview of the genuine signatures for the twisted 2HDM at the Large Hadron Collider. We emphasise the most important signals (and the main associated backgrounds) to provide a phenomenological basis to future, more in-depth, experimental analysis. The principal production mechanisms of the Higgs bosons are first examined (most of them being similar to those encountered in the SM or in the MSSM), together with their decay properties where most of the characteristic features of the twisted 2HDM arise. Particularly relevant signatures for the exotic scalar decays $h^0 \rightarrow A^0 A^0$, $H^\pm \rightarrow W^\pm A^0$ and $H^0 \rightarrow Z A^0$ are then considered in the context of LHC. As for the content of chapter 3, a large part of the material presented here will appear in [148].

Unless mentioned otherwise, all the decay widths and branching ratios have been computed using TwoHiggsCalc, a tree-level 2HDM parameter calculator described in Appendix B. Tree-level cross sections and parton-level Monte-Carlo events have been obtained using the MadGraph/MadEvent v4.2 event generator [149] based on exact matrix elements calculations, and the “simplified 2HDM” model. The default SM input parameters for all simulations are: $\alpha^{-1}(m_Z) = 127.934$, $G_F = 1.16637 \times 10^{-5} \text{ GeV}^{-2}$, $\alpha_s(m_Z) = 0.1172$, $m_Z(\text{pole}) = 91.1876 \text{ GeV}$, $m_\tau = 1.777 \text{ GeV}$, $m_b(\text{pole}) = 4.2 \text{ GeV}$ and $m_t(\text{pole}) = 174.3 \text{ GeV}$. The quark masses appearing in the Yukawa couplings are the running masses at the scalar mass scale. By default,

the selected set of Parton Distribution Functions (PDFs) is CTEQ6L1 and the renormalisation/factorisation scales are fixed on an event by event basis to the mass of the heaviest final state particle plus the sum of the massless particles transverse momenta. No cuts are applied on the final state objects except when mentioned explicitly.

4.1 Decays and production modes

4.1.1 Type I models

Production mechanisms

The type I twisted 2HDM is characterised by the reduced couplings of H^0 , A^0 , and H^\pm to the SM fermions (all of them being scaled by $\tan\beta < 1$), while the h^0 couplings are identical to the SM case due to the presence of the twisted symmetry introduced in section 2.6. As a matter of fact, the only relevant production mechanisms for H^0 , A^0 , H^\pm involve heavy fermions (e.g., $gg \rightarrow t\bar{t}H^0/A^0$) and/or gauge interactions (e.g., $q\bar{q} \rightarrow Z^* \rightarrow H^0A^0$), while all the production modes described in 1.4.5 for the SM Higgs boson are also pertinent for h^0 (see Figure 4.1(a)).

Cross sections of the scalar pair production mechanisms, which mainly involve the decay of an off-shell s -channel vector boson, are summarized on Figures 4.1(b), (c) and (d). In the most optimistic situations, the total cross sections barely reach the 1 pb level, or even less for the H^+H^- and H^0H^0 pairs production where both scalars have to satisfy $m_S \gtrsim 130$ GeV. If H^\pm is light, a potentially more interesting possibility is the $t \rightarrow H^+b$ exotic decay. Due to the very large $t\bar{t}$ production cross section at the LHC, the resulting $W^\pm H^\mp b\bar{b}$ final state may emerge from the background (depending on the actual H^\pm decay modes), despite the reduced $t \rightarrow H^+b$ branching ratio (see Figure 4.2(a)).

If $m_{H^\pm} \gtrsim 150$ GeV, the associated production of the charged Higgs boson with a single top quark becomes dominant compared to the $t \rightarrow H^+b$ decay which goes down quickly when m_{H^\pm} gets closer to the $m_t - m_b$ mass threshold. The corrected LO cross section for the $gb \rightarrow tH^-$ process is shown on figure 4.2(b) for two different $\tan\beta$ hypothesis. The $gg \rightarrow tH^-b$ process (which is part of the NLO corrections to the previous one), where the initial state b quarks comes from a gluon splitting instead of the proton sea, gives also a sizeable ($\simeq 50\%$) contribution to the total production rate and should be taken into account, e.g. see Ref. [97] for a review.

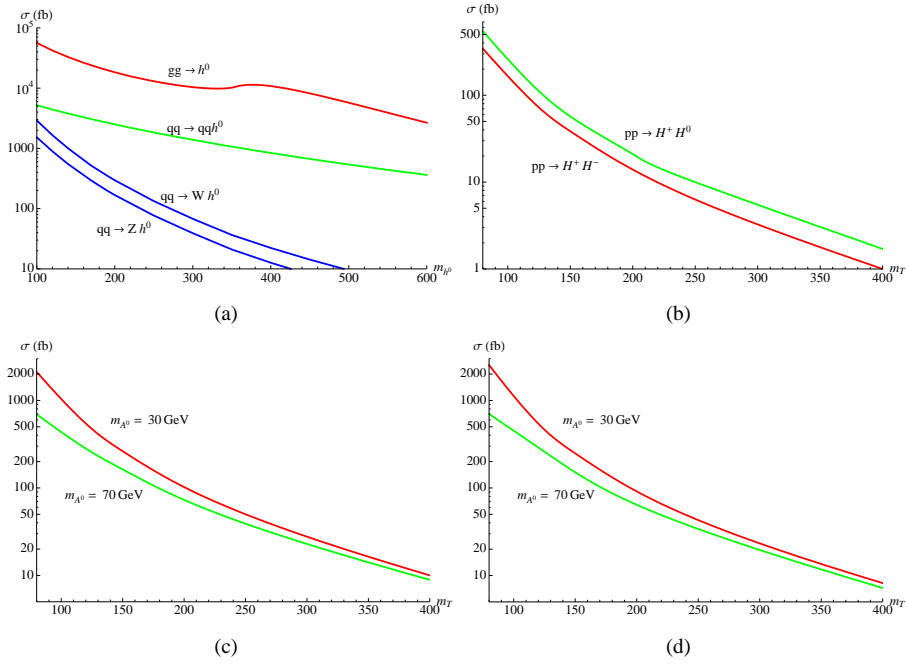


Figure 4.1: Type independent production cross sections. (a) Main h^0 production cross sections, with respect to m_{h^0} (data from Ref. [34]). (b) H^+H^- and H^+H^0 pairs production cross section with respect to m_T . H^+A^0 (c) and H^0A^0 (d) pairs production cross section, with respect to m_T and for two different values of m_{A^0} .

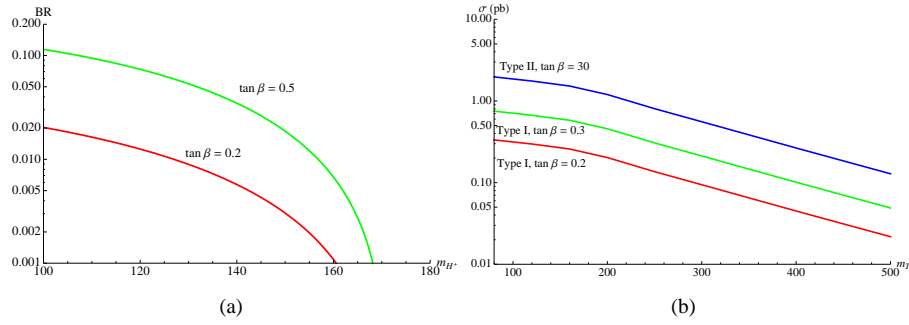


Figure 4.2: (a) Branching ratio of the top decay into charged Higgs $t \rightarrow H^+ b$, as a function of the charged Higgs mass and for two different values of $\tan \beta$ (type I). (b) Corrected LO cross sections of the charged Higgs production in association with top quark, $gb \rightarrow tH^-$, as a function of the triplet mass and for different Yukawa couplings. The renormalization and factorisation scale are fixed to $\mu_F = \mu_R = \frac{1}{3}(m_t + m_T)$, the running b quark mass is set to 3.0 GeV and an overall K -factor of 1.45 (1.25) is applied for type I (type II) couplings. The sizeable difference between these two K -factors is explained by the fact that the running bottom Yukawa coupling, which is dominant in type II models, absorbs a larger correction than the running top Yukawa coupling, see Ref. [150].

Finally, the $t\bar{t}$ associated production of the neutral Higgs bosons, which has been demonstrated to be challenging for most decay modes in the Standard Model, does not offer a viable alternative to the other channels for discovery, and is not considered in the following.

Decay modes

The principal decay modes of h^0 , which are shown in Figure 4.3 for two different

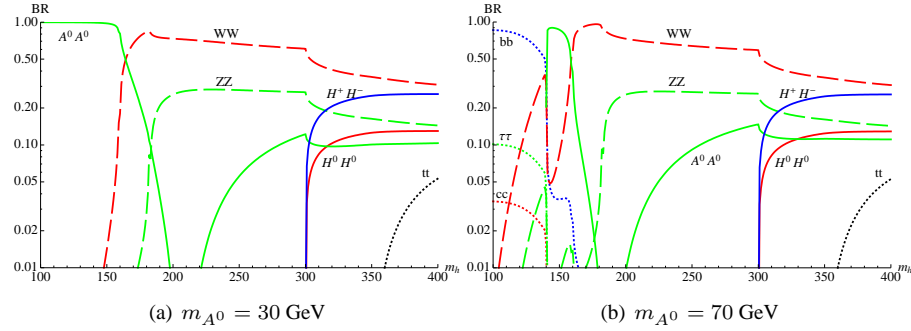


Figure 4.3: Branching ratio of h^0 into fermions (dotted lines), vector bosons (dashed lines) and scalars (plain lines), with respect to its mass and for two different values of m_{A^0} .

values of the A^0 mass, can be qualitatively very different from those observed in the Standard Model, or even in the MSSM. In the low mass region, i.e. if $m_{h^0} < 2m_{A^0}$, the h^0 Higgs boson primarily decays to b , τ and c pairs (in order of importance) like in the Standard Model. When $2m_{A^0} < m_{h^0} < 2m_W$, the main decay is $h^0 \rightarrow A^0 A^0$ thanks to the large trilinear scalar coupling. Note however that this coupling goes to zero when $m_{h^0} = \sqrt{2(m_T^2 - m_{A^0}^2)}$ (see Appendix A), such that the $h^0 \rightarrow A^0 A^0$ branching ratio vanishes in the narrow mass window containing this critical value. If $m_{h^0} > 2m_W$ and, at the same time, $m_{h^0} < 2m_T$, the decay into a pair of gauge bosons dominates with BRs similar to the SM ones. Above the $2m_T$ threshold, both the $h^0 \rightarrow H^0 H^0$ and the $h^0 \rightarrow H^+ H^-$ decays are kinematically allowed. For large m_{h^0} , the $H^+ H^-$ and $W^+ W^-$ decays account for half of the total decay width, while the other half is divided between the $H^0 H^0$, $A^0 A^0$, ZZ and $t\bar{t}$ pair decays. As can be seen in Figure 4.4(a), the total decay width of h^0 is sizeably bigger than in the Standard Model at low masses (around 1 GeV for $m_{h^0} = 100$ GeV), due to the $h^0 \rightarrow A^0 A^0$ exotic decay mode, but remains of the same order of magnitude at higher masses.

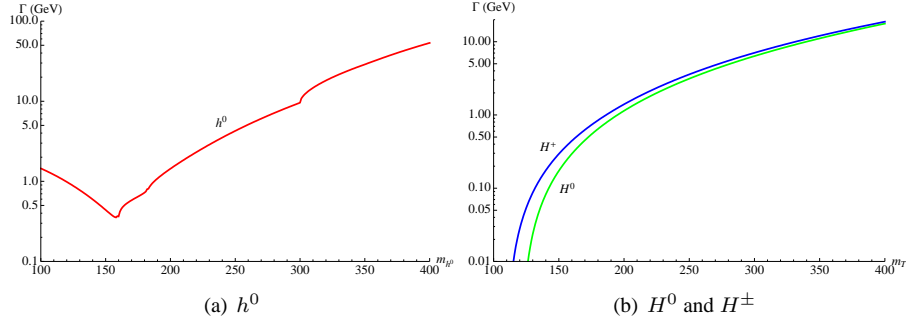


Figure 4.4: Total decay width of h^0 (left), H^0 (right, in green) and H^\pm (right, in blue), in GeV (type I, $m_{A^0} = 30$ GeV, $\tan \beta = 0.2$).

For the other Higgs bosons, A^0 , H^0 and H^\pm , the situation is somehow simpler. On the whole mass range, or below the $Z A^0$ and $W^\pm A^0$ mass threshold for H^0 and H^\pm , the only possible decays are into SM particles. Since the coupling of these scalars are identical to those of the SM Higgs boson, up to an overall $\tan \beta$ scaling factor, their decay patterns are straightforward to determine. The A^0 and H^0 bosons decay mainly into $b\bar{b}$ pairs ($\sim 85\%$), $\tau^+\tau^-$ pairs ($\sim 10\%$) and $c\bar{c}$ pairs ($\sim 3\%$). The H^\pm boson decays mainly into $\tau^+\nu_\tau$ ($\sim 75\%$) and $c\bar{s}$ ($\sim 25\%$), or into $t\bar{b}$ if $m_{H^\pm} > m_t + m_b$. If H^0 (respectively H^\pm) is heavier than the $Z A^0$ (respectively $W^\pm A^0$) threshold, the $H^0 \rightarrow Z A^0$ bosonic decay (respectively $H^\pm \rightarrow W^\pm A^0$) clearly dominates over all fermionic modes and has a branching ratio equal to unity. Like for h^0 , the H^0 and H^\pm decay widths remain however at most of the order of the SM Higgs one, as seen in Figure 4.4(b).

4.1.2 Type II models

Production mechanisms

All production mechanisms for h^0 , and those involving only gauge and scalar interactions for H^0 , A^0 and H^\pm , are identical to those described in section 4.1.1. The main difference with type I models is the enhanced coupling of the extra Higgs bosons to down-type quarks and to charged leptons. The associated production with b quarks, or the direct production through a b quark loop in the low mass region, becomes by far the principal production mechanism at the LHC, see Figure 4.5.

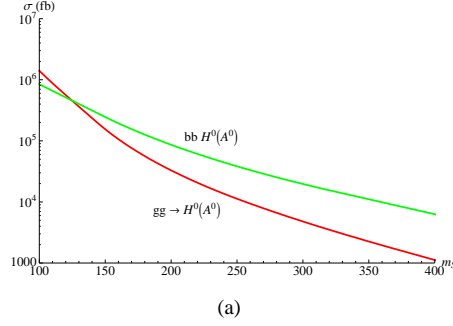


Figure 4.5: NLO cross sections for the direct production (through a b quark loop) and for the associated production of H^0 (A^0) with a b quarks pair as a function of m_T (m_{A^0}). Type II, $\tan \beta = 30$. Data from Ref. [34]

Decay modes

The h^0 couplings being the same in type II as in type I model, the branching ratio patterns shown on Figure 4.3 remain valid. The total decay width is shown in Figure 4.6(a) for $m_{A^0} = 50$ GeV.

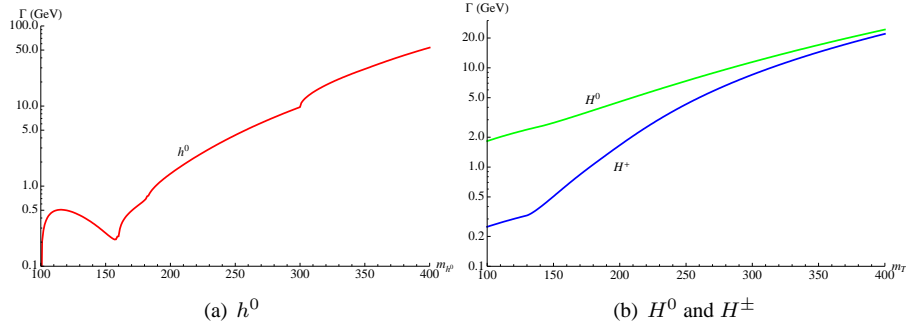


Figure 4.6: Total decay width of h^0 (left), H^0 (right, in green) and H^\pm (right, in blue), in GeV (type II, $m_{A^0} = 50$ GeV, $\tan \beta = 30$).

The H^0 and H^\pm decays are dominated by the $Z A^0$ and $W^\pm A^0$ at high masses, as seen in Figure 4.7. But, contrary to what happens for type I models, the associated branching ratio is no longer equal to unity above the kinematical threshold. The $b\bar{b}$ and $t\bar{t}$ decays are indeed non negligible anymore, in particular in the moderate mass

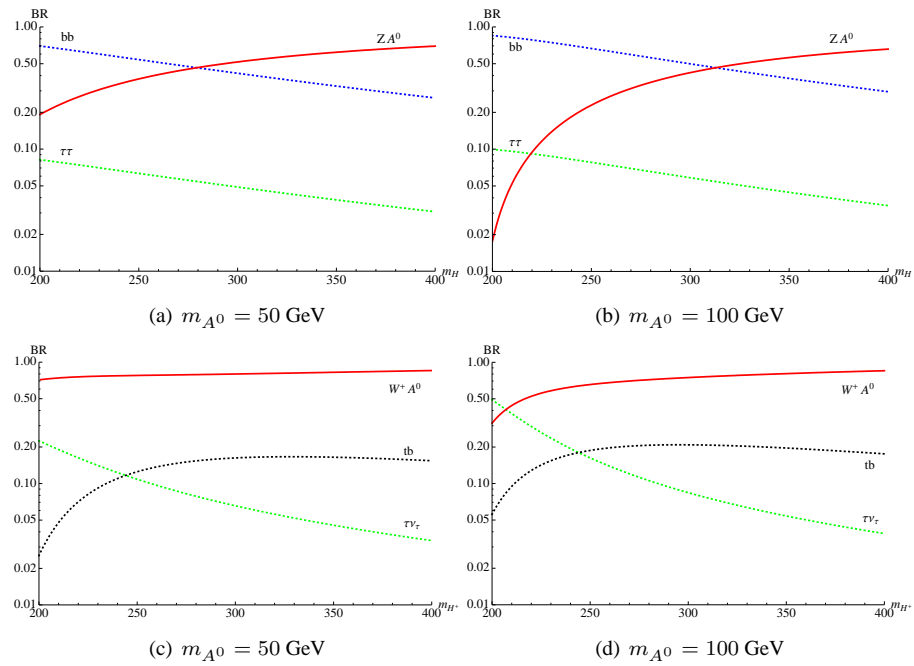


Figure 4.7: Branching ratio of H^0 (top) and H^+ (bottom) into fermions (dotted lines), and scalar plus vector boson (plain line), with respect to their mass and for two different values of m_{A^0} (type II, $\tan\beta = 30$).

regime $m_T < 300$ GeV. The effect of these enhanced fermionic modes on the total width of H^0 and H^\pm can be seen in Figure 4.6(b).

4.1.3 Benchmark points

Our choice of benchmark points in the twisted 2HDM parameter space is summarised in Table 4.1. These points are chosen in order to cover the different possibilities of

	Type	m_{h^0}	m_{A^0}	m_T	$\tan\beta$
BP0	Type I	120 GeV	50 GeV	300 GeV	0.2
BP1	Type I	300 GeV	30 GeV	140 GeV	0.2
BP2	Type I	450 GeV	60 GeV	200 GeV	0.2
BP3	Type II	400 GeV	30 GeV	300 GeV	30

Table 4.1: Set of benchmark points for the phenomenological analysis of the twisted 2HDM.

unusual signatures at the LHC. Even if they satisfy all the direct and indirect constraints displayed in Table 3.1, they do not necessarily correspond to the regions of the parameter space most favoured by a global fit of model parameters.

The benchmark point 0 (BP0) is characterised by a relatively light SM Higgs boson which decays predominantly into a pair of light pseudoscalars A^0 . The typical signatures, i.e. $h^0 \rightarrow A^0 A^0 \rightarrow b\bar{b}b\bar{b}$ or $h^0 \rightarrow A^0 A^0 \rightarrow b\bar{b}\tau^+\tau^-$, are considered in section 4.2. The triplet mass being relatively high, and the couplings of the associated scalars to fermions suppressed by a low $\tan\beta$ factor, experimental evidences for the presence of H^0 and H^\pm will require an important integrated luminosity.

In benchmarks BP1 and BP2, the h^0 mass is larger than the $2m_T$ threshold. The SM Higgs boson can then decay into $H^0 H^0$ and $H^+ H^-$ pairs. For each case, the pseudoscalar mass m_{A^0} is low enough to ensure that the exotic decays $H^0 \rightarrow Z A^0$ and $H^\pm \rightarrow W^\pm A^0$ are kinematically allowed. The typical signatures associated to these benchmarks are $gg \rightarrow h^0 \rightarrow H^0 H^0 \rightarrow Z A^0 Z A^0$ and $gg \rightarrow h^0 \rightarrow H^+ H^- \rightarrow W^+ A^0 W^- A^0$, both with $A^0 \rightarrow b\bar{b}$ or $A^0 \rightarrow \tau^+ \tau^-$ (see sections 4.3 and 4.4). The mass of A^0 (and those of all other scalars) is lower in BP1 than in BP2.

Finally, BP3 is the only type II benchmark point. The triplet mass being strongly constrained by the $b \rightarrow s\gamma$ measurement, the h^0 decay to $H^0 H^0$ and $H^+ H^+$ pairs is not longer possible due to unitarity constraints. Nevertheless, the presence of a light A^0 favoured by the a_μ data still allows for the $H^0 \rightarrow Z A^0$ and $H^+ \rightarrow W^+ A^0$ decays.

Regarding the main production modes in the large $\tan\beta$ case, the main signatures are $gg \rightarrow H^0 \rightarrow ZA^0$ and $b\bar{b}H^0 \rightarrow b\bar{b}ZA^0$ with $A^0 \rightarrow b\bar{b}$ or $A^0 \rightarrow \tau^+\tau^-$, see section 4.3.

4.2 Signals with $h^0 \rightarrow A^0A^0$

Taking into account the branching ratios for $h^0 \rightarrow A^0A^0$ ($\sim 100\%$), $A^0 \rightarrow b\bar{b}$ ($\sim 85\%$) and $A^0 \rightarrow \tau^+\tau^-$ ($\sim 10\%$) for the benchmark BP0, the total branching ratio of $h^0 \rightarrow A^0A^0 \rightarrow 4b$ is $\sim 72\%$, $\sim 17\%$ for $h^0 \rightarrow A^0A^0 \rightarrow 2b2\tau$ and around one percent for $h^0 \rightarrow A^0A^0 \rightarrow 4\tau$. Since the four τ final state signal is suppressed at least by a factor of a hundred compared to the $m_{A^0} < 2m_b$ scenarios studied in the framework of the NMSSM (e.g., see [40] and [151] for recent overviews), the LHC discovery of h^0 and A^0 in this channel is probably difficult. On the other hand, the four b final state has a large BR, but suffers from important QCD backgrounds. This final state has been investigated in direct production mode at the Tevatron (where it is overwhelmed by the backgrounds [139]) and in W/Z associated production [140, 141]. At the LHC, a discovery significance may still be reached in this last mode [141, 152].

In the context of the present work, we focus on the intermediate $2b2\tau$ final state, which has a smaller (but still sizable) BR than the $4b$ final state, together with a much lower background. This final state has been considered in the framework of the associated production of h^0 with a W/Z boson at the Tevatron in [141, 34]. However, in this case, only a few events could be observed (at best) after a few fb^{-1} due to the cuts and b/τ tagging necessary to remove the large reducible background. Similar difficulties with the reducible background are also expected at LHC [141]. In the present study¹ [151], we focus on the Vector Boson Fusion (VBF) production mode for h^0 , which has been shown to be a promising channel at the LHC for the SM decay $h^0 \rightarrow \tau^+\tau^-$ both in parton-level analysis [153, 154] and after full detector simulation [155, 156, 157]. After the end of the redaction of [151], it has been brought to our knowledge that a study on similar lines in the context of the NMSSM, using parton shower based simulations, can be found in [158, 159]. A short comparison of the results from both approaches, underlying a possible difference, can be found at the end of the section.

¹The author wishes to acknowledge and thank Nadia Adam and Valerie Halyo from Princeton University, and Sergei Gleyzer from Florida State University, for collaboration on this study.

Signal and background

In order to improve efficiency, some production cuts have been applied already at the parton level. To ensure a possibility for tagging/reconstruction, a minimal p_T of 20 GeV is required for all (non b) jets and 10 GeV for b -jets² and leptons. For the same reason, a maximal pseudorapidity of 5 is required for jets and of 2.5 for b -jets and leptons, and a minimal separation cut, i.e. $\Delta R > 0.3$, is also imposed on all objects pairs. Furthermore, regarding the particular kinematic configuration of signal events, standard VBF cuts are applied, i.e. $|\Delta\eta| > 4$ and $m_{jj} > 700$ GeV for the two forward jets.

The signal is characterized by a populated final state with two central b jets, two central τ 's and two forward jets. To avoid triggering issues, we focus on the leptonic decays of both τ 's. The associated tree level cross section (after τ 's decays and cuts) is rather low, around 9 fb, mainly due to the low average p_T of b 's and τ 's from A^0 decays.

The irreducible background where the τ pair is coming from an off shell photon or Z , and the b pair from a gluon splitting is rather low, with a 1fb cross section. The same process with a e or μ pair replacing the τ pair has a more sizable cross section, around 8.7 fb, due to the absence of the τ branching ratio. The most dangerous reducible background is the $t\bar{t}$ pairs produced by gluon fusion in the VBF kinematic configuration and fully leptonic top decays (through an intermediate τ or not). Even if the total cross section is almost three order of magnitude larger than the signal (3.2 pb), the associated distributions (in particular the invariant mass of b 's and τ 's) and the total amount of missing transverse energy are different.

Results

Regarding the expected kinematic distributions of the signal and background samples, it is evident that a cut based technique can be defined to achieve a first separation. The chosen selection criteria are:

$$M_{ll} \leq 30, \quad 40 \leq M_{bb} \leq 60, \quad \Delta R_{ll} \leq 2, \quad \text{and} \quad \Delta R_{bb} \leq 2. \quad (4.1)$$

Figure 4.8 shows the invariant mass M_{bbll} , of the four body final state after these simple cuts. The signal and the background considered are stacked and normalized by cross-section.

A crude estimate of the significance around M_{bbll} , in the region $50 \leq M_{bbll} \leq 110$, yields $S/\sqrt{B} = 4$ for an integrated luminosity of 100 fb^{-1} , with approximatively

²This rather optimistic choice does not affect our final (pessimistic) conclusion regarding the feasibility of this study.

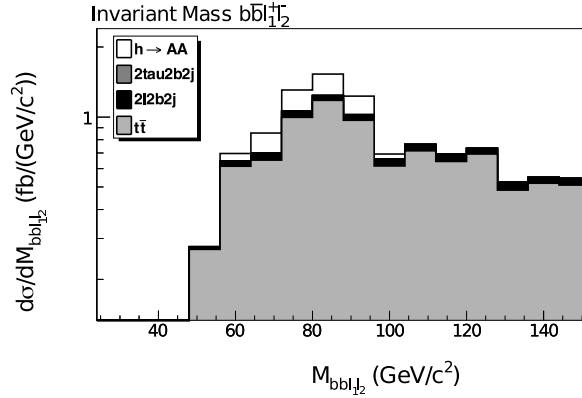
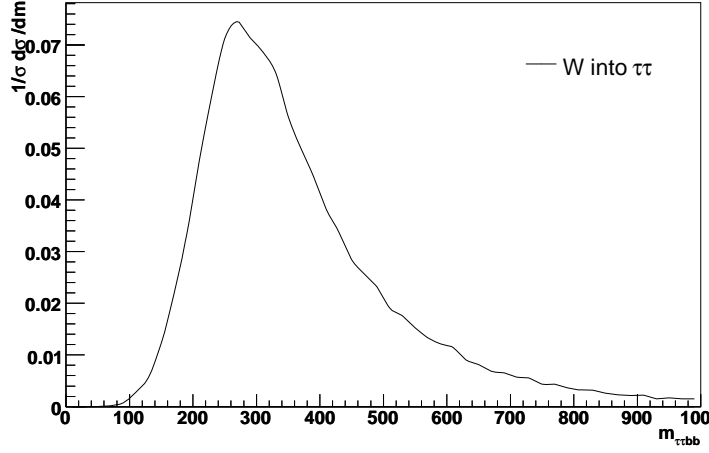


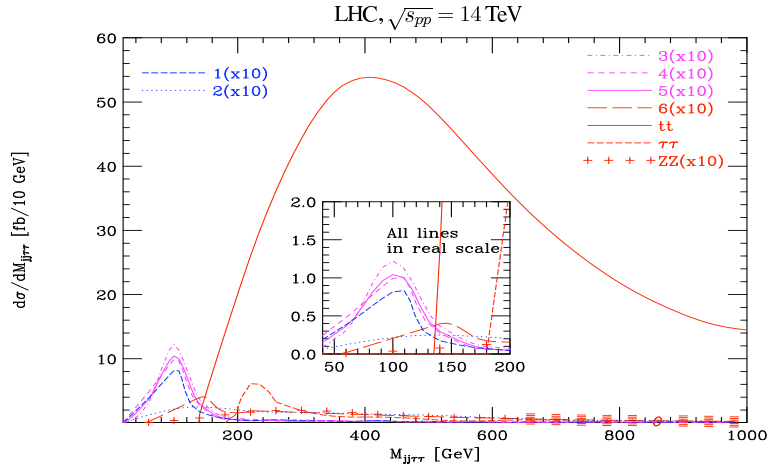
Figure 4.8: Invariant mass M_{bblj_2} of the four-body final state after selection cuts 4.1. The signal and background histograms are stacked and normalized by their corresponding cross-sections. From Ref. [151].

100 signal events. B-tagging efficiency will impact the number of both signal and background events, and reduces this significance by a factor of ~ 2 if an optimistic b -tagging efficiency of 50% is assumed. From this naive cut based parton-level analysis, one can conclude that the $h^0 \rightarrow A^0 A^0 \rightarrow b\bar{b}\tau^+\tau^-$ channel in VBF at the LHC is (at best) very challenging, at least for our specific choice of masses and couplings.

Our conclusion regarding the feasibility of this signal is significantly more pessimistic than the one first obtained in [158, 159], where an approximate significance above 20 is claimed at the parton-level. The main reason for this discrepancy is the difference between the $m_{2\tau 2b}$ invariant mass distribution of the $t\bar{t}jj$ background obtained by these authors using a parton shower event generator, and the one obtained using MadGraph/MadEvent, see Figure 4.9. Even in the presence of additional production cuts (which may explain partially the difference between the two distribution shapes at high invariant masses), our exact matrix element calculation shows a non negligible tail (when compared to the signal) in the region $80 \lesssim m_{2\tau 2b} \lesssim 150$ GeV which is apparently not reproduced in the original simulation.



(a)



(b)

Figure 4.9: Differential cross section of the $t\bar{t}jj$ background with respect to the invariant mass of the four-body $bb\tau^+\tau^-$ final state from (a) our simulation (normalised, with all the production cuts on b quarks described in the text applied) and (b) Refs. [158, 159] (without cuts). Notice in particular the slight discrepancy between the two shapes in the low invariant mass region, where the signal stands. The signal distributions on Figure (b) are not relevant in the context of this comparison.

4.3 Signals with $H^0 \rightarrow A^0 Z^0$

4.3.1 Process $gg \rightarrow h^0 \rightarrow H^0 H^0 \rightarrow ZA^0 ZA^0$

Due to both the relatively high gluon fusion cross section (see Figure 4.1(a)) and the sizeable $h^0 \rightarrow H^0 H^0$ branching ratio (see Figure 4.3), the $gg \rightarrow h^0 \rightarrow H^0 H^0$ process offers an interesting possibility for the H^0 boson production in type I models. Considering that H^0 decays almost exclusively to ZA^0 in these models, the decay chain $gg \rightarrow h^0 \rightarrow H^0 H^0 \rightarrow ZA^0 ZA^0$ (see Figure 4.10(a)) has a total cross section of order 1 pb at the LHC. In the following, the production cross section of Monte-Carlo signal events is scaled to fit the NLO theoretical prediction from [34].

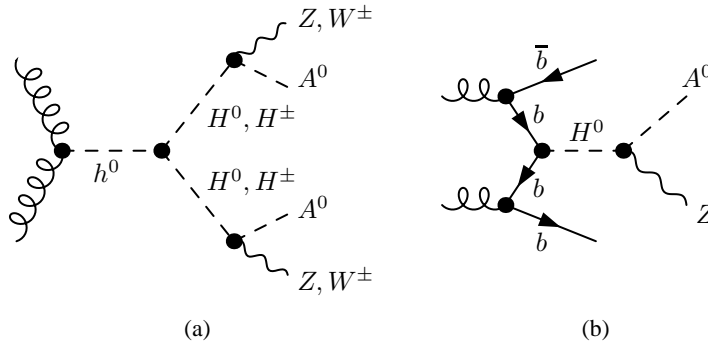


Figure 4.10: Sample Feynman diagrams for (a) the $gg \rightarrow h^0 \rightarrow H^0 H^0 \rightarrow ZA^0 ZA^0$ process and (b) the $gg \rightarrow b\bar{b}H^0 \rightarrow b\bar{b}ZA^0$ process.

Signal and background

In order to allow for a maximal rejection of the possible backgrounds, we require that both Z gauge bosons decay into light leptons. Since this last requirement decreases significantly the signal cross section, we focus only on the main A^0 decay mode, i.e. $A^0 \rightarrow b\bar{b}$. The signal final state is then $l^+ l^- \tilde{l}^+ \tilde{l}^- b\bar{b}b\bar{b}$, with $l^\pm = e^\pm, \mu^\pm$

Signal events have been first produced without any cut on the final state partons, except an acceptance $\eta < 2.5$ cut on the b -quarks. Thanks to the kinematic of the Z decay, the four leptons have generally sizeable transverse momenta ($p_T > 20$ GeV), are well separated ($\Delta R > 1$) and mainly distributed in the central region ($|\eta| < 3$). The

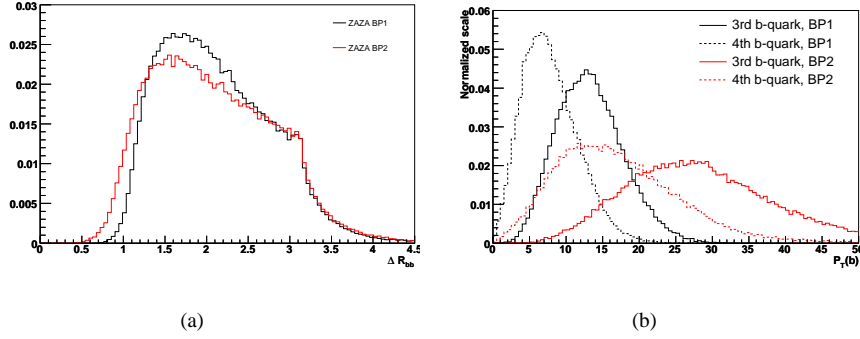


Figure 4.11: (a) Normalized ΔR distributions for the b -quark pairs coming from A^0 for the $gg \rightarrow h^0 \rightarrow H^0 H^0 \rightarrow ZA^0 ZA^0 \rightarrow ZZ4b$ signal, for the benchmarks BP1 (in black) and BP2 (in red). (b) p_T distributions of the third (plain lines) and fourth (dotted lines) b -quarks (ordered in p_T), for the same signal and benchmark points.

same is not necessarily true for b -quarks, as shown in Figure 4.11. The ΔR distribution displays a fairly good angular separation between the b -quarks coming from the same A^0 decay, especially for the benchmark point BP2, thanks to a higher A^0 mass. However, Figure 4.11(b) clearly shows that the same b -quarks are mainly distributed in the low p_T region. Indeed, A^0 is not only light, but also produced with a relatively low momentum since both the $h^0 \rightarrow H^0 H^0$ and $H^0 \rightarrow ZA^0$ decays occur close to their kinematic thresholds, especially in the BP1 case.

Because of this particular feature of the signal, the signal isolation strategy will be different for the benchmark points BP1 and BP2. In the BP1 scenario, the average p_T of the b -quarks coming from the A^0 is clearly not sufficient to envisage the reconstruction and the tagging of the resulting single jet. Since, in this case, the minimal angular separation between the two b -quarks is of order $\Delta R \sim 1$, a possible solution is to group the closest jets two-by-two and to tag the two resulting “super” b -jets. The only Standard Model irreducible background is then $ZZb\bar{b}$ which appears to be relatively low ($\sim 10\%$ of the signal before any isolation cut).

In the BP2 scenario, the average p_T of the b -quarks is slightly higher than BP1 case, and the simultaneous reconstruction (and potentially tagging) of the resulting four jets could be envisaged for $p_T > 15$ GeV without losing too much signal events. Assuming two B -tagging, the irreducible SM backgrounds are $ZZb\bar{b}jj$ and $ZZb\bar{b}b\bar{b}$ but both of them have cross sections two order of magnitude smaller the signal one, even after considering the signal loss due to acceptance cuts.

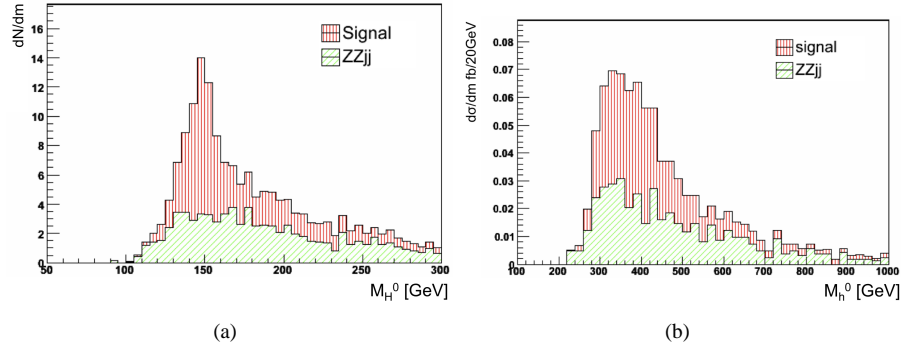


Figure 4.12: (a) Distribution of the reconstructed mass for the candidate H^0 boson after full simulation of the signal $gg \rightarrow h^0 \rightarrow H^0 H^0 \rightarrow Z A^0 Z A^0$ (red) and the main background ($ZZjj$ in green). There are two entries per event, and the total integrated luminosity is 100 fb^{-1} . (b) Same for the candidate h^0 boson mass (with one entry per event), normalised to the total cross section. From Ref. [160].

Results

Any quantitative result obtained at the parton-level would reveal itself partially meaningless due to the very low contribution of SM backgrounds and to the expected importance of additional soft radiations and pile-up effects. We only report here the results obtained recently in [160] after parton showering and hadronization with Pythia [161] and fast detector simulation with PGS [162].

The scenario considered in this work corresponds to $m_{h^0} = 400 \text{ GeV}$, $m_T = 150 \text{ GeV}$ and $m_{A^0} = 20 \text{ GeV}$. Since h^0 is significantly heavier than $2m_T$, and H^0 significantly heavier than $m_{A^0} + m_Z$, the A^0 bosons turn out to be notably more boosted and the associated b -quarks are more colinear than in the benchmarks BP1 and BP2. In order to avoid possible technical issues related to B -tagging the resulting “super” b -jets, no tagging is assumed in this preliminary analysis and the relevant background is then $ZZjj$. The Z bosons decay into muon pairs which are forced to be located inside the active region of the detector. To achieve the best possible background rejection, a minimum p_T of 40 GeV (20 GeV) is required for highest (lowest) p_T jet. The reconstructed h^0 ($ZZbb$) and H^0 (Zb) masses after the complete simulation chain are shown on Figure 4.12.

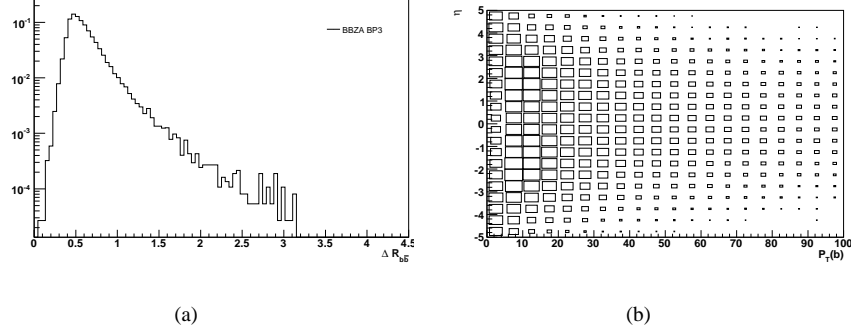


Figure 4.13: (a) Normalized ΔR distributions for the b -quark pairs coming from A^0 for the $gg \rightarrow b\bar{b}H^0 \rightarrow b\bar{b}ZA^0$ signal, for the benchmark point BP3. (b) (η, p_T) distribution of the the b -quarks produced in association with A^0 , for the same signal and benchmark point (the area of the boxes are proportional to the bin heights).

4.3.2 Process $gg \rightarrow b\bar{b}H^0 \rightarrow b\bar{b}ZA^0$

The $b\bar{b}$ associated production of A^0 or H^0 in a type II 2HDM (like the MSSM scalar sector) has been shown to be a promising discovery channel at the LHC when the Higgs boson decays into a $\tau^+\tau^-$ pair (e.g. see Ref. [97] and references therein) mainly thanks its very large cross section. As seen in Figure 4.5, this associated production mechanism dominates over the gluon fusion production through a b -quark loop for large scalar masses. In the context of a type II twisted 2HDM, a particularly interesting signature is the $gg \rightarrow b\bar{b}H^0 \rightarrow b\bar{b}ZA^0$ channel (see Figure 4.10(b)).

Signal and background

As shown in Figure 4.13(a) for the benchmark BP3, the decay products of A^0 in $gg \rightarrow b\bar{b}H^0 \rightarrow b\bar{b}ZA^0$ are very close from each other, due to high H^0 mass. For the $A^0 \rightarrow b\bar{b}$ main decay mode, the corresponding (large) SM backgrounds would then be Zj and/or Zb , depending on the actual efficiency of the B -tagging method applied on the super b -jet. Regarding the typically low p_T distributions of the two “spectator” b ’s produced in association with H^0 (see Figure 4.13(b)), they are assumed to be hard to reconstruct and are not taken into account in the signal final state.

Regarding the large $b\bar{b}ZA^0$ production cross section ($\sim 20\text{pb}$ for BP3), the secondary $A^0 \rightarrow \tau^+\tau^-$ decay could also be considered. When only the leptonic decays of Z and τ ’s are taken into account, the resulting final state $l^+l^- \bar{l}^+ \bar{l}^- (b\bar{b}) + E_{T\text{miss}}$ is cleaner

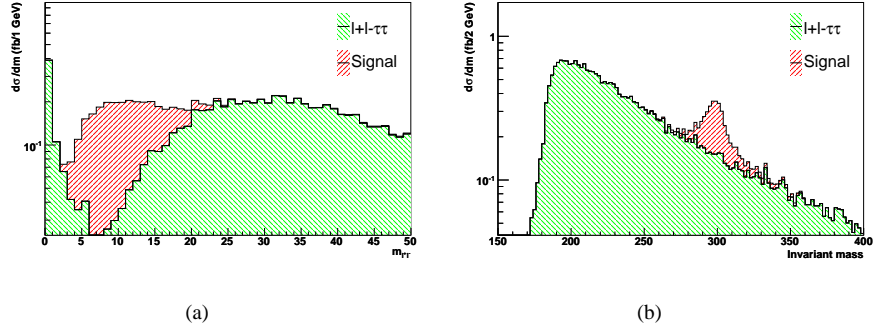


Figure 4.14: (a) Signal (BP3, in red) and background (in green) stacked invariant mass distributions for the candidate lepton pair coming from A^0 (see text) in the $gg \rightarrow b\bar{b}H^0 \rightarrow b\bar{b}ZA^0 \rightarrow b\bar{b}Z\tau^+\tau^-$ signal (with both τ 's decaying into leptons). (b) Same for the four leptons invariant mass (taking into account the total missing transverse energy).

than for the b decay mode. The main SM irreducible background is $Z(Z/\gamma)^*$ where a Z decays into e 's or μ 's and the τ pair originates from a photon or an off-shell Z . The same process with two e/μ pairs can also be considered as a background when the total missing transverse energy of the signal is too small to conclude about the presence of τ leptons.

Results

For reasonable acceptance cuts on all leptons in the final state ($p_T > 20$ GeV and $\eta < 2.5$), the signal cross section is 3.1 fb while the $Z(Z/\gamma)^*$ backgrounds have a total cross section of approximately 34 fb.

The proposed parton-level analysis method is straightforward. The lepton pair reconstructing the closest invariant mass to the real Z mass (used as an input) is “removed” from the event and the other one is used to reconstruct the invariant mass distribution shown in Figure 4.14(a). As seen on this Figure, the background is only important in the very low invariant mass region (due to the γ tail) and in the intermediate region $m_Z/3$ around which the $Z \rightarrow 2\tau \rightarrow 2l4\nu$ process stands (and, of course, also in the m_Z region which is not shown). In the signal region $\sim m_{A^0}/3$, it is rather low and a good significance could probably be achieved.

Since both τ 's are coming from the same scalar, the total missing transverse energy of the event can be used to reconstruct the invariant mass of the $l^+l^-\tau^+\tau^-$ four-body

final state. The result is shown in Figure 4.14(b). Since the background is mainly distributed around $2m_Z$, the signal should be clearly visible in the m_{H^0} region.

4.4 Signals with $H^\pm \rightarrow A^0 W^\pm$

4.4.1 Process $gg \rightarrow h^0 \rightarrow H^+ H^- \rightarrow W^+ A^0 W^- A^0$

The $gg \rightarrow h^0 \rightarrow H^+ H^- \rightarrow W^+ A^0 W^- A^0$ process (see Figure 4.10(a)) is very similar to the $gg \rightarrow h^0 \rightarrow H^0 H^0 \rightarrow Z A^0 Z A^0$ channel. The major difference is an higher cross section, due to the higher $h^0 \rightarrow H^+ H^-$ branching ratio compared to $h^0 \rightarrow H^0 H^0$, and the presence of W bosons in the final state. Since $BR(W^\pm \rightarrow l^\pm \nu_l) > BR(Z \rightarrow l^+ l^-)$, the leptonic and semi-leptonic final states have larger cross sections but suffer from the presence of very large $t\bar{t}$ backgrounds and are more difficult to reconstruct due to the presence of various sources of missing transverse energy.

Signal and background

The first considered final state is $l^+ l^- b\bar{b}b\bar{b} + E_{T,miss}$ where both A^0 scalars decay into $b\bar{b}$ and both W bosons decay leptonically. The kinematic distributions of the signal b -quarks are shown in Figure 4.15. Like already emphasised for the $Z A^0 Z A^0$ channel, the b -quarks coming from light A^0 boson are very soft and close to be collinear for the benchmark BP1. This renders any B -tagging attempt for the third and fourth jets (ordered in p_T) very difficult, to say the least. The resulting final state is $W^+ W^- b\bar{b}$ where the four b -quarks have been paired up into two super b -jets, and the main background, i.e. $t\bar{t}$, is three orders of magnitude larger than the signal.

The situation is slightly more favourable for the benchmark BP2. As seen in Figure 4.15, the good angular separation of the four b -quarks, together with an higher p_T distributions may allow for the reconstruction of four jets and the B -tagging of three of them. The main backgrounds, i.e. $t\bar{t}b\bar{b}$ and $t\bar{t}jj$ (where one of the jets is mistagged as coming from a b), have cross section only one order of magnitude larger than the signal.

Another potentially interesting final state is $l^\pm jj\tau^+\tau^-(b\bar{b}) + E_{T,miss}$ where one of the A^0 scalars decays into a soft $b\bar{b}$ pair and the other one into $\tau^+\tau^-$, while one of the W boson decays leptonically and the other one hadronically. To have a cleaner signature, we focus on the leptonic decays of both τ 's. Since the b -quark pair is likely

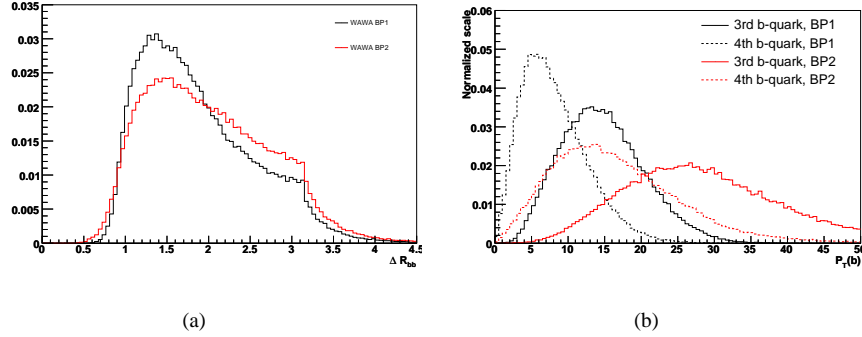


Figure 4.15: (a) Normalized ΔR distributions for the b -quark pairs coming from A^0 for the $gg \rightarrow h^0 \rightarrow H^+H^- \rightarrow W^+A^0W^-A^0 \rightarrow W^+W^-4b$ signal, for the benchmarks BP1 (in black) and BP2 (in red). (b) p_T distributions of the third (plain lines) and fourth (dotted lines) b -quarks (ordered in p_T), for the same signal and benchmark points.

to be hard to reconstruct, the main backgrounds are $W^\pm Zjj$ with $W^\pm \rightarrow l^\pm \nu_l$ and $Z \rightarrow l^+l^-$, and $t\bar{t}l^+l^-$ where the lepton pair originates from a photon or an off-shell Z boson radiated from a top quark or an initial state quark.

Results

For the benchmark BP2 and the final state W^+W^-4b , the signal cross section (before any acceptance cut) is 36.1 fb. After requiring $p_T > 15$ GeV for b -quarks, $p_T > 10$ GeV for leptons from the W 's decays and $|\eta| < 2.5$ for all objects, it drops down to 6.5 fb for a B -tagging efficiency of 40%. This should be compared to the background cross sections under the same hypothesis: 25 fb for $t\bar{t}b\bar{b}$ and 120 fb (taking into account a 2% mistagging probability) for $t\bar{t}jj$. As seen in Figure 4.16(a), inclusive quantities like the total invariant mass of all final states object do not allow for a good separation of the signal over the main background leading to a pessimistic preliminary conclusion regarding the feasibility of this analysis.

The situation is clearer for the benchmark BP1 and the final state $l^\pm jj\tau^+\tau^-(b\bar{b}) + E_{T,miss}$. After imposing acceptance cuts on all leptons ($p_T > 5$ GeV, $|\eta| < 2.5$), including those coming from τ decays, and on all jets ($p_T > 20$ GeV, $|\eta| < 2.5$), the main background (i.e., $WZ/\gamma jj$) can be further reduced by imposing $70 < m_{jj} < 90$ GeV for the two leading jets. The signal and background can be separated in kinematical distributions like the total invariant mass of all three leptons, as seen in Figure

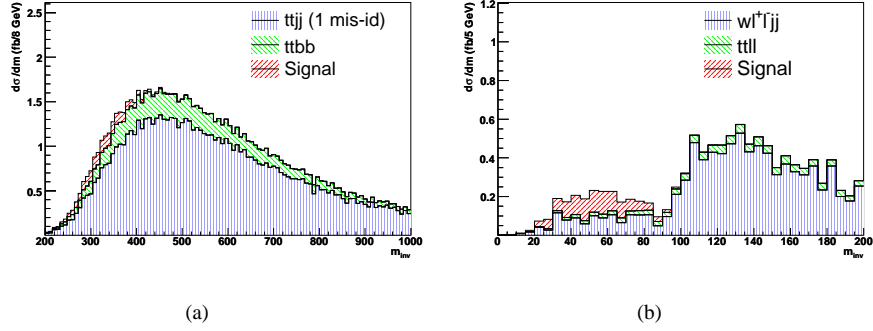


Figure 4.16: (a) Total invariant mass of all visible final state objects for the $gg \rightarrow h^0 \rightarrow H^+H^- \rightarrow W^+A^0W^- \rightarrow l^+l^-b\bar{b}b\bar{b} + E_{T,mis}$ signal and the main backgrounds (stacked) after acceptance cuts (see text). (b) Invariant mass of the three leptons for the $gg \rightarrow h^0 \rightarrow H^+H^- \rightarrow W^+A^0W^-A^0 \rightarrow l^\pm jj\tau^+\tau^- (b\bar{b}) + E_{T,mis}$ signal and the main backgrounds (stacked) after acceptance and isolation cuts (see text).

4.16(b). A discovery significance could probably be reached after a total integrated luminosity of a few tens of fb^{-1} . This already encouraging result could even be improved in a straightforward way by requiring that the two lowest p_T leptons have different flavours, thus reducing dramatically the main $W\gamma jj$ background where they are most likely to originate from the photon.

4.4.2 Process $pp \rightarrow tt \rightarrow W^\pm H^\mp bb \rightarrow W^+W^-A^0bb$

As mentioned previously, if the charged Higgs boson is light enough it could be produced through the top decay $t \rightarrow H^+b$. In the benchmark BP1, the charged Higgs subsequently decays into $W^\pm A^0$ (see Figure 4.17(a)), giving a $W^+W^-b\bar{b}b\bar{b}$ or a $W^+W^-b\bar{b}\tau^+\tau^-$ signature depending on the considered A^0 decay mode.

Signal and background

The $l^+l^-4b + E_{T,mis}$ final state, where $A^0 \rightarrow b\bar{b}$ and both W 's decay leptonically, has been investigated in [163] in the specific context of the CP violating MSSM and NMSSM. Preliminary studies of this signal in ATLAS [164] and CMS [151] collaborations show that this signal may emerge significantly from the main QCD background, i.e., $t\bar{t}b\bar{b}$, when heavy mass reconstruction and B -tagging techniques are used.

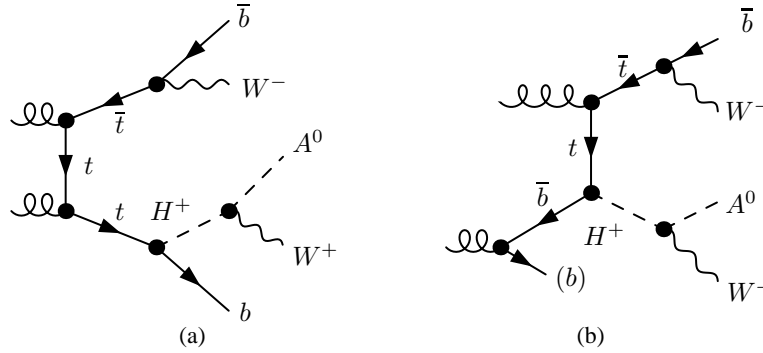


Figure 4.17: Sample Feynman diagrams for (a) the $gg \rightarrow t\bar{t} \rightarrow W^+W^-b\bar{b}A^0$ process and (b) the $gg(\bar{b}) \rightarrow \bar{t}H^+ \rightarrow W^+W^-(b)\bar{b}A^0$ process.

In the present work, we focus only on the somehow simpler final state $l^\pm l^+ l^- 2b + E_{T,miss}$ for the benchmark BP1, where $A^0 \rightarrow \tau^+ \tau^- \rightarrow l^+ l^- + E_{T,miss}$, one W boson decays leptonically and the other one hadronically. The main issue regarding this process is the relatively low momenta of the two leptons produced in τ decay due to the low A^0 mass and the small amount of boost available. Assuming the B -tagging of at least one of the two b -jets coming from tops, the only relevant background is the $t\bar{t}l^+l^-$ process with semileptonic decays³.

Results

With loose but reasonable acceptance cuts on leptons ($p_T > 5$ GeV and $|\eta| < 2.5$) and jets ($p_T > 20$ GeV and $|\eta| < 2.5$) and one B -tag (with a 40% efficiency), the total cross section is 2.2 fb for the signal (with a 23% acceptance) and 5.2 fb for the background (with a 62% acceptance). As shown in Figure 4.18(a), a clean kinematical variable like the reconstructed invariant mass of the three final state leptons allows for a good separation of signal and background events. The reconstruction of the A^0 and H^0 masses seems however challenging due to the various sources of missing transverse energy.

³All the quoted acceptance for this background refers to a “bare” generation cross section where only an invariant mass cut $m_{ll} > 5$ GeV has been applied to avoid the γ soft divergence.

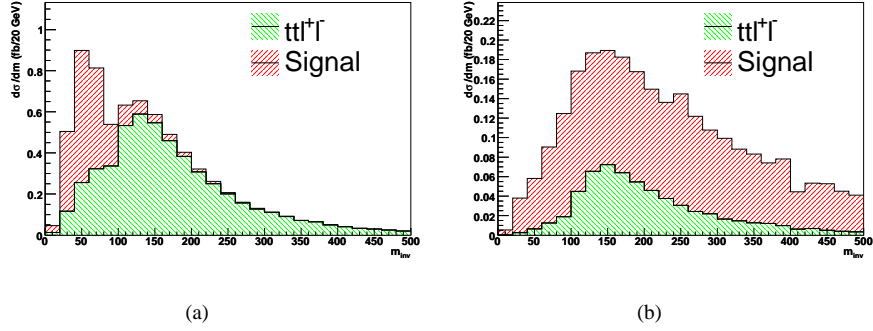


Figure 4.18: Invariant mass distributions of the three final state leptons for the $t \rightarrow H^+ b$ (a) and tH^+ signals (b), together with the $t\bar{t}l^+l^-$ background (stacked).

4.4.3 Process $pp \rightarrow tH^\pm(b) \rightarrow W^- b W^+ A^0(b)$

The cross section for the charged Higgs production in top decays drops down rapidly for increasing charged Higgs masses. For $m_{H^\pm} \gtrsim (m_t - m_b)$, the charged Higgs associated production with a single top (see Figure 4.17(b)) is by far a more promising channel, especially with type II Yukawa couplings like in the benchmark scenario BP3 considered here.

Signal and background

For the same decay hypothesis for A^0 and the W 's as in the previous section, the signal final state is $l^\pm l^+ l^- b(b) + E_{T,miss}$ where the presence of the extra b quark between parenthesis depends on the considered initial state (gg or gb). In the following, both possibilities are treated inclusively. Compared to the previous process $t \rightarrow H^+ b$, the leptons coming from the A^0 decay are considerably more boosted due to the higher charged Higgs mass, and a simple minimum p_T cut on all final state leptons may be already sufficient to achieve an impressive separation of the signal events.

Results

With simple acceptance cuts on leptons ($p_T > 15$ GeV and $|\eta| < 2.5$) and jets ($p_T > 20$ GeV and $|\eta| < 2.5$), together with one B -tag (with a 40% efficiency) and a simple selection cut $60 < m_{jj} < 100$ on the two hardest jets (which affects mainly the background where the b -jets are often harder than those coming from the W), the total cross section is 2.4 fb for the signal (with a 26% acceptance) and 0.6 fb for the

background (with a 7.3% acceptance). As seen in 4.18(b), there is no clear separation between signal and background events in the invariant mass distribution of the final state leptons, but the overall S/B ratio looks large enough to envisage a discovery significance after approximately 5 fb^{-1} of integrated luminosity.

4.5 Summary

The constrained twisted two-Higgs-doublet introduced in Chapters 2 and 3 clearly offers opportunities for interesting and unusual signatures at the LHC.

The $h^0 \rightarrow A^0 A^0$ decay favoured in the $m_{h^0} > 2m_T$ region of the model parameter space may be studied when h^0 is produced in association with a W/Z boson, as argued in [141, 152]. The same process could also be studied for a VBF production of h^0 , but the original optimistic conclusion [158, 159] about the feasibility of this channel when one A^0 decays into a b -quark pair and the other one into a τ pair is tempered by our matrix-element based simulation of the $t\bar{t}jj$ background.

The $H^0 \rightarrow ZA^0$ decay appears as one of the most striking signature of the model, in particular due to the presence of a Z boson in the final state. The $gg \rightarrow h^0 \rightarrow H^0 H^0 \rightarrow ZA^0 ZA^0$ process, with both Z bosons decaying into charged leptons and both A^0 into b -quarks, is almost free of SM background. A complete fast-simulation study of the signal [160] for a specific benchmark has shown promising results, and our parton-level kinematic analysis emphasises the possible importance of soft “super” b -jets tagging techniques, in particular for light and/or mildly boosted A^0 configurations. The $b\bar{b}H^0 \rightarrow b\bar{b}ZA^0$ process where A^0 decays into a τ pair may also offer good detection opportunities for type II models, in particular thanks to the very large signal cross section (around 100 signal events with a significance above 10 for a total integrated luminosity of 30 fb^{-1}).

The $H^\pm \rightarrow W^\pm A^0$ decay, finally, may also gives genuine signatures despite the presence of larger backgrounds like $t\bar{t}$ and the difficulties associated to mass reconstruction due to the presence of large amount of missing transverse energy. The $gg \rightarrow h^0 \rightarrow H^+ H^- \rightarrow W^+ A^0 W^- A^0$ may be detectable even for a rather light A^0 if at least one A^0 boson decays into a τ pair. But the detection will rely crucially on the detector performance for low p_T leptons identification. When the charged Higgs is produced in association with top quarks, the $H^\pm \rightarrow W^\pm A^0 \rightarrow W^\pm \tau^+ \tau^-$ decay chain also offers good detection opportunities, in particular in the high m_{H^\pm} region, mainly due to the low cross section of the $t\bar{t}l^+l^-$ background.

Conclusion

In the course of this thesis we have examined the possibility for an extension of the Standard Model scalar sector which can, simultaneously, be justified on the basis of natural symmetries, satisfy existing theoretical and experimental constraints and give rise to unexpected phenomenology at forthcoming high energy colliders.

Our starting point, the generic two-Higgs-doublet model, is a simple yet rich framework which may arise naturally in the context of various BSM theories. On the other hand, genuine SM properties give grounds for specific symmetries, like the custodial and CP symmetries, which may or may not be satisfied by new interactions. The extension of these symmetries in the context of the 2HDM sheds new light on their possible interplay and allows us to naturally introduce a new “twisted” scenario. In this scenario, the successful $\rho \approx 1$ phenomenological relation is ensured by the degeneracy of a pair of charged scalars with a scalar (H^0), and not with a pseudoscalar (A^0) as it is usually done in the literature.

Surprisingly enough, this seemingly mild difference opens in fact a window to novel and, to a large extent, unexplored phenomenology for the Higgs sector. Indeed, due to its vanishing coupling to pairs of gauge bosons, a light pseudoscalar, say A^0 , may escape the LEP II direct bound while the same is not true for a charged Higgs boson, whose mass is already strongly constrained by indirect measurements. The twisted scenario we proposed allows us to naturally reconcile a large mass splitting between (H^\pm, H^0) and A^0 with tight electroweak precision constraints. In this scenario, a SM Higgs boson mass larger than ~ 200 GeV may also be accommodated through small breaking of the custodial symmetry, driven for example by loop corrections.

An “inverted” mass spectrum $m_{A^0} < m_{H^0, H^\pm} < m_{h^0}$, as compared for example to the typical MSSM scenario, with a relatively light A^0 (e.g., $m_{A^0} \approx 30$ GeV) is still allowed by all the theoretical, indirect and direct constraints we extensively reviewed

and applied to the specific twisted 2HDM case. This particular mass spectrum leads to interesting new signal opportunities, mainly related to the presence of new exotic decay channels like $h^0 \rightarrow H^0 H^0$, $H^+ H^-$, $H^\pm \rightarrow W^\pm A^0$ or $H^0 \rightarrow Z A^0$. These signals are covered only very partially (to say the least) by analysis in the context of more restricted BSM models. This motivated us to implement the generic 2HDM in the framework of the MadGraph/MadEvent matrix-element based Monte-Carlo event generator. Incidentally, this implementation triggered extensive modifications of the original code structure towards larger flexibility. The parton-level analysis of the most important twisted 2HDM signals together with their main backgrounds, for different representative benchmark points, allowed us to conclude positively regarding their possible experimental interest.

The perspectives for extending the present work are likely to be numerous but can be categorised along two main directions. On the theoretical side, the twisted version of the custodial and CP symmetries can probably be generalised to other sectors of the theory, like the Yukawa sector, or to more complex scalar sector extensions, i.e., models with more than two Higgs doublets or involving higher representations. Applications to more “realistic” BSM scenarios like Technicolor-inspired models could also be envisaged. The additional degrees of freedom emphasised by our approach may indeed offer an appreciable latitude when considering the impact of the presence of low-scale approximate symmetries on higher scale structures.

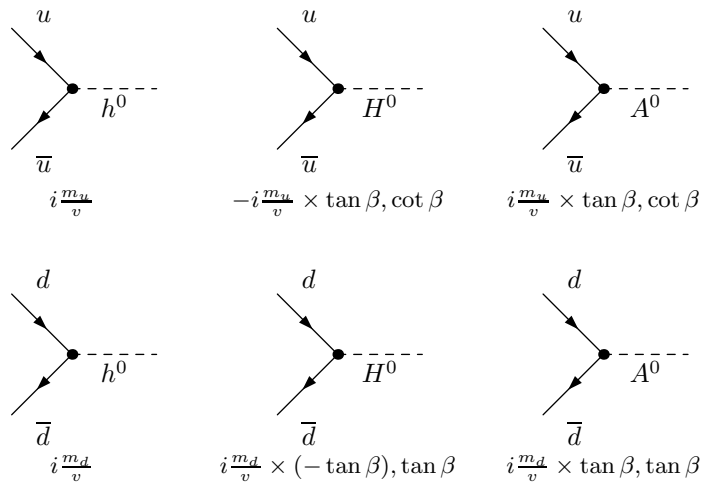
On the experimental side, our limited phenomenological analysis clearly highlights the feasibility of more detailed studies. Beyond this pragmatic conclusion, it also reveals some unusual and specific challenges which may be encountered in such studies. Among others, let us quote the identification of “super b -jets” which appears as a recurrent requirement for several processes, or the resolution of overconstrained systems of several kinematical variables. Various innovative solutions to these problems may exist, or have already been proven to exist, and some of them are expected to be applied to the twisted 2HDM in a near future.


In summary, the generic approach advocated in our introduction, where recurrent structures in BSM theories are considered from the point of view of specific symmetries motivated by low energy constraints, has been successfully followed in the present work. From our point of view, this alternative investigation method between “pure” top-down and bottom-up strategies offers interesting insights for our never-ending quest towards a unified physical interpretation of high energy phenomena.

Appendix A

Higgs boson Feynman rules in the twisted 2HDM

The first value is for type I models, and the second one for type II models.



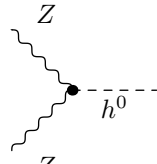


$$-\frac{iV_{ud}^*}{\sqrt{2}v} [m_d X(1 + \gamma_5) + m_u Y(1 - \gamma_5)]$$

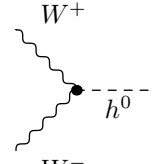
$$-\frac{iV_{ud}}{\sqrt{2}v} [m_d X(1 - \gamma_5) + m_u Y(1 + \gamma_5)]$$

$$\text{Type I : } X = -\tan\beta \quad Y = \tan\beta \quad (\text{A.1})$$

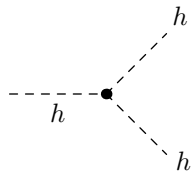
$$\text{Type II : } X = \tan\beta \quad Y = \cot\beta \quad (\text{A.2})$$



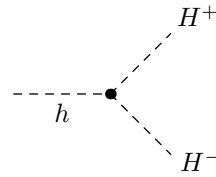
$$\frac{-2ig_{\mu\nu}m_Z^2}{v}$$



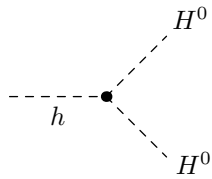
$$\frac{-2ig_{\mu\nu}m_W^2}{v}$$



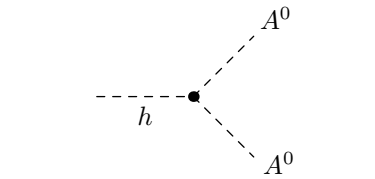
$$6\Lambda_S v = \frac{3m_{h^0}^2}{v}$$



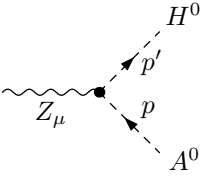
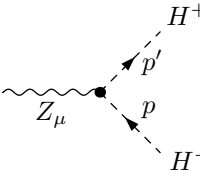
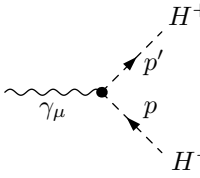
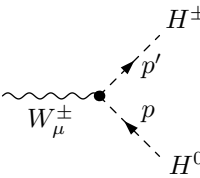
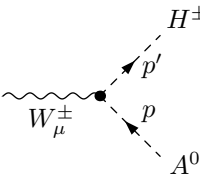
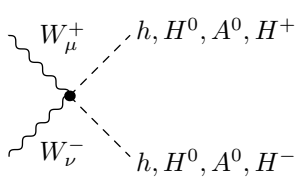
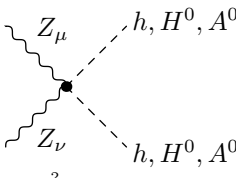
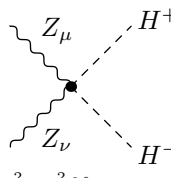
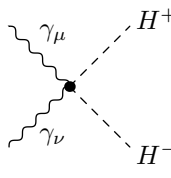
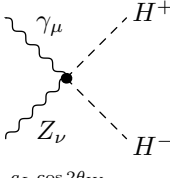
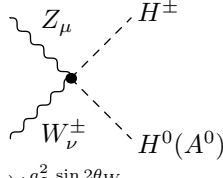
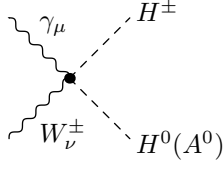
$$2\Lambda_S v = \frac{m_{h^0}^2}{v}$$



$$2\Lambda_S v = \frac{m_{h^0}^2}{v}$$



$$(2\Lambda_S + \Lambda_{AS})v = \frac{m_{h^0}^2 + 2(m_{A^0}^2 - m_T^2)}{v}$$

 <p style="text-align: center;">Z_μ</p> <p style="text-align: center;">$-\frac{g_L}{2 \cos \theta_W} (p + p')_\mu$</p>	 <p style="text-align: center;">Z_μ</p> <p style="text-align: center;">$-\frac{g_L \cos 2\theta_W}{2 \cos \theta_W} (p + p')_\mu$</p>	 <p style="text-align: center;">γ_μ</p> <p style="text-align: center;">$-ie(p + p')_\mu$</p>
 <p style="text-align: center;">W_μ^\pm</p> <p style="text-align: center;">$\pm i \frac{g_L}{2} (p + p')_\mu$</p>	 <p style="text-align: center;">W_μ^\pm</p> <p style="text-align: center;">$\frac{g_L}{2} (p + p')_\mu$</p>	 <p style="text-align: center;">W_μ^+</p> <p style="text-align: center;">W_ν^-</p> <p style="text-align: center;">$i \frac{g_L^2}{2} g_{\mu\nu}$</p>
 <p style="text-align: center;">Z_μ</p> <p style="text-align: center;">Z_ν</p> <p style="text-align: center;">$i \frac{g_L^2}{2 \cos^2 \theta_W} g_{\mu\nu}$</p>	 <p style="text-align: center;">Z_μ</p> <p style="text-align: center;">Z_ν</p> <p style="text-align: center;">$i \frac{g_L^2 \cos^2 2\theta_W}{2 \cos^2 \theta_W} g_{\mu\nu}$</p>	 <p style="text-align: center;">γ_μ</p> <p style="text-align: center;">γ_ν</p> <p style="text-align: center;">$2ie^2 g_{\mu\nu}$</p>
 <p style="text-align: center;">γ_μ</p> <p style="text-align: center;">Z_ν</p> <p style="text-align: center;">$ie \frac{g_L \cos 2\theta_W}{\cos \theta_W} g_{\mu\nu}$</p>	 <p style="text-align: center;">Z_μ</p> <p style="text-align: center;">W_ν^\pm</p> <p style="text-align: center;">$(\pm) i \frac{g_L^2 \sin 2\theta_W}{2 \cos^2 \theta_W} g_{\mu\nu}$</p>	 <p style="text-align: center;">γ_μ</p> <p style="text-align: center;">W_ν^\pm</p> <p style="text-align: center;">$-(\pm) i \frac{g_L e}{2} g_{\mu\nu}$</p>

Appendix **B**

The 2HDM implementation into MadGraph/MadEvent v4

The MadGraph/MadEvent package [165, 166] is a multi-purpose Monte Carlo event generator based on exact matrix elements calculations at tree-level using the helicity amplitude formalism implemented in the HELAS library [167].

The first versions of MadGraph/MadEvent were dedicated to SM processes and, even if the MSSM was also available in the independent package SMadGraph [168], the implementation of new physics models was not a straightforward task. Starting from version 4 [149], the MadGraph/MadEvent code structure has been redesigned in order to simplify this step, and the fully generic 2HDM has been implemented as a first application of this new framework. The current version of the code includes various additional improvements, like interfaces for matching the matrix element description with parton showers, implementation of the Les Houches standards, decay chains syntax, analysis platforms, and a user-friendly web interface for online event generation on computer farms. Recent developments also include FeynRules, a Mathematica module to automatically derive Feynman rules from a given Lagrangian, and a specific version of the code optimised to run over the Grid.

B.1 The implementation of the 2HDM into MadGraph

In the so called “general” version of the model, we do not have put any further restrictions on the interactions allowed by gauge invariance. Many diagrams involving tree-level FCNCs and violating the CP symmetry are thus present. The user who has no interest in these phenomena should use the “simplified” version of the model where the number of generated diagrams (and thus the computing time) is much smaller in many cases. We use the following naming convention: h^+ and h^- stand for the positively and negatively charged Higgs bosons, while h_1 , h_2 and h_3 stand for the neutral ones. Since we do not assume CP invariance of the potential, the neutral bosons are not necessarily CP eigenstates and we are thus using the standard naming convention in this case, h_1 being the lightest one and h_3 the heavier one.

TwoHiggsCalc is a 2HDM parameters calculator written in C and is accessible from a web interface. It has been designed to compute input values for the 2HDM extension of MadGraph/MadEvent but it can also be used as an independent tool. Starting from parameters of the Lagrangian, such as the v.e.v. or the Yukawa couplings, the program computes useful physical quantities at leading order such as the mass spectrum, the mixing matrix, the total decay widths and the branching ratios.

Basis conventions

In the general 2HDM, one has the freedom to choose a specific basis for entering parameters. All the possible choices should be physically equivalent. TwoHiggsCalc works with parameters given in a particular basis, called the “Higgs basis” where only one Higgs doublet gets a vev. An independent software called Gen2HB has been written to allow the user to first convert the parameters given in an arbitrary basis, called the “generic basis” where both Higgs doublet get a vev, to parameters in the Higgs basis. See [90] for more information on basis invariance and for more information on our notations.

Input/output format

The program reads input and writes out results in a specific format close to the “SUSY Les Houches Accord” [169, 170] convention for SUSY parameters. This format can later be read by MadGraph/MadEvent to perform numerical computations of 2HDM processes. If the program is downloaded as a stand alone application, you should read

the README file which describe the modified version of LHA used as input convention. To facilitate online use of TwoHiggsCalc, a web form has been designed to simplify the input file writing process. In this form, you can enter numerical values for the parameters, the units being fixed when needed. Some simple algebraic expressions can also be used. The $+$, $-$, $*$, $/$ operators and the `PI` reserved keyword, e.g. in `PI/2+3*PI/2`, are correctly interpreted.

Lagrangian convention for the Higgs basis

The scalar potential is written

$$\begin{aligned}
 V = & \mu_1 H_1^\dagger H_1 + \mu_2 H_2^\dagger H_2 - \left(\mu_3 H_1^\dagger H_2 + \text{h.c.} \right) \\
 & \lambda_1 \left(H_1^\dagger H_1 \right)^2 + \lambda_2 \left(H_2^\dagger H_2 \right)^2 \\
 & + \lambda_3 \left(H_1^\dagger H_1 \right) \left(H_2^\dagger H_2 \right) + \lambda_4 \left(H_1^\dagger H_2 \right) \left(H_2^\dagger H_1 \right) \\
 & + \left[\left(\lambda_5 H_1^\dagger H_2 + \lambda_6 H_1^\dagger H_1 + \lambda_7 H_2^\dagger H_2 \right) \left(H_1^\dagger H_2 \right) + \text{h.c.} \right]
 \end{aligned}$$

All quartic terms parameters (in red) must be input, all the masses terms parameters (μ_1 , μ_2 and μ_3) being fixed by the minimization constraints. λ_1 to λ_4 are real parameters. λ_5 could be in general a complex parameter but since only the phase differences between λ_5 , λ_6 , λ_7 and μ_3 matters, the phase of λ_5 can always be rotated out. We will thus consider it as a real parameter here while λ_6 and λ_7 are a priori complex.

The Yukawa interactions read

$$\begin{aligned}
 \mathcal{L}_Y = & \frac{\overline{Q}_L \sqrt{2}}{v} \left[(M_d H_1 + Y_d H_2) d_R + (M_u \tilde{H}_1 + Y_u \tilde{H}_2) u_R \right] \\
 & + \frac{\overline{E}_L \sqrt{2}}{v} [(M_e H_1 + Y_e H_2) e_R]
 \end{aligned}$$

Yukawa couplings must be given in the physical basis, i.e. in the basis where the mass matrix is diagonal. Since in the Higgs basis only the first Higgs doublet gets a non zero vev, the M matrix is completely fixed by the observed fermion masses while the Y matrix (giving the couplings of the second Higgs doublet) is a priori free. For this matrix, the first indice refers to doublet generation while the second one refers to the singlet generation. For example, `Y2B` stands for the complex Yukawa couplings of the second Higgs doublet to the second generation quark left doublet and to the bottom singlet.

Lagrangian convention for the generic basis

The scalar potential is written

$$\begin{aligned}
 V = & \mu_1 \phi_1^\dagger \phi_1 + \mu_2 \phi_2^\dagger \phi_2 - \left(\mu_3 \phi_1^\dagger \phi_2 + \text{h.c.} \right) \\
 & \lambda_1 \left(\phi_1^\dagger \phi_1 \right)^2 + \lambda_2 \left(\phi_2^\dagger \phi_2 \right)^2 \\
 & + \lambda_3 \left(\phi_1^\dagger \phi_1 \right) \left(\phi_2^\dagger \phi_2 \right) + \lambda_4 \left(\phi_1^\dagger \phi_2 \right) \left(\phi_2^\dagger \phi_1 \right) \\
 & + \left[\left(\lambda_5 \phi_1^\dagger \phi_2 + \lambda_6 \phi_1^\dagger \phi_1 + \lambda_7 \phi_2^\dagger \phi_2 \right) \left(\phi_1^\dagger \phi_2 \right) + \text{h.c.} \right]
 \end{aligned}$$

All quartic terms parameters must be given as well as $\tan(\beta)$, the μ_3 norm and the phase of v_2 . Additional parameters are computed automatically. The overall v.e.v. is extracted from SM parameters while masses terms parameters like mu_1 , mu_2 and the phase of mu_3 are fixed by the minimization constraints. λ_1 to λ_4 are real parameters, λ_5 , λ_6 and λ_7 are a priori complex. The accuracy value at which minimization equations in terms of invariants are going to be checked can also be provided, the web interface use the default value $1e-10$.

The Yukawa interactions read

$$\begin{aligned}
 \mathcal{L}_Y = & \frac{\overline{Q}_L \sqrt{2}}{v} \left[(\Delta_d H_1 + \Gamma_d H_2) d_R + (\Delta_u \tilde{H}_1 + \Gamma_u \tilde{H}_2) u_R \right] \\
 & + \frac{\overline{E}_L \sqrt{2}}{v} [(\Delta_e H_1 + \Gamma_e H_2) e_R]
 \end{aligned}$$

Yukawa couplings must be given in the physical basis, i.e. in the basis where the mass matrix is diagonal. Since the mass matrix is fixed, only the Γ matrix, i.e. the Yukawa couplings of the second Higgs doublet, is required. The other one (Δ) is going to be automatically evaluated to match observed fermion masses. For the Γ matrix, the first indice refers to doublet generation while the second one refers to the singlet generation. For example, G2B stands for the complex Yukawa couplings of the second Higgs doublet to the second generation quark left doublet and to the bottom singlet.

TwoHiggsCalc output

Given the above parameters plus some SM parameters as an input, `TwoHiggsCalc` computes the following quantities

- Scalar particles mass spectrum

Block	Comment
SMINPUTS	From 1 to 4, SM parameters, see the SM section for more details
MGSMPARAM	Extra block with $\sin \theta_W$ and M_W , see the SM section for more details
MGYUKAWA	“Yukawa” masses used in the Yukawa couplings evaluation
MGCKM	The full CKM matrix
BASIS	Basis choice, must be 1 (Higgs basis) for MadEvent !
MINPAR	Scalar potential parameters in the Higgs basis
YUKAWA2	Yukawa couplings of the second Higgs doublet
MASS	All SM particles masses, plus the five new Higgs boson masses
TMIX	The scalar mixing matrix
DECAY	For all the Higgs bosons, top, W^\pm and Z

Table B.1: LHA blocks used by 2HDM MadEvent

- Mixing matrix of neutral scalars (called T in [51])
- Decay widths for all scalars as well as for W and Z bosons and the top quark. All widths are evaluated at tree-level using the same couplings as in MadEvent. Under threshold formula are included for the scalar into two vector bosons decays and the one loop driven scalar into two gluons decay is also computed.

B.2 The implementation of the 2HDM into MadEvent

The LHA blocks and parameters used by MadEvent are given in table B.1. All blocks in the table are provided by TwoHiggsCalc. Note that if parton density functions (PDFs) are used in the MadEvent run, the value for α_s at M_Z and the order of its running is given by the PDF. Otherwise $\alpha_s(M_Z)$ is given by block SMINPUTS, parameter 3, and the order of running is taken to be 2-loop. The scale where α_s is evaluated is however always given by the “scale” parameter in the `run_card.dat`.

Appendix C

Higgs bosons production in association with single top

The $t\bar{t}$ associated Higgs boson production is known to have a non negligible ($\simeq 1$ pb) cross section at LHC for moderate value of m_h ($m_h \simeq 100$ GeV). This is in great part due to the very large $t\bar{t}$ pair production cross section. Since the single top production has also a sizeable rate at LHC (more or less half of the $t\bar{t}$ production), in particular in the t -channel, one could naively expect that the single top associated production of the Higgs boson is still competitive. Nevertheless it has been shown in [171] that this naive guess is false.

The single top associated production of the SM Higgs boson appears to be relatively small, of order 100 fb for $m_h \simeq 100$ GeV instead of the 500 fb that one could have expected. The main reason for this is a particularly strong destructive interference between the two dominant amplitudes associated with the diagrams shown on figure C.1.

Even though the sign of this interference can be guessed from unitarity requirement, its absolute magnitude at moderate energy compared to the masses involved (e.g. the top mass) is surprising. The integrated squared amplitude for each of these diagram is indeed three to five times larger than the total cross section. The total SM cross section at LHC as a function of m_h is shown on figure C.2.

If one considers the MSSM instead of the SM, this negative result still holds. To illustrate this, let's consider the decoupling regime where the mixing between h^0 and

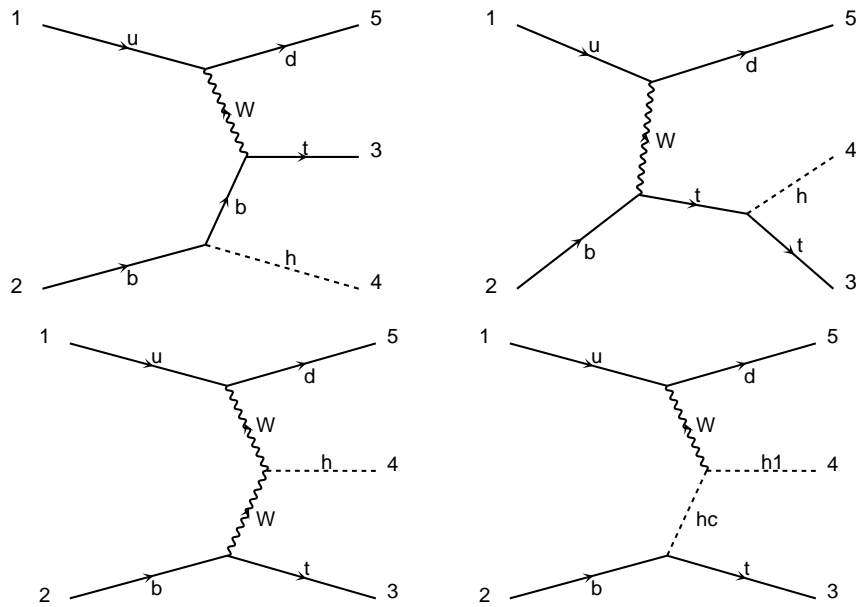


Figure C.1: Top and bottom left: Diagrams contributing to single-top and Higgs associated production in the SM. Bottom right: Extra diagram contributing to single-top and Higgs associated production in the 2HDM.

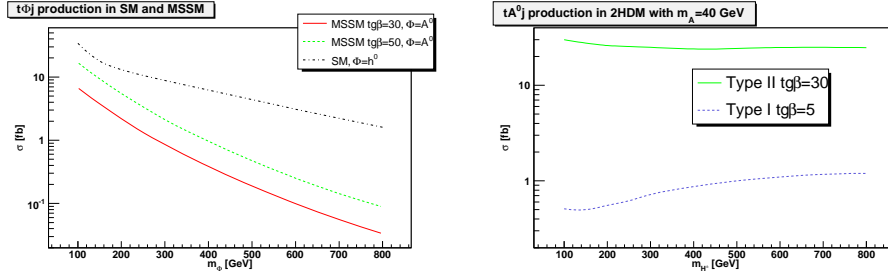


Figure C.2: Cross sections of single top associated production of different Higgs bosons. On the left, the SM Higgs boson production cross section is shown together with the 2HDM type II pseudoscalar A^0 production cross section for two different $\tan\beta$ values, both as a function of their mass. On the right, the MSSM pseudoscalar A^0 production cross section is shown as a function of m_{H^\pm} both for type I and type II. For all these cross sections, a minimal p_T of 20 GeV and a maximal rapidity of 2.5 is assumed for the (non b) jet. The factorisation and renormalisation scales are both set equal to m_ϕ . The b quark mass involved in the Yukawa coupling is the running mass at m_ϕ . The PDF is CTEQ6L1.

H^0 is small. For the lightest Higgs boson, the situation is similar to the SM. The $WW h^0$ coupling is close to the SM value and even if h^0 is coupling mainly to b , the $b\bar{b}$ coupling is close to the $t\bar{t}$ one in the SM in the limit of large $\tan\beta$. For the heaviest scalar H^0 the coupling $WW H^0$ almost vanishes and one could then expect an enhancement of the total cross section. But an additional diagram involving a charged Higgs boson (see figure C.1) should also be taken into account due to the large $W^\pm H^\mp H^0$ coupling. This diagram leads to an amplitude of the same order and the same sign as the one involving only the W boson and thus no particular enhancement is observed [171]. The situation is similar for the pseudoscalar A^0 but in this case the $WW A^0$ coupling is strictly zero due to CP invariance.

The last hope one could have to get a sizeable cross section for this process is to consider a 2HDM where the pseudoscalar A^0 is relatively light and where the charged Higgs pair is much heavier so that the negative interference cannot occur (i.e., the amplitudes associated with the SM like diagrams on figure C.1 are dominant). This of course cannot be considered in the MSSM case since the masses of H^\pm and A^0 are linked through the mass relation $m_{H^\pm}^2 = m_{A^0}^2 + m_{W^\pm}^2$. The resulting cross section for $m_{A^0} = 40$ GeV is plotted on figure C.2 as a function of the charged Higgs mass both in case of type I and of type II 2HDM. A small enhancement at high m_{H^\pm} is well observed in the 2HDM type I case but the overall cross section is expected to stay much smaller than the SM one due to the reduced top quark Yukawa coupling. In type

In models, the effect of varying m_{H^\pm} is almost invisible. At low m_{H^\pm} , the diagram involving the charged Higgs boson should contribute but its squared amplitude is more or less of the order of magnitude of the negative interference it creates so that its total contribution is negligible.

To conclude we propose a “no hope” conjecture stating that the associated production of Higgs bosons and single top in any realistic extension of the scalar sector will always have a cross section at best of order of the SM one, the latter appearing to be itself probably too small to be successfully exploited at LHC.

Bibliography

- [1] J. F. Gunion, H. E. Haber, G. L. Kane, and S. Dawson, *The Higgs hunter's guide*. Perseus Publishing, 1989. SCIPP-89/13.
- [2] A. Djouadi, *The anatomy of electro-weak symmetry breaking. I: The Higgs boson in the standard model*, hep-ph/0503172.
- [3] E. Fermi, *An attempt of a theory of beta radiation. I*, *Z. Phys.* **88** (1934) 161–177.
- [4] T. van Ritbergen and R. G. Stuart, *Complete 2-loop quantum electrodynamic contributions to the muon lifetime in the fermi model*, *Phys. Rev. Lett.* **82** (1999) 488–491, [hep-ph/9808283].
- [5] **Particle Data Group** Collaboration, W. M. Yao *et. al.*, *Review of particle physics*, *J. Phys.* **G33** (2006) 1–1232.
- [6] S. L. Glashow, *Partial symmetries of weak interactions*, *Nucl. Phys.* **22** (1961) 579–588.
- [7] S. Weinberg, *A model of leptons*, *Phys. Rev. Lett.* **19** (1967) 1264–1266.
- [8] A. Salam, *Weak and electromagnetic interactions*, *Svartholm: Elementary Particle Theory, Proceedings Of The Nobel Symposium Held 1968 At Lerum, Sweden* (1968) 367–377.
- [9] C.-N. Yang and R. L. Mills, *Conservation of isotopic spin and isotopic gauge invariance*, *Phys. Rev.* **96** (1954) 191–195.
- [10] F. Englert and R. Brout, *Broken symmetry and the mass of gauge vector mesons*, *Phys. Rev. Lett.* **13** (1964) 321–322.

- [11] P. W. Higgs, *Broken symmetries and the masses of gauge bosons*, *Phys. Rev. Lett.* **13** (1964) 508–509.
- [12] G. S. Guralnik, C. R. Hagen, and T. W. B. Kibble, *Global conservation laws and massless particles*, *Phys. Rev. Lett.* **13** (1964) 585–587.
- [13] M. S. Chanowitz, *Strong $W W$ scattering at the end of the 90's: Theory and experimental prospects*, hep-ph/9812215.
- [14] W. J. Marciano and S. S. D. Willenbrock, *Radiative corrections to heavy higgs scalar production and decay*, *Phys. Rev.* **D37** (1988) 2509.
- [15] K. Riesselmann and S. Willenbrock, *Ruling out a strongly-interacting standard Higgs model*, *Phys. Rev.* **D55** (1997) 311–321, [hep-ph/9608280].
- [16] T. P. Cheng, E. Eichten, and L.-F. Li, *Higgs Phenomena in Asymptotically Free Gauge Theories*, *Phys. Rev.* **D9** (1974) 2259.
- [17] M. Gockeler, H. A. Kastrup, T. Neuhaus, and F. Zimmermann, *Scaling analysis of the $O(4)$ symmetric ϕ^4 theory in the broken phase*, *Nucl. Phys.* **B404** (1993) 517–555, [hep-lat/9206025].
- [18] P. Arnold and S. Vokos, *Instability of hot electroweak theory: bounds on $m(h)$ and $m(t)$* , *Phys. Rev.* **D44** (1991) 3620–3627.
- [19] T. Hambye and K. Riesselmann, *Matching conditions and higgs mass upper bounds revisited*, *Phys. Rev.* **D55** (1997) 7255–7262, [hep-ph/9610272].
- [20] W. J. Marciano and A. Sirlin, *Radiative corrections to neutrino induced neutral current phenomena in the $SU(2)_L \times U(1)$ theory*, *Phys. Rev.* **D22** (1980) 2695.
- [21] M. J. G. Veltman, *Limit on mass differences in the Weinberg model*, *Nucl. Phys.* **B123** (1977) 89.
- [22] M. Gell-Mann and M. Levy, *The axial vector current in beta decay*, *Nuovo Cim.* **16** (1960) 705.
- [23] P. Sikivie, L. Susskind, M. B. Voloshin, and V. I. Zakharov, *Isospin breaking in technicolor models*, *Nucl. Phys.* **B173** (1980) 189.
- [24] R. Lytel, *Weak isospin breaking and higher order corrections*, *Phys. Rev.* **D22** (1980) 505.
- [25] M. J. G. Veltman, *Second threshold in weak interactions*, *Acta Phys. Polon.* **B8** (1977) 475.

- [26] M. B. Einhorn and J. Wudka, *Screening of heavy Higgs radiative effects*, *Phys. Rev.* **D39** (1989) 2758.
- [27] G. Passarino and M. J. G. Veltman, *One Loop Corrections for $e^+ e^-$ Annihilation Into $\mu^+ \mu^-$ in the Weinberg Model*, *Nucl. Phys.* **B160** (1979) 151.
- [28] M. B. Einhorn, D. R. T. Jones, and M. J. G. Veltman, *Heavy particles and the rho parameter in the standard model*, *Nucl. Phys.* **B191** (1981) 146.
- [29] M. Herquet, *Symétries custodiales dans les modèles à deux doublets de Higgs*, *Rapport d'activité DEA* (2004).
- [30] "LEP Electroweak Working Group." <http://lepewwg.web.cern.ch/>.
- [31] G. F. Giudice, *Theories for the fermi scale*, 0710.3294.
- [32] **ECFA/DESY LC Physics Working Group** Collaboration, E. Accomando *et. al.*, *Physics with $e^+ e^-$ linear colliders*, *Phys. Rept.* **299** (1998) 1–78, [hep-ph/9705442].
- [33] **LEP Working Group for Higgs boson searches** Collaboration, R. Barate *et. al.*, *Search for the standard model Higgs boson at LEP*, *Phys. Lett.* **B565** (2003) 61–75, [hep-ex/0306033].
- [34] U. Aglietti *et. al.*, *Tevatron-for-LHC Report: Higgs*, hep-ph/0612172.
- [35] **TEVNPH Working Group** Collaboration, *Combined CDF and Dzero Upper Limits on Standard Model Higgs-Boson Production*, 0712.2383.
- [36] M. Pieri, *Searches for Higgs Bosons at LHC*, *CMS CR-2005/031* (2005).
- [37] M. J. G. Veltman, *The Infrared - Ultraviolet Connection*, *Acta Phys. Polon.* **B12** (1981) 437.
- [38] H. P. Nilles, *Supersymmetry, Supergravity and Particle Physics*, *Phys. Rept.* **110** (1984) 1.
- [39] P. Fayet, *Supersymmetry and Weak, Electromagnetic and Strong Interactions*, *Phys. Lett.* **B64** (1976) 159.
- [40] E. Accomando *et. al.*, *Workshop on CP studies and non-standard Higgs physics*, hep-ph/0608079.
- [41] H. Georgi and S. L. Glashow, *Unity of All Elementary Particle Forces*, *Phys. Rev. Lett.* **32** (1974) 438–441.

- [42] H. Georgi and C. Jarlskog, *A New Lepton - Quark Mass Relation in a Unified Theory*, *Phys. Lett.* **B86** (1979) 297–300.
- [43] S. Dimopoulos and F. Wilczek, *Supersymmetric Unified Models*, . In *Erice 1981, Proceedings, The Unity Of The Fundamental Interactions*, 237-249.
- [44] H. Georgi and A. Pais, *Calculability and Naturalness in Gauge Theories*, *Phys. Rev.* **D10** (1974) 539.
- [45] H. Georgi and A. Pais, *Vacuum Symmetry and the PseudoGoldstone Phenomenon*, *Phys. Rev.* **D12** (1975) 508.
- [46] N. Arkani-Hamed, A. G. Cohen, and H. Georgi, *Electroweak symmetry breaking from dimensional deconstruction*, *Phys. Lett.* **B513** (2001) 232–240, [hep-ph/0105239].
- [47] M. Schmaltz, *The simplest little Higgs*, *JHEP* **08** (2004) 056, [hep-ph/0407143].
- [48] N. Arkani-Hamed *et al.*, *The minimal moose for a little Higgs*, *JHEP* **08** (2002) 021, [hep-ph/0206020].
- [49] S. Chang and J. G. Wacker, *Little Higgs and custodial SU(2)*, *Phys. Rev.* **D69** (2004) 035002, [hep-ph/0303001].
- [50] S. R. Coleman and E. Weinberg, *Radiative Corrections as the Origin of Spontaneous Symmetry Breaking*, *Phys. Rev.* **D7** (1973) 1888–1910.
- [51] G. C. Branco, L. Lavoura, and J. P. Silva, *CP violation*, . Oxford, UK: Clarendon (1999) 511 p.
- [52] A. D. Sakharov, *Violation of CP Invariance, c Asymmetry, and Baryon Asymmetry of the Universe*, *Pisma Zh. Eksp. Teor. Fiz.* **5** (1967) 32–35.
- [53] G. W. Anderson and L. J. Hall, *The Electroweak phase transition and baryogenesis*, *Phys. Rev.* **D45** (1992) 2685–2698.
- [54] M. B. Gavela, P. Hernandez, J. Orloff, and O. Pene, *Standard model CP violation and baryon asymmetry*, *Mod. Phys. Lett.* **A9** (1994) 795–810, [hep-ph/9312215].
- [55] P. Huet and E. Sather, *Electroweak baryogenesis and standard model CP violation*, *Phys. Rev.* **D51** (1995) 379–394, [hep-ph/9404302].
- [56] T. D. Lee, *A Theory of Spontaneous T Violation*, *Phys. Rev.* **D8** (1973) 1226–1239.

- [57] G. C. Branco, *Spontaneous CP nonconservation and natural flavor conservation: A minimal model*, *Phys. Rev.* **D22** (1980) 2901.
- [58] G. 't Hooft, *Symmetry breaking through Bell-Jackiw anomalies*, *Phys. Rev. Lett.* **37** (1976) 8–11.
- [59] C. A. Baker *et al.*, *An improved experimental limit on the electric dipole moment of the neutron*, *Phys. Rev. Lett.* **97** (2006) 131801, [hep-ex/0602020].
- [60] J. M. Gerard, *The light quark current mass ratios and eta - eta-prime mixing*, *Mod. Phys. Lett.* **A5** (1990) 391.
- [61] H. Leutwyler, *The ratios of the light quark masses*, *Phys. Lett.* **B378** (1996) 313–318, [hep-ph/9602366].
- [62] S. Weinberg, *The Problem of Mass*, *Trans. New York Acad. Sci.* **38** (1977) 185–201.
- [63] R. D. Peccei and H. R. Quinn, *CP Conservation in the Presence of Instantons*, *Phys. Rev. Lett.* **38** (1977) 1440–1443.
- [64] Y. Koide, *Fermion-Boson two-body model of quarks and leptons and Cabibbo mixing*, *Nuovo Cim. Lett.* **34** (1982) 201.
- [65] Y. Koide, *Charged lepton mass sum rule from U(3) family Higgs potential model*, *Mod. Phys. Lett.* **A5** (1990) 2319–2324.
- [66] J. M. Gerard, F. Goffinet, and M. Herquet, *A new look at an old mass relation*, *Phys. Lett.* **B633** (2006) 563–566, [hep-ph/0510289].
- [67] Y. Koide, *Permutation symmetry S(3) and VEV structure of flavor- triplet Higgs scalars*, *Phys. Rev.* **D73** (2006) 057901, [hep-ph/0509214].
- [68] **WMAP** Collaboration, D. N. Spergel *et al.*, *Wilkinson Microwave Anisotropy Probe (WMAP) three year results: Implications for cosmology*, *Astrophys. J. Suppl.* **170** (2007) 377, [astro-ph/0603449].
- [69] U. Seljak, A. Slosar, and P. McDonald, *Cosmological parameters from combining the Lyman-alpha forest with CMB, galaxy clustering and SN constraints*, *JCAP* **0610** (2006) 014, [astro-ph/0604335].
- [70] E. Ma, *Verifiable radiative seesaw mechanism of neutrino mass and dark matter*, *Phys. Rev.* **D73** (2006) 077301, [hep-ph/0601225].

- [71] R. Barbieri, L. J. Hall, and V. S. Rychkov, *Improved naturalness with a heavy Higgs: An alternative road to LHC physics*, *Phys. Rev.* **D74** (2006) 015007, [hep-ph/0603188].
- [72] M. Cirelli, N. Fornengo, and A. Strumia, *Minimal dark matter*, *Nucl. Phys.* **B753** (2006) 178–194, [hep-ph/0512090].
- [73] L. Lopez Honorez, E. Nezri, J. F. Oliver, and M. H. G. Tytgat, *The inert doublet model: An archetype for dark matter*, *JCAP* **0702** (2007) 028, [hep-ph/0612275].
- [74] Q.-H. Cao, E. Ma, and G. Rajasekaran, *Observing the Dark Scalar Doublet and its Impact on the Standard-Model Higgs Boson at Colliders*, *Phys. Rev.* **D76** (2007) 095011, [0708.2939].
- [75] P. Chankowski *et. al.*, *Do precision electroweak constraints guarantee e^+e^- collider discovery of at least one Higgs boson of a two Higgs doublet model?*, *Phys. Lett.* **B496** (2000) 195–205, [hep-ph/0009271].
- [76] J. M. Gerard and M. Herquet, *A twisted custodial symmetry in the two-Higgs-doublet model*, *Phys. Rev. Lett.* **98** (2007) 251802, [hep-ph/0703051].
- [77] A. Strumia and F. Vissani, *Neutrino masses and mixings*, hep-ph/0606054.
- [78] B. W. Lee, *Perspectives on theory of weak interactions*, *eConf* **C720906V4** (1972) 249–305.
- [79] J. C. Pati and A. Salam, *Lepton Number as the Fourth Color*, *Phys. Rev.* **D10** (1974) 275–289.
- [80] R. N. Mohapatra and J. C. Pati, *Left-Right Gauge Symmetry and an Isoconjugate Model of CP Violation*, *Phys. Rev.* **D11** (1975) 566–571.
- [81] G. Senjanovic and R. N. Mohapatra, *Exact Left-Right Symmetry and Spontaneous Violation of Parity*, *Phys. Rev.* **D12** (1975) 1502.
- [82] U. Amaldi *et. al.*, *A Comprehensive Analysis of Data Pertaining to the Weak Neutral Current and the Intermediate Vector Boson Masses*, *Phys. Rev.* **D36** (1987) 1385.
- [83] T. G. Rizzo, *Updated bounds on Higgs triplet vacuum expectation values and the tree level rho parameter from radiative corrections*, *Mod. Phys. Lett.* **A6** (1991) 1961–1966.
- [84] H. Georgi, H. R. Quinn, and S. Weinberg, *Hierarchy of Interactions in Unified Gauge Theories*, *Phys. Rev. Lett.* **33** (1974) 451–454.

- [85] J. F. Gunion, *Extended Higgs sectors*, hep-ph/0212150.
- [86] G. C. Branco, J. M. Gerard, R. Gonzalez Felipe, and B. M. Nobre, *Polychromatic grand unification*, hep-ph/0305092.
- [87] J. L. Diaz-Cruz and A. Mendez, *Vacuum alignment in multiscalar models*, *Nucl. Phys.* **B380** (1992) 39–50.
- [88] P. M. Ferreira, R. Santos, and A. Barroso, *Stability of the tree-level vacuum in two Higgs doublet models against charge or CP spontaneous violation*, hep-ph/0406231.
- [89] I. F. Ginzburg and M. Krawczyk, *Symmetries of two Higgs doublet model and CP violation*, *Phys. Rev.* **D72** (2005) 115013, [hep-ph/0408011].
- [90] S. Davidson and H. E. Haber, *Basis-independent methods for the two-Higgs-doublet model*, *Phys. Rev.* **D72** (2005) 035004, [hep-ph/0504050].
- [91] H. E. Haber and D. O’Neil, *Basis-independent methods for the two-Higgs-doublet model. II: The significance of $\tan(\beta)$* , *Phys. Rev.* **D74** (2006) 015018, [hep-ph/0602242].
- [92] W. Grimus and M. N. Rebelo, *Automorphisms in gauge theories and the definition of CP and P*, *Phys. Rept.* **281** (1997) 239–308, [hep-ph/9506272].
- [93] A. Pomarol and R. Vega, *Constraints on CP violation in the Higgs sector from the rho parameter*, *Nucl. Phys.* **B413** (1994) 3–15, [hep-ph/9305272].
- [94] S. L. Glashow and S. Weinberg, *Natural conservation laws for neutral currents*, *Phys. Rev.* **D15** (1977) 1958.
- [95] A. Pilaftsis, *Higgs scalar-pseudoscalar mixing in the minimal supersymmetric standard model*, *Phys. Lett.* **B435** (1998) 88–100, [hep-ph/9805373].
- [96] A. Pilaftsis, *CP-odd tadpole renormalization of Higgs scalar-pseudoscalar mixing*, *Phys. Rev.* **D58** (1998) 096010, [hep-ph/9803297].
- [97] A. Djouadi, *The anatomy of electro-weak symmetry breaking. II: The Higgs bosons in the minimal supersymmetric model*, hep-ph/0503173.
- [98] D. Keira, *Determination of the Discovery Potential for Higgs Bosons in MSSM*, 0710.1957.
- [99] D. Toussaint, *Renormalization effects from superheavy higgs particles*, *Phys. Rev.* **D18** (1978) 1626.

- [100] G. C. Branco, A. J. Buras, and J. M. Gerard, *CP Violation in models with two and three scalar doublets*, *Nucl. Phys.* **B259** (1985) 306.
- [101] N. G. Deshpande and E. Ma, *Pattern of Symmetry Breaking with Two Higgs Doublets*, *Phys. Rev.* **D18** (1978) 2574.
- [102] A. Barroso, P. M. Ferreira, and R. Santos, *Neutral minima in two-Higgs doublet models*, *Phys. Lett.* **B652** (2007) 181–193, [hep-ph/0702098].
- [103] A. G. Akeroyd, A. Arhrib, and E.-M. Naimi, *Note on tree-level unitarity in the general two Higgs doublet model*, *Phys. Lett.* **B490** (2000) 119–124, [hep-ph/0006035].
- [104] I. F. Ginzburg and I. P. Ivanov, *Tree-level unitarity constraints in the most general 2HDM*, *Phys. Rev.* **D72** (2005) 115010, [hep-ph/0508020].
- [105] K. Tobe and J. D. Wells, *Higgs boson mass limits in perturbative unification theories*, *Phys. Rev.* **D66** (2002) 013010, [hep-ph/0204196].
- [106] I. Maksymyk, C. P. Burgess, and D. London, *Beyond S, T and U*, *Phys. Rev.* **D50** (1994) 529–535, [hep-ph/9306267].
- [107] W. Grimus, L. Lavoura, O. M. Ogreid, and P. Osland, *The oblique parameters in multi-Higgs-doublet models*, 0802.4353.
- [108] M. E. Peskin and T. Takeuchi, *Estimation of oblique electroweak corrections*, *Phys. Rev.* **D46** (1992) 381–409.
- [109] W. Grimus, L. Lavoura, O. M. Ogreid, and P. Osland, *A precision constraint on multi-Higgs-doublet models*, 0711.4022.
- [110] H. E. Haber, *Introductory low-energy supersymmetry*, hep-ph/9306207.
- [111] H.-J. He, N. Polonsky, and S.-f. Su, *Extra families, Higgs spectrum and oblique corrections*, *Phys. Rev.* **D64** (2001) 053004, [hep-ph/0102144].
- [112] R. Barbieri and G. F. Giudice, *$b \rightarrow s$ gamma decay and supersymmetry*, *Phys. Lett.* **B309** (1993) 86–90, [hep-ph/9303270].
- [113] T. Inami and C. S. Lim, *Effects of Superheavy Quarks and Leptons in Low-Energy Weak Processes $k(L) \rightarrow \mu$ anti- μ , $K^+ \rightarrow \pi^+$ Neutrino anti-neutrino and $K^0 \leftrightarrow$ anti- K^0* , *Prog. Theor. Phys.* **65** (1981) 297.
- [114] B. Grinstein and M. B. Wise, *Weak Radiative B Meson Decay as a Probe of the Higgs Sector*, *Phys. Lett.* **B201** (1988) 274.

- [115] W.-S. Hou and R. S. Willey, *Effects of Charged Higgs Bosons on the Processes $b \rightarrow s$ Gamma, $b \rightarrow s g^*$ and $b \rightarrow s$ Lepton+ Lepton-, Phys. Lett. B202 (1988) 591.*
- [116] **Heavy Flavor Averaging Group (HFAG)** Collaboration, E. Barberio *et. al.*, *Averages of b -hadron properties at the end of 2006*, 0704 . 3575.
- [117] M. Misiak *et. al.*, *The first estimate of $B(\text{anti-}B \rightarrow X/s \text{ gamma})$ at $O(\alpha(s)^2)$* , *Phys. Rev. Lett.* **98** (2007) 022002, [hep-ph/0609232].
- [118] F. Borzumati and C. Greub, *2HDMs predictions for anti- $B \rightarrow X/s$ gamma in NLO QCD*, *Phys. Rev.* **D58** (1998) 074004, [hep-ph/9802391].
- [119] Z.-j. Xiao and L. Guo, *$B0$ anti- $B0$ mixing and $B \rightarrow X/s$ gamma decay in the third type 2HDM: Effects of NLO QCD contributions*, *Phys. Rev.* **D69** (2004) 014002, [hep-ph/0309103].
- [120] **BABAR** Collaboration, B. Aubert *et. al.*, *Observation of the Semileptonic Decays $B \rightarrow D^* \tau \text{ nubar}$ and Evidence for $B \rightarrow D \tau \text{ nubar}$* , *Phys. Rev. Lett.* **100** (2008) 021801, [0709 . 1698].
- [121] U. Nierste, S. Trine, and S. Westhoff, *Charged-Higgs effects in a new $B \rightarrow D \tau \nu$ differential decay distribution*, 0801 . 4938.
- [122] K. Ikado *et. al.*, *Evidence of the purely leptonic decay $B \rightarrow \tau \text{ anti-} \nu/\tau$* , *Phys. Rev. Lett.* **97** (2006) 251802, [hep-ex/0604018].
- [123] C. Smith, *Minimal Flavour Violation, Lectures notes* (2008).
- [124] **BABAR** Collaboration, B. Aubert *et. al.*, *A search for $B^+ \rightarrow \tau^+ \nu$ with Hadronic B tags*, *Phys. Rev.* **D77** (2008) 011107, [0708 . 2260].
- [125] A. Wahab El Kaffas, P. Osland, and O. Magne Ogreid, *Constraining the Two-Higgs-Doublet-Model parameter space*, *Phys. Rev.* **D76** (2007) 095001, [0706 . 2997].
- [126] C. Q. Geng and J. N. Ng, *Charged Higgs effect in $B(d)0$ - anti- $B(d)0$ mixing, $K \rightarrow \pi$ neutrino anti-neutrino decay and rare decays of B mesons*, *Phys. Rev.* **D38** (1988) 2857.
- [127] P. Ball and R. Fleischer, *Probing new physics through B mixing: Status, benchmarks and prospects*, *Eur. Phys. J.* **C48** (2006) 413–426, [hep-ph/0604249].
- [128] J. Urban, F. Krauss, U. Jentschura, and G. Soff, *Next-to-leading order QCD corrections for the $B0$ anti- $B0$ mixing with an extended Higgs sector*, *Nucl. Phys.* **B523** (1998) 40–58, [hep-ph/9710245].

- [129] H. E. Logan, *Radiative corrections to the $Z b$ anti- b vertex and constraints on extended Higgs sectors*, hep-ph/9906332.
- [130] K. Hagiwara, A. D. Martin, D. Nomura, and T. Teubner, *Improved predictions for $g-2$ of the muon and $\alpha_{\text{QED}}(M_Z^2)$* , *Phys. Lett.* **B649** (2007) 173–179, [hep-ph/0611102].
- [131] **Muon G-2** Collaboration, G. W. Bennett *et. al.*, *Final report of the muon E821 anomalous magnetic moment measurement at BNL*, *Phys. Rev.* **D73** (2006) 072003, [hep-ex/0602035].
- [132] M. Krawczyk, *The new $(g-2)(\mu)$ measurement and limits on the light Higgs bosons in 2HDM. II*, hep-ph/0103223.
- [133] B. Heltsley, *Bottomonium results from cleo - qwg talk*, .
- [134] D. Chang, W.-F. Chang, C.-H. Chou, and W.-Y. Keung, *Large two-loop contributions to $g-2$ from a generic pseudoscalar boson*, *Phys. Rev.* **D63** (2001) 091301, [hep-ph/0009292].
- [135] **LEP Working Group for Higgs boson searches** Collaboration, S. Schael *et. al.*, *Search for neutral MSSM Higgs bosons at LEP*, *Eur. Phys. J.* **C47** (2006) 547–587, [hep-ex/0602042].
- [136] **DELPHI** Collaboration, J. Abdallah *et. al.*, *Searches for neutral Higgs bosons in extended models*, *Eur. Phys. J.* **C38** (2004) 1–28, [hep-ex/0410017].
- [137] M. Krawczyk, J. Zochowski, and P. Mattig, *Process $Z \rightarrow h(A) + \gamma$ in the 2HDM and the experimental constraints from LEP*, *Eur. Phys. J.* **C8** (1999) 495–505, [hep-ph/9811256].
- [138] **DELPHI** Collaboration, J. Abdallah *et. al.*, *Search for charged Higgs bosons at LEP in general two Higgs doublet models*, *Eur. Phys. J.* **C34** (2004) 399–418, [hep-ex/0404012].
- [139] T. Stelzer, S. Wiesenfeldt, and S. Willenbrock, *Higgs at the Tevatron in extended supersymmetric models*, *Phys. Rev.* **D75** (2007) 077701, [hep-ph/0611242].
- [140] A. Djouadi *et. al.*, *Benchmark scenarios for the NMSSM*, 0801.4321.
- [141] M. Carena, T. Han, G.-Y. Huang, and C. E. M. Wagner, *Higgs Signal for h to aa at Hadron Colliders*, 0712.2466.
- [142] M. Roco *FERMILAB-Conf*(2001), no. 00/203-E.

- [143] CDF Collaboration, *Search for Neutral MSSM Higgs Bosons Decaying to Tau Pairs with 1.8fb^{-1} of Data*, *CDF Note* (2007), no. 9071.
- [144] A. G. Akeroyd, *Searching for a very light Higgs boson at the Tevatron*, *Phys. Rev.* **D68** (2003) 077701, [hep-ph/0306045].
- [145] CDF Collaboration, *Search for anomalous tau production in b-tagged top quark events*, *CDF Note* (2006), no. 8353.
- [146] CDF Collaboration, *A search of charged Higgs in the decay products of pair-produced top quarks.*, *CDF Note* (2006), no. 7712.
- [147] B. C. Allanach *et. al.*, *The Snowmass points and slopes: Benchmarks for SUSY searches*, hep-ph/0202233.
- [148] S. de Visscher, J.-M. Gérard, M. Herquet, V. Lemaitre, and F. Maltoni *To be published* (2008).
- [149] J. Alwall *et. al.*, *MadGraph/MadEvent v4: The New Web Generation*, *JHEP* **09** (2007) 028, [arXiv:0706.2334].
- [150] T. Plehn, *Charged Higgs boson production in bottom gluon fusion*, *Phys. Rev.* **D67** (2003) 014018, [hep-ph/0206121].
- [151] S. Dawson *et. al.*, *Les Houches 2008 Higgs Working Group Summary Report*, arXiv:0803.1154.
- [152] K. Cheung, J. Song, and Q.-S. Yan, *Role of $h \rightarrow \eta \eta$ in Intermediate-Mass Higgs Boson Searches at the Large Hadron Collider*, *Phys. Rev. Lett.* **99** (2007) 031801, [hep-ph/0703149].
- [153] D. L. Rainwater, D. Zeppenfeld, and K. Hagiwara, *Searching for $h \rightarrow \tau \tau$ in weak boson fusion at the lhc*, *Phys. Rev.* **D59** (1999) 014037, [hep-ph/9808468].
- [154] T. Plehn, D. L. Rainwater, and D. Zeppenfeld, *Probing the MSSM Higgs sector via weak boson fusion at the LHC*, *Phys. Lett.* **B454** (1999) 297–303, [hep-ph/9902434].
- [155] S. Asai *et. al.*, *Prospects for the search for a standard model higgs boson in atlas using vector boson fusion*, *Eur. Phys. J.* **C32S2** (2004) 19–54, [hep-ph/0402254].
- [156] D. Cavalli *et. al.*, *The higgs working group: Summary report*, hep-ph/0203056.
- [157] M. Klute *ATLAS Note ATL-PHYS-2002-018* (2002).

- [158] U. Ellwanger, J. F. Gunion, C. Hugonie, and S. Moretti, *Towards a no-lose theorem for NMSSM Higgs discovery at the LHC*, hep-ph/0305109.
- [159] U. Ellwanger, J. F. Gunion, C. Hugonie, and S. Moretti, *NMSSM Higgs discovery at the LHC*, hep-ph/0401228.
- [160] A. Pin Master's thesis, Université catholique de Louvain, June, 2008.
- [161] T. Sjostrand, S. Mrenna, and P. Skands, *PYTHIA 6.4 physics and manual*, *JHEP* **05** (2006) 026, [hep-ph/0603175].
- [162] J. Conway *et al.*, "Pgs 4: Pretty good simulation of high energy collisions."
www.physics.ucdavis.edu/~conway/research/software/pgs/pgs4-general.htm
- [163] D. K. Ghosh, R. M. Godbole, and D. P. Roy, *Probing the CP-violating light neutral Higgs in the charged Higgs decay at the LHC*, *Phys. Lett.* **B628** (2005) 131–140, [hep-ph/0412193].
- [164] M. Schumacher, "Les Houches Workshop." In summary talk by T. Lari, 2005.
- [165] T. Stelzer and W. F. Long, *Automatic generation of tree level helicity amplitudes*, *Comput. Phys. Commun.* **81** (1994) 357–371, [hep-ph/9401258].
- [166] F. Maltoni and T. Stelzer, *MadEvent: Automatic event generation with MadGraph*, *JHEP* **02** (2003) 027, [hep-ph/0208156].
- [167] H. Murayama, I. Watanabe, and K. Hagiwara, *HELAS: HELicity amplitude subroutines for Feynman diagram evaluations*, . KEK-91-11.
- [168] G. C. Cho *et al.*, *Weak boson fusion production of supersymmetric particles at the LHC*, *Phys. Rev.* **D73** (2006) 054002, [hep-ph/0601063].
- [169] P. Skands *et al.*, *SUSY Les Houches accord: Interfacing SUSY spectrum calculators, decay packages, and event generators*, *JHEP* **07** (2004) 036, [hep-ph/0311123].
- [170] B. Allanach *et al.*, *SUSY Les Houches Accord 2*, arXiv:0801.0045.
- [171] F. Maltoni, K. Paul, T. Stelzer, and S. Willenbrock, *Associated production of Higgs and single top at hadron colliders*, *Phys. Rev.* **D 64** (2001) 094023, [hep-ph/0106293].